Antiproton-to-Proton flux ratio measurement of AMS02

Ziyuan.Li / Sun-Yet-Sen University

IHEP, Beijing, Aug.22,2017

Evidence of Dark Matter

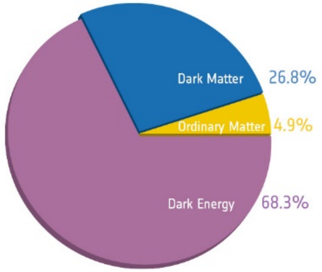

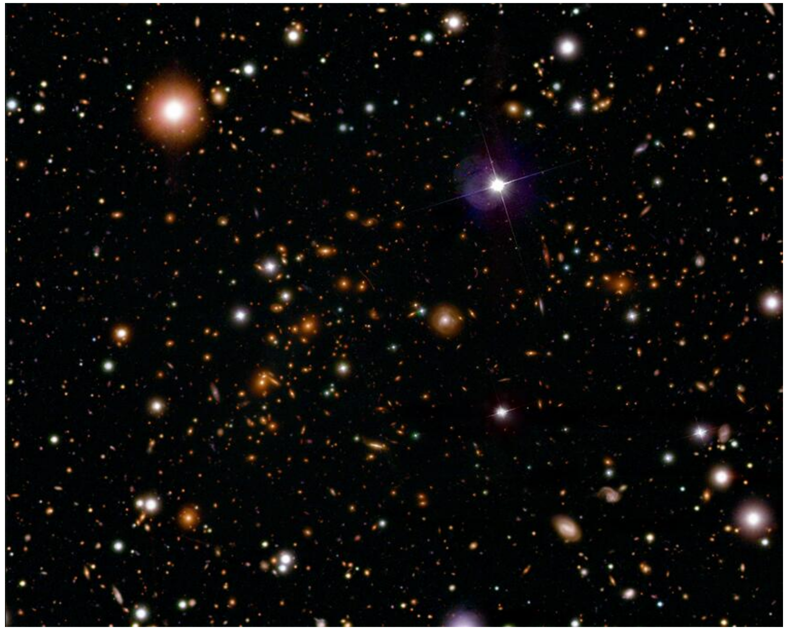

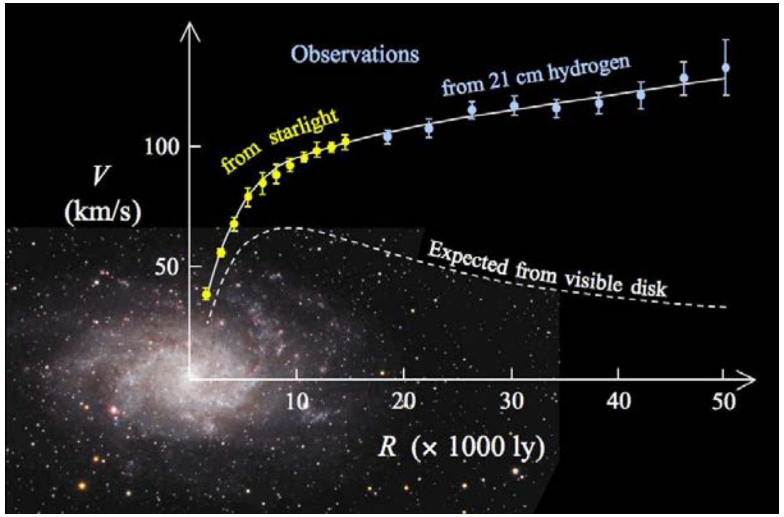

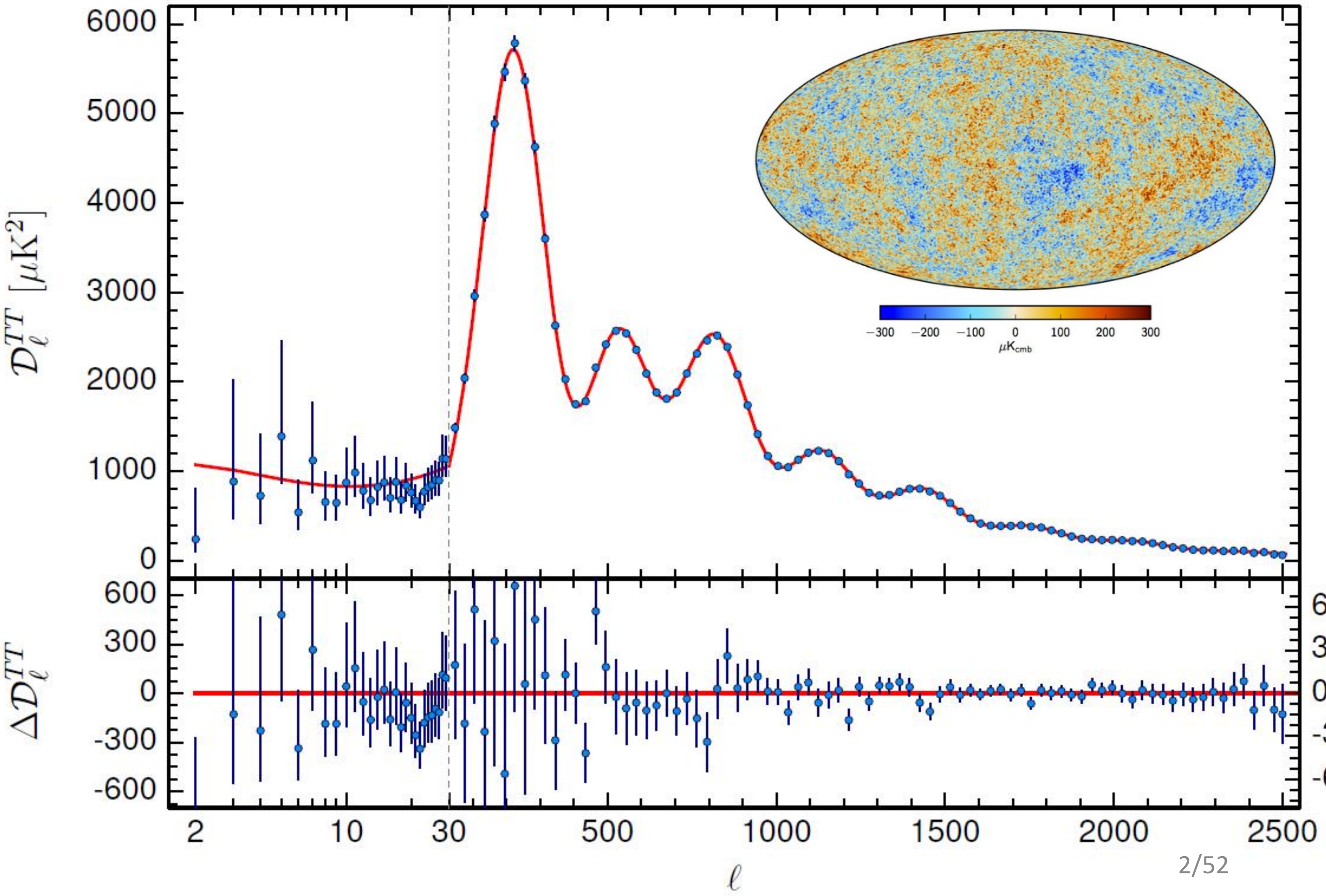

Three independent methods to search for Dark Matter

Annihilation

HESS, HAWC, VERITAS, MAGIC, IceCube, …

PAMELA, FERMI, CALET, DAMPE, AMS, …

$\chi + \chi \rightarrow e^{+}, \bar{p}, \gamma, \ldots$

Scattering

CDEX
CDMS
CRESST
DARKSIDE
DEAP
LUX
PandaX
PICO
XENON
…

$\chi + N \rightarrow \chi + N$

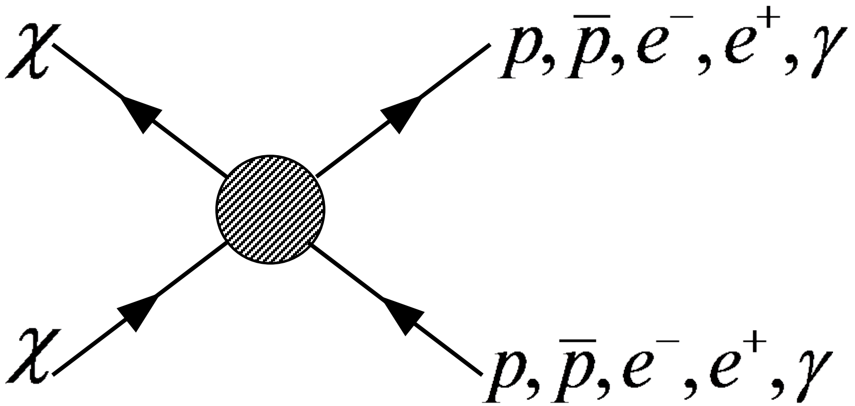

$\ldots + \chi + \chi \leftarrow p + p$

LHC

Production

Dark Matter Searches at AMS

e^+ and $\bar{p}$ are rare species in cosmic rays
The collision of cosmic rays with interstellar medium(ISM) will produce e^+ and $\bar{p}$

$p, He + ISM \rightarrow e^+, \bar{p} + \ldots$

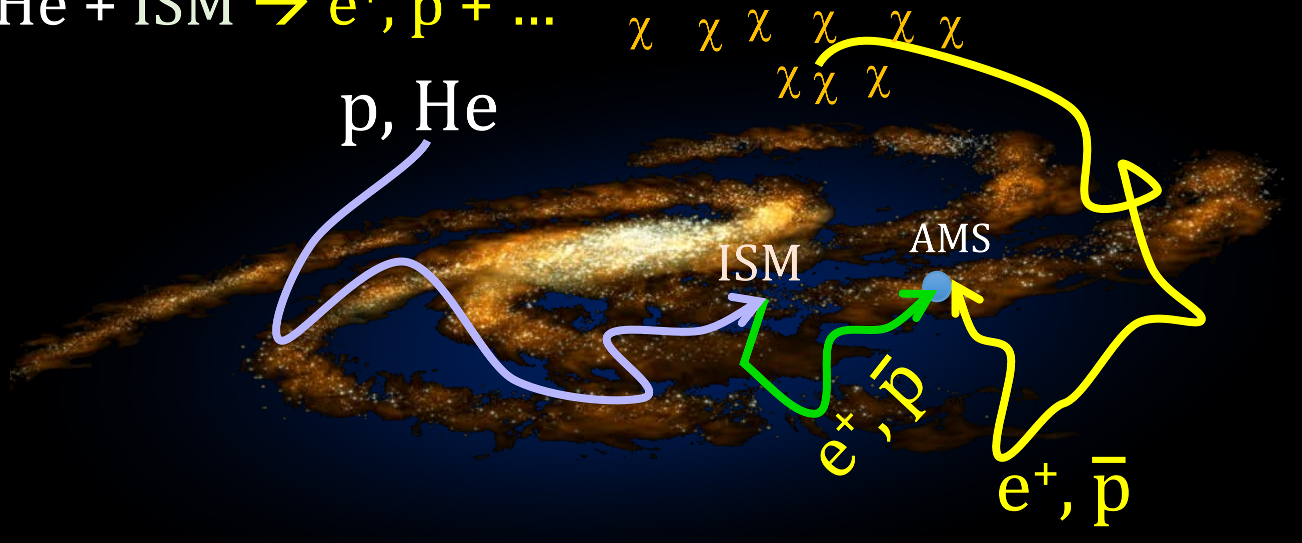

M. Turner and F. Wilczek, Phys. Rev. D42 (1990) 1001; J. Ellis 26th ICRC (1999)

$\chi + \chi \rightarrow e^+, \bar{p} + \ldots$

The collision of dark matter particles will produce additional e^+ and $\bar{p}$

The excess of e^+ and $\bar{p}$ can be accurately measured by AMS

Physics of AMS

- Searches for Dark Matter through simultaneous observation of positron, antiproton, …
- A long duration mission for precision measurements of elementary particles and nuclei in cosmic rays
- Searches for primordial antimatter
- Understanding the origin and propagation of cosmic rays

Alpha Magnetic Spectrometer

Transition Radiation Detector
Identify $e^{\pm}/p$

Silicon Tracker
Z, Rigidity(R=P/Z)

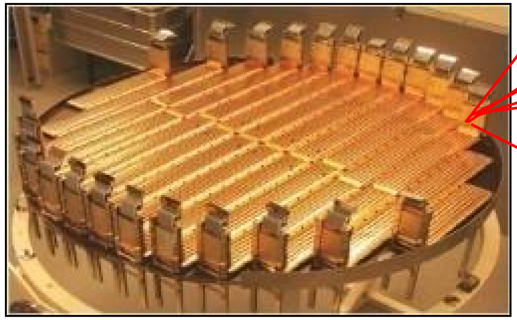

Electromagnetic Calorimeter
Identify $e^{\pm}/p$, E of $e^{\pm}$

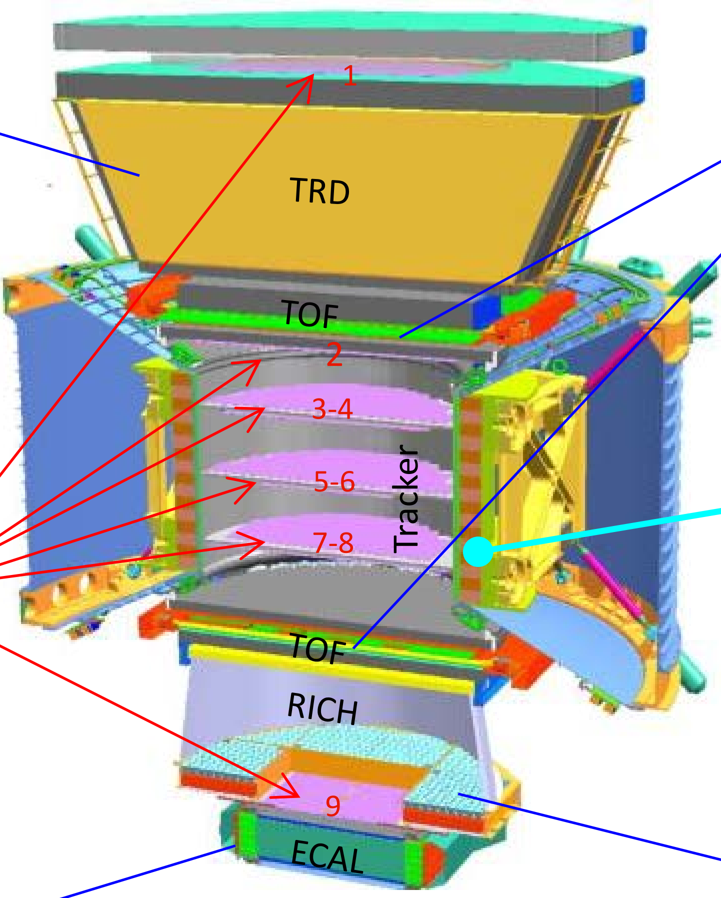

Time of Flight
V, Z

Magnet
$\pm$Z

Ring Imaging Cherenkov
V, Z

The Charge(Z) and Energy(E) are measured independently by several detectors

Precise identification of particle and nuclei species

Transition Radiation Detector (TRD)

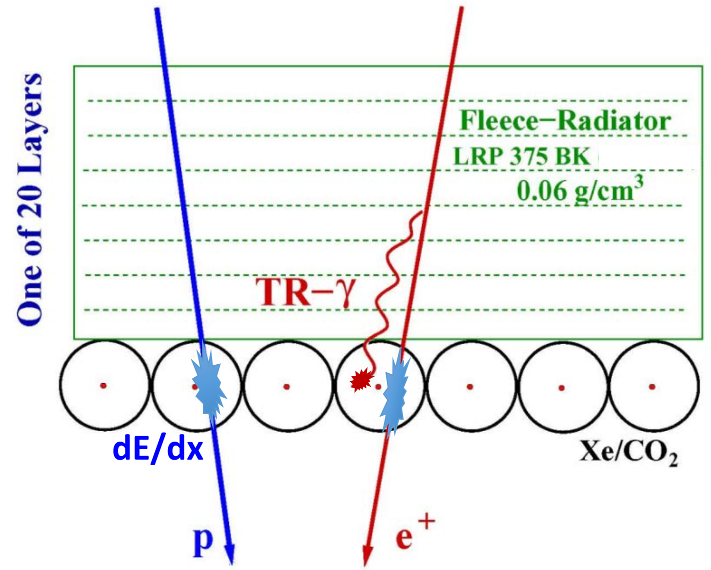

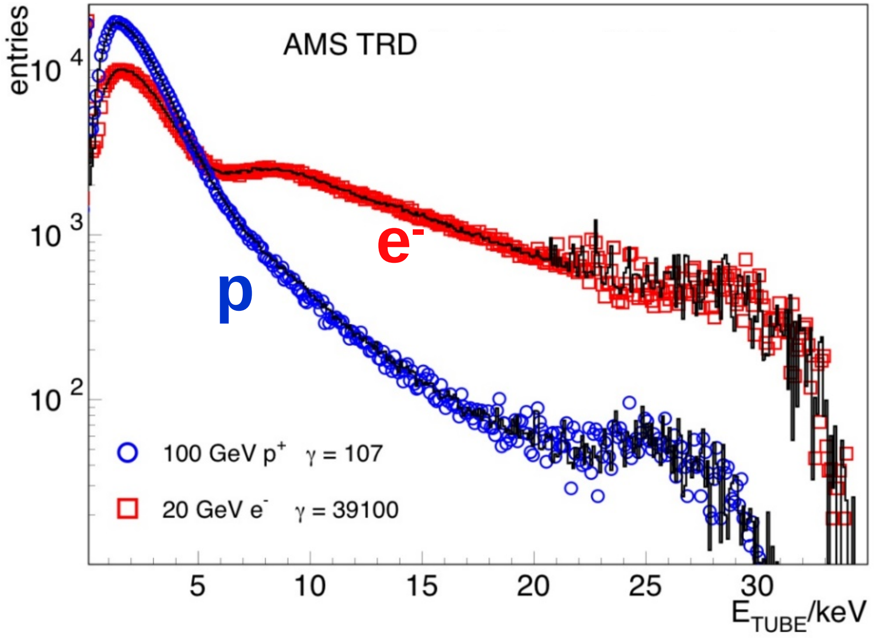

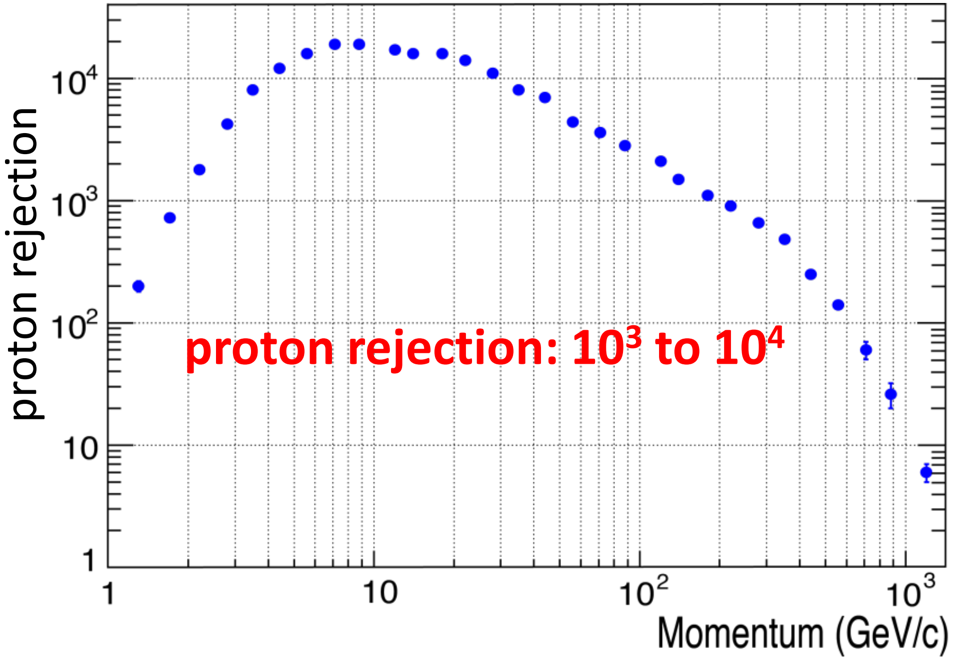

Silicon Tracker and Magnet

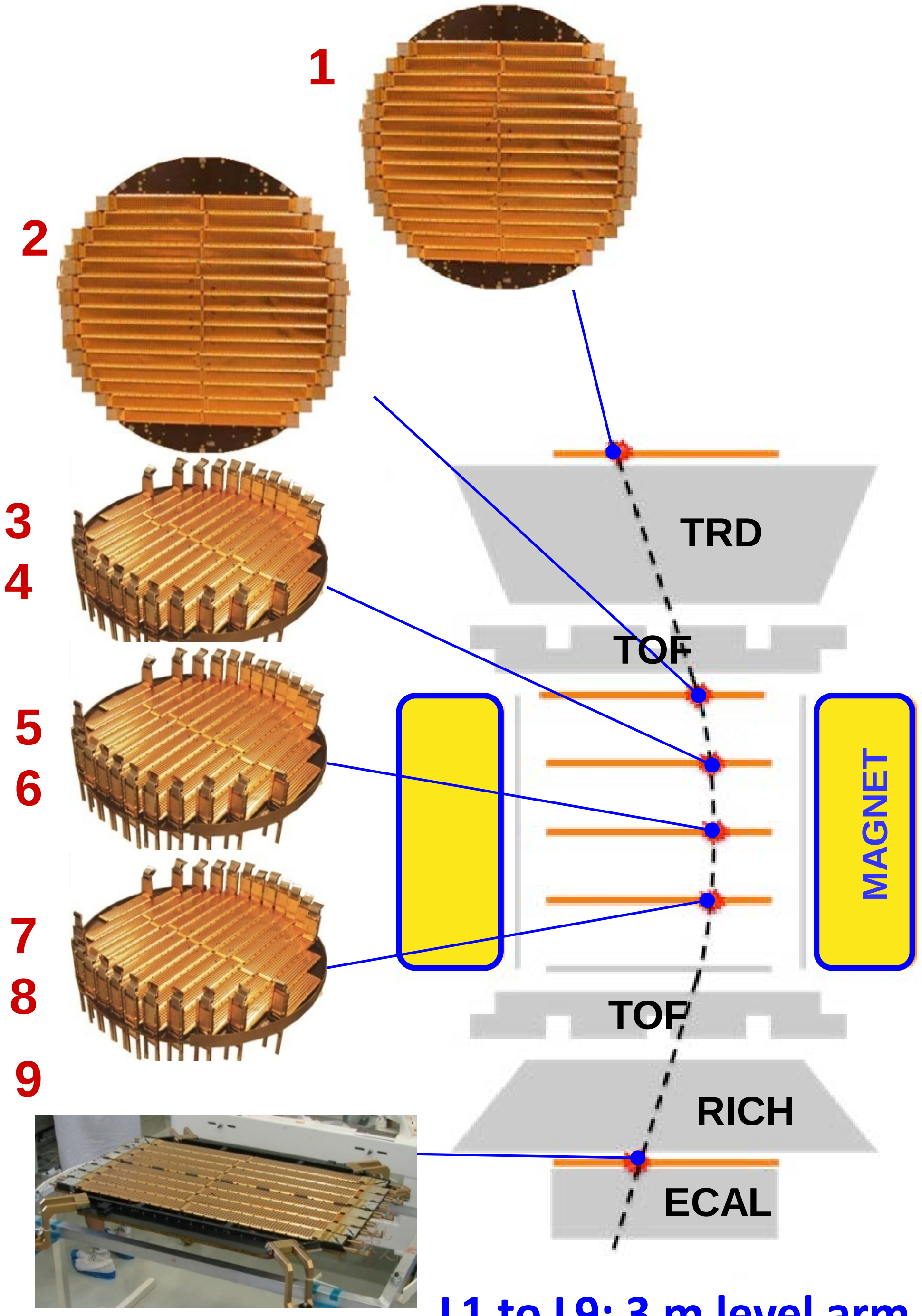

L1 to L9: 3 m level arm

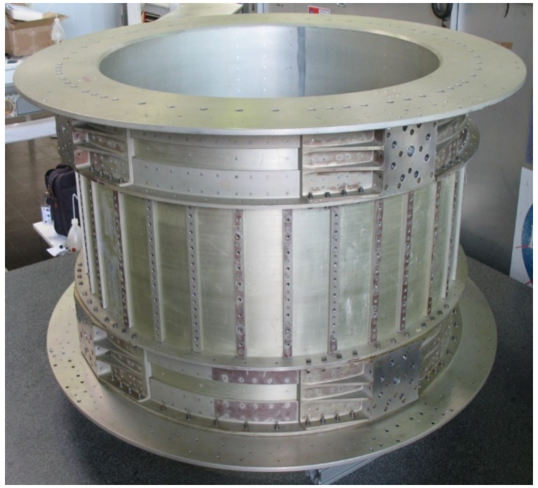

1.4 kG

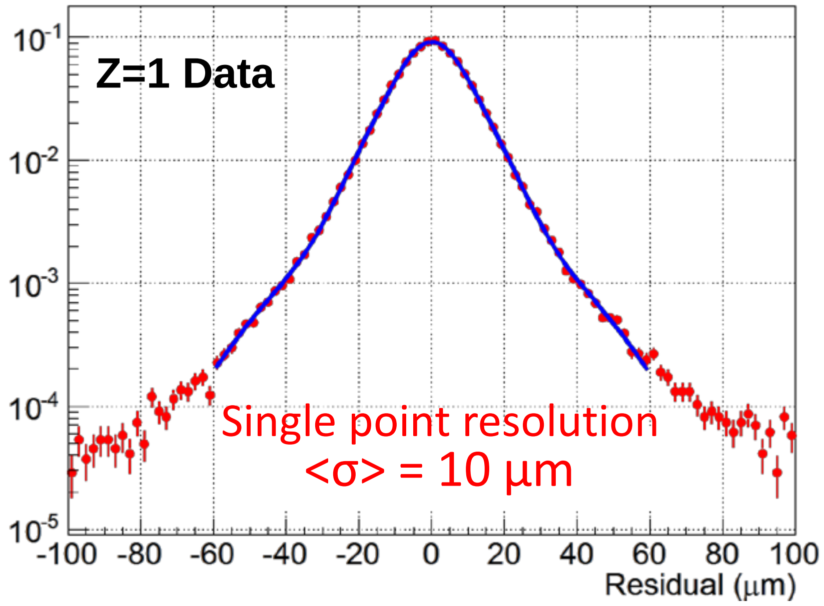

Maximum Detectable Rigidity(MDR)

2.0 TV for Z=1 particles

Electromagnetic Calorimeter (ECAL)

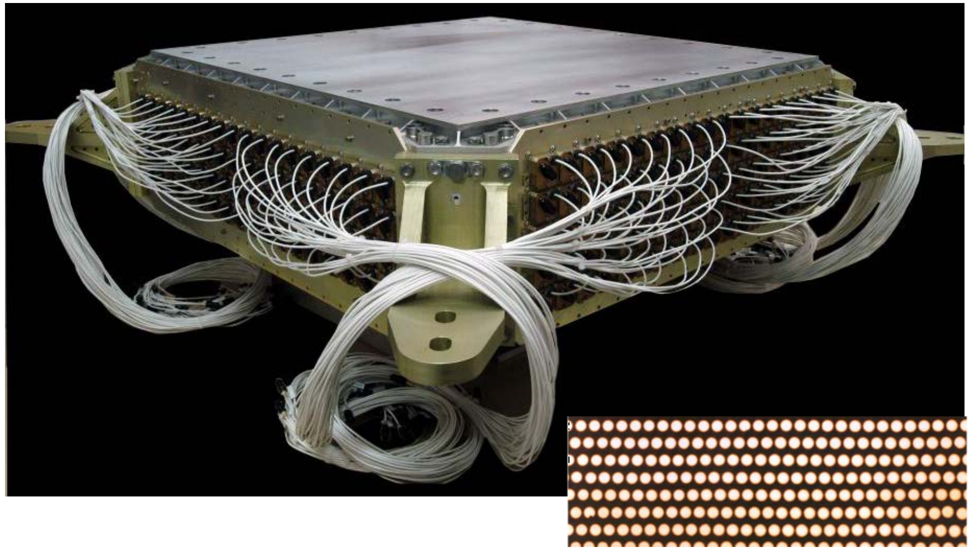

- **17 X_0, 3D measurement of the directions and energies of $e^{\pm}$ to TeV**
- **Energy scale and resolution measured with test beam**
- **Identify $e^{\pm}$ by 3D shower shape**
- **Proton rejection is above 10^4 with ECAL and Tracker**

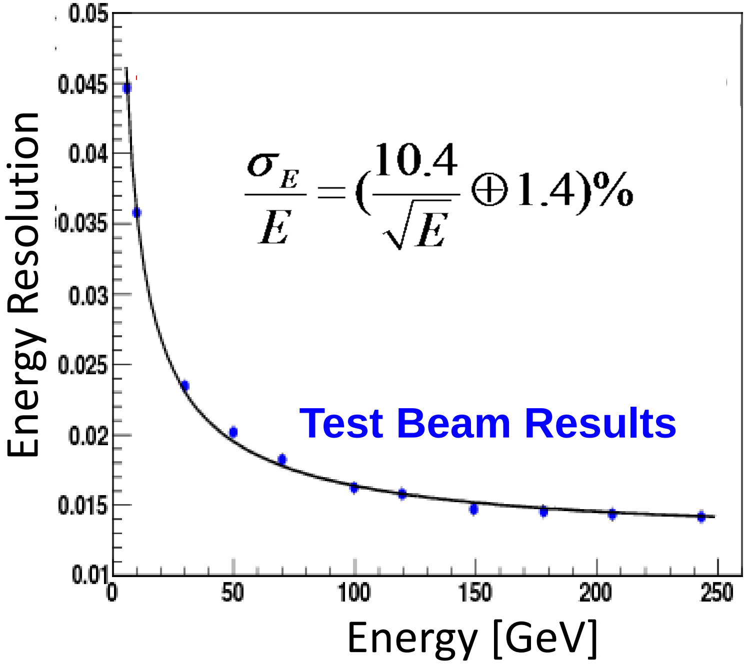

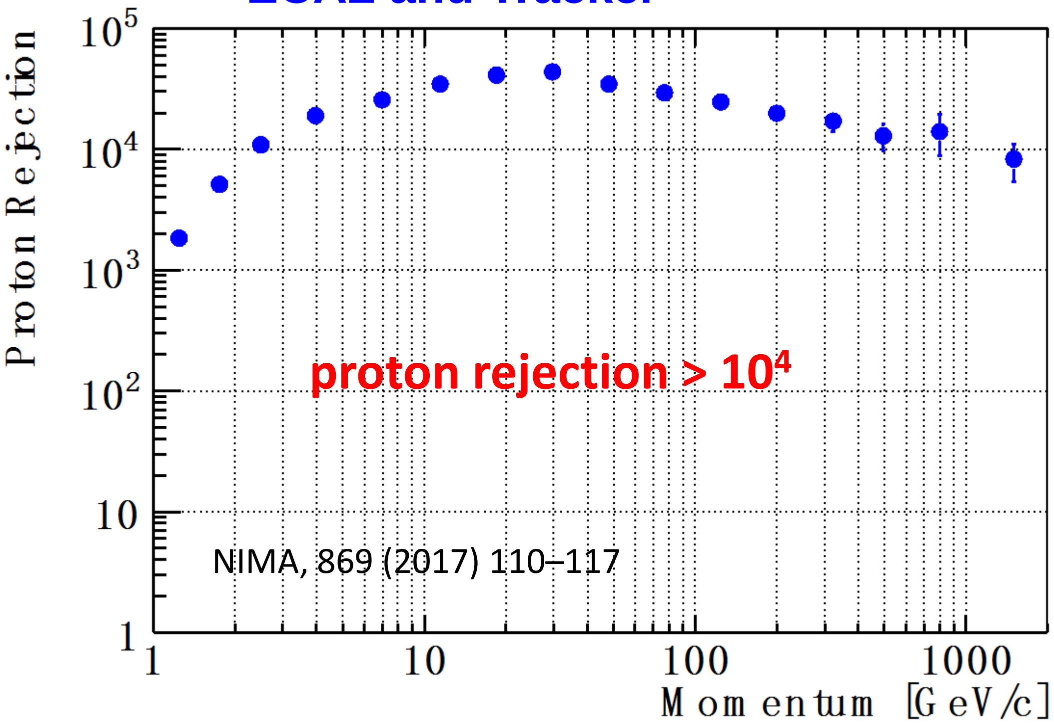

Particle signals in AMS detector

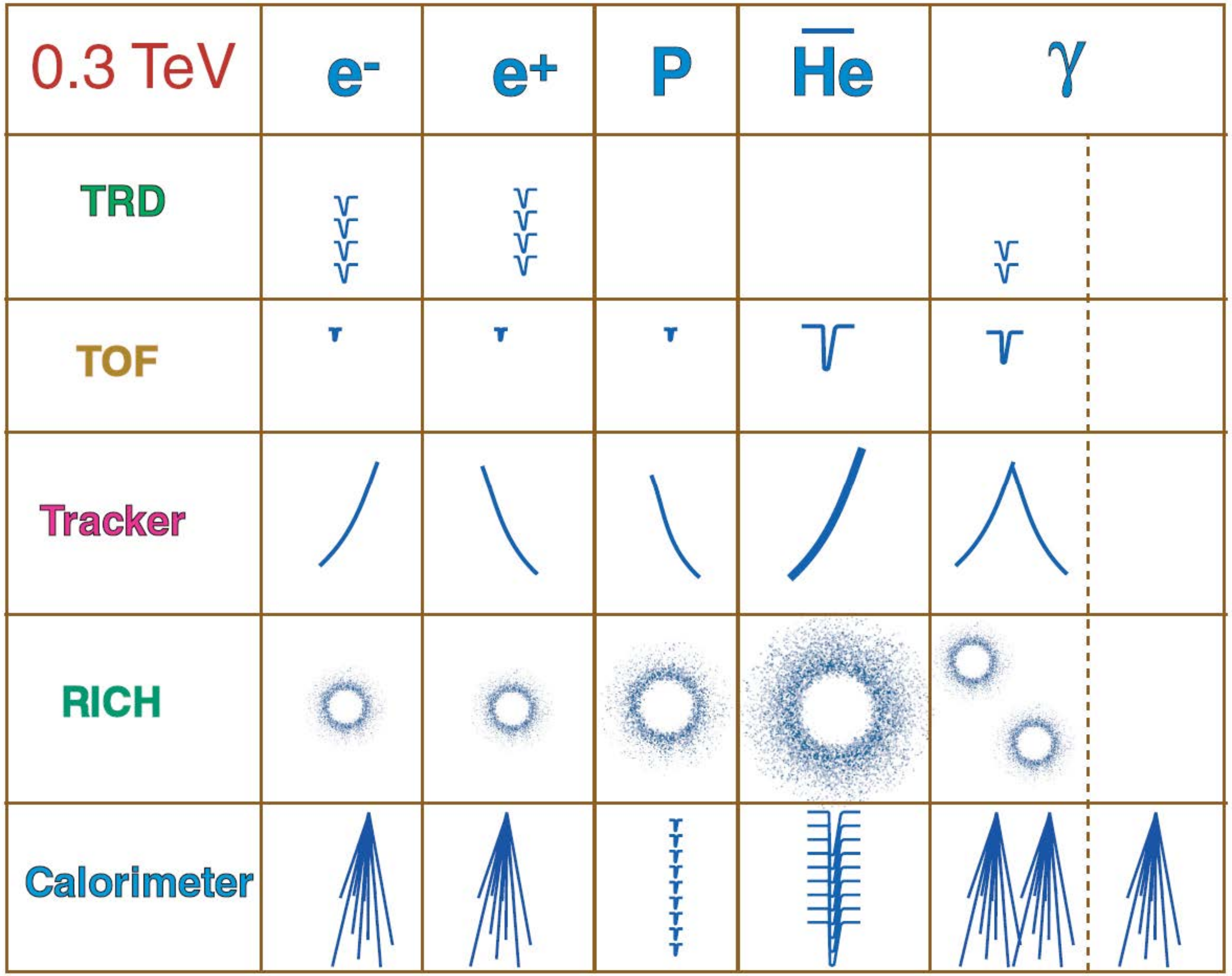

Electron and Proton identification in AMS

Redundant particle identification using TRD, ECAL and Tracker

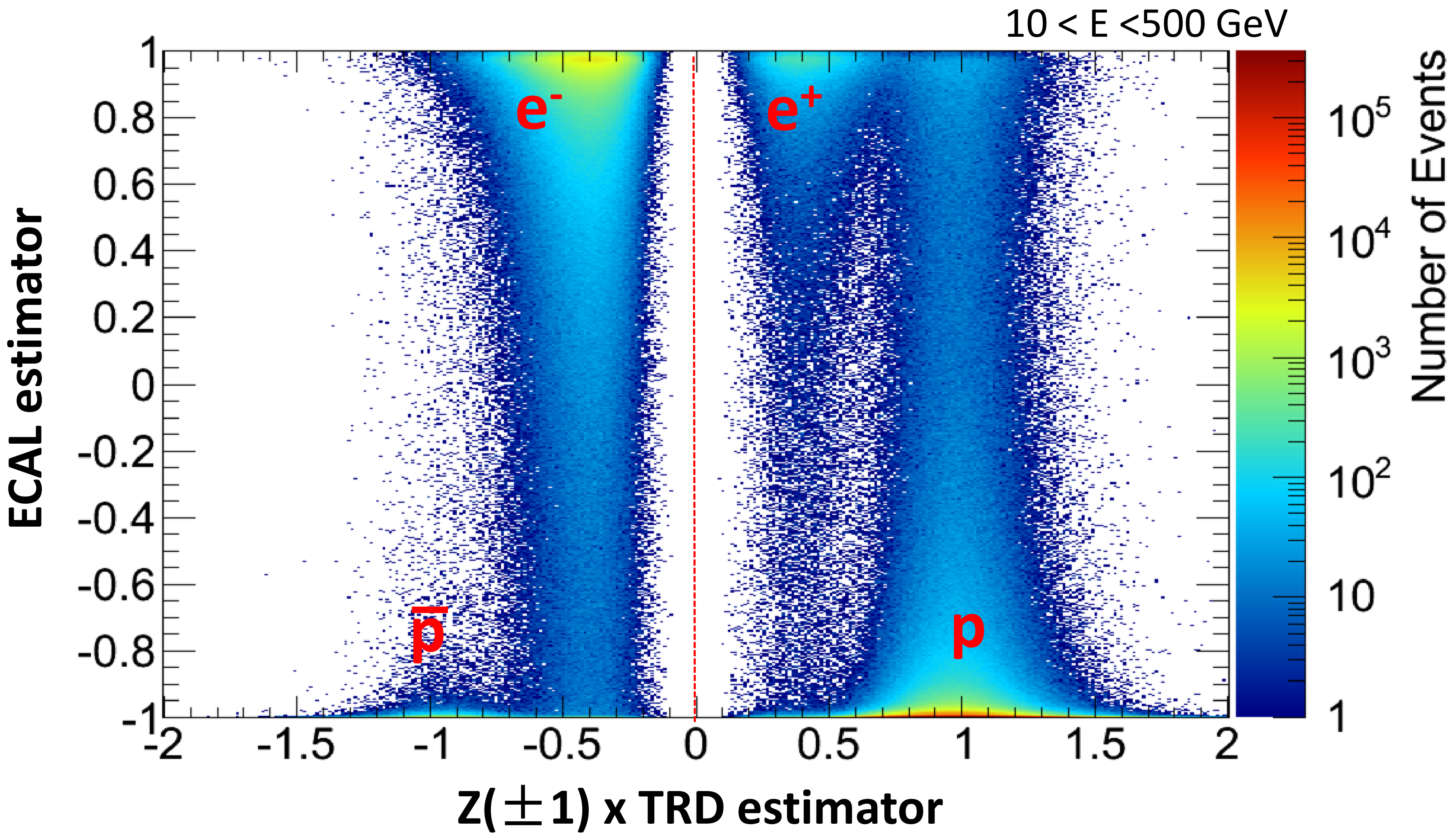

Event pre-selection for the $\bar{p}/p$ analysis

- **Primary cosmic ray particle:**
  - **|R| > 1.2 × max cutoff**
  - **Good RTI**
- **TOF:**
  - **Down-going particle**
  - **β>0.3**
  - **0.8 < |Q| < 1.6**
- **TRD:**
  - **Single TRD track**
  - **at least 12 hits**
- **TRACKER:**
  - **Single Tracker track**
  - **Track quality**
  - **0.7 < |Q| < 1.4**
- **ECAL:**
  - **ECAL quality**
  - **Hadron shower shape**

Event Display

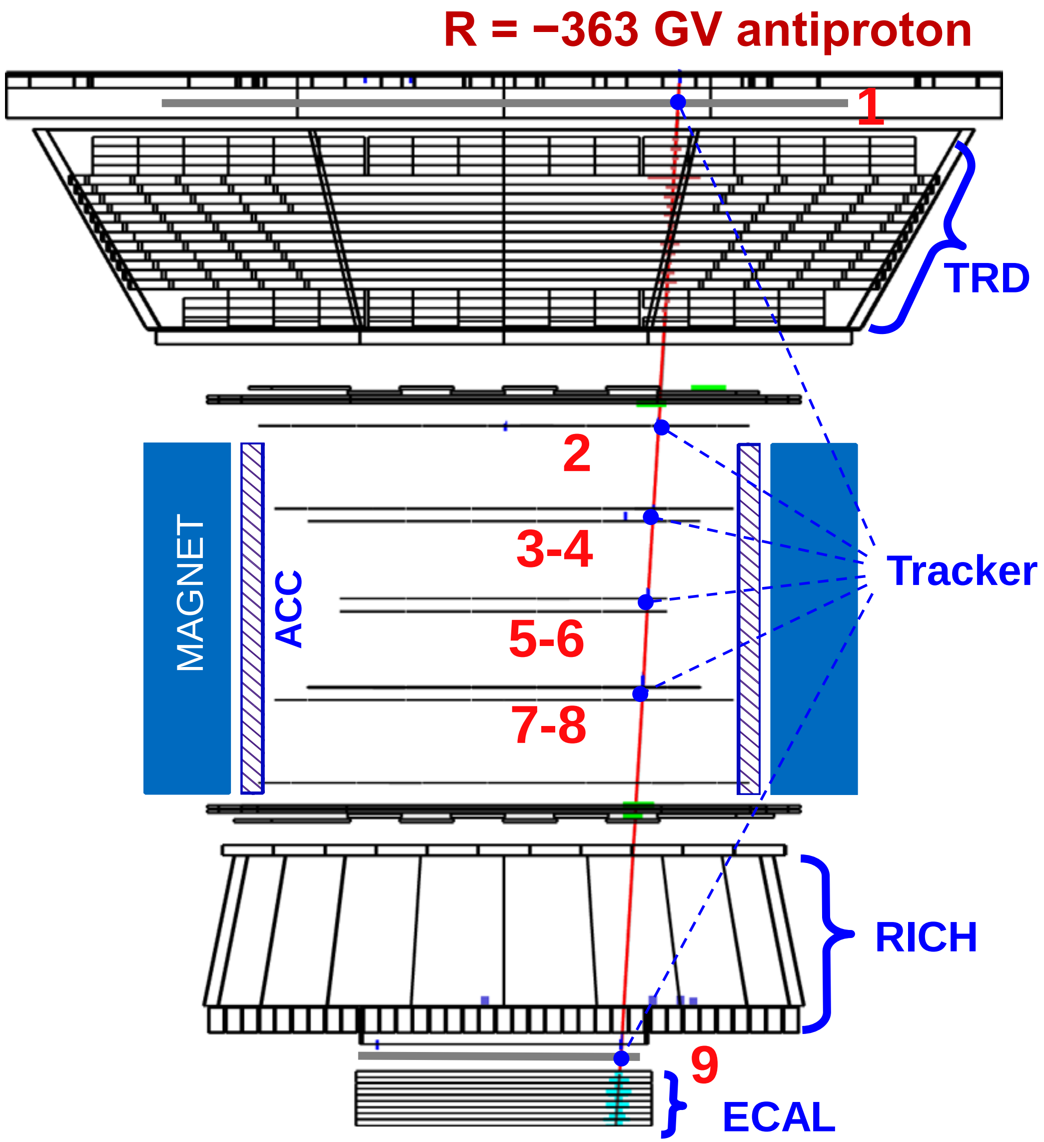

Data sample

350,000 antiprotons are selected in the rigidity range 1–450 GV

Analysis strategy

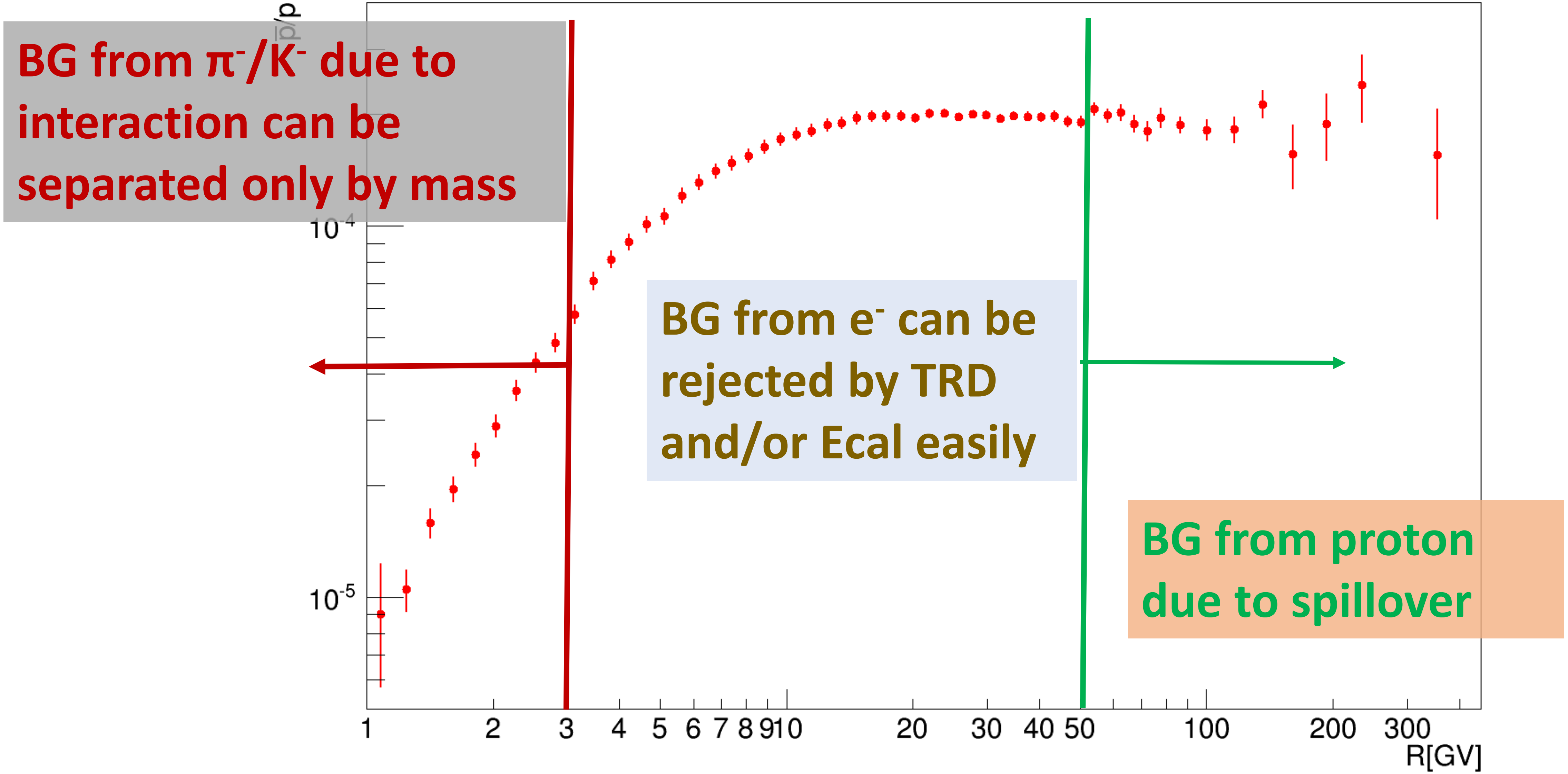

Low rigidity region (R < 3 GV)

Key analysis : RICH Veto
Goal : Control π/e^- B.G.

- **RICH Veto to control π/e^- background. (Develop together with CIEMAT group, publish in Chinese Physic C)**
  Ziyuan Li *et al.*, Chinese Physics C Vol. 41, No. 5 (2017) 056001

- **Template fitting on $1/\beta_{TOF}$ distribution to get the final antiproton counting**

Low rigidity challenge

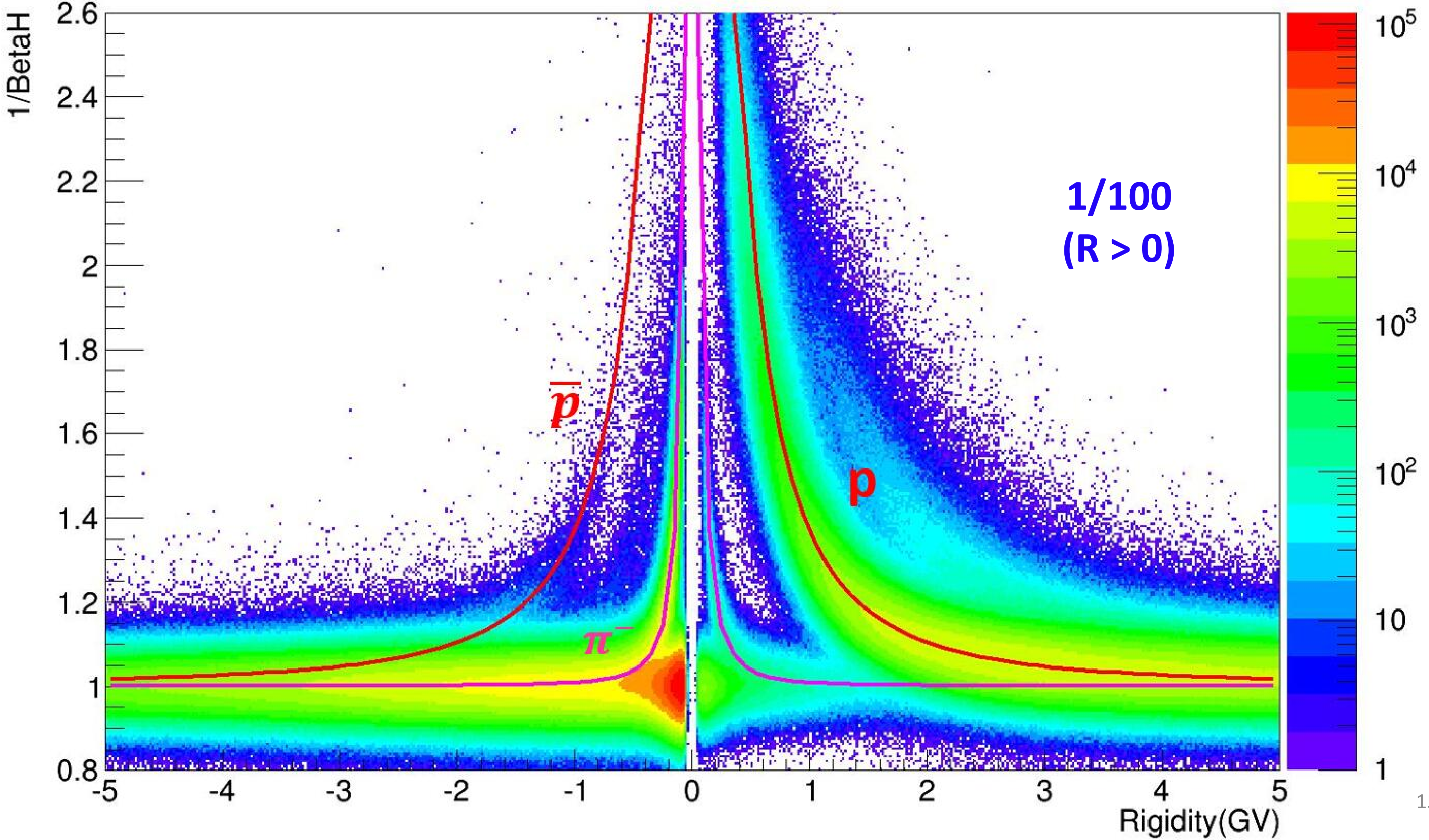

Interaction removal cuts

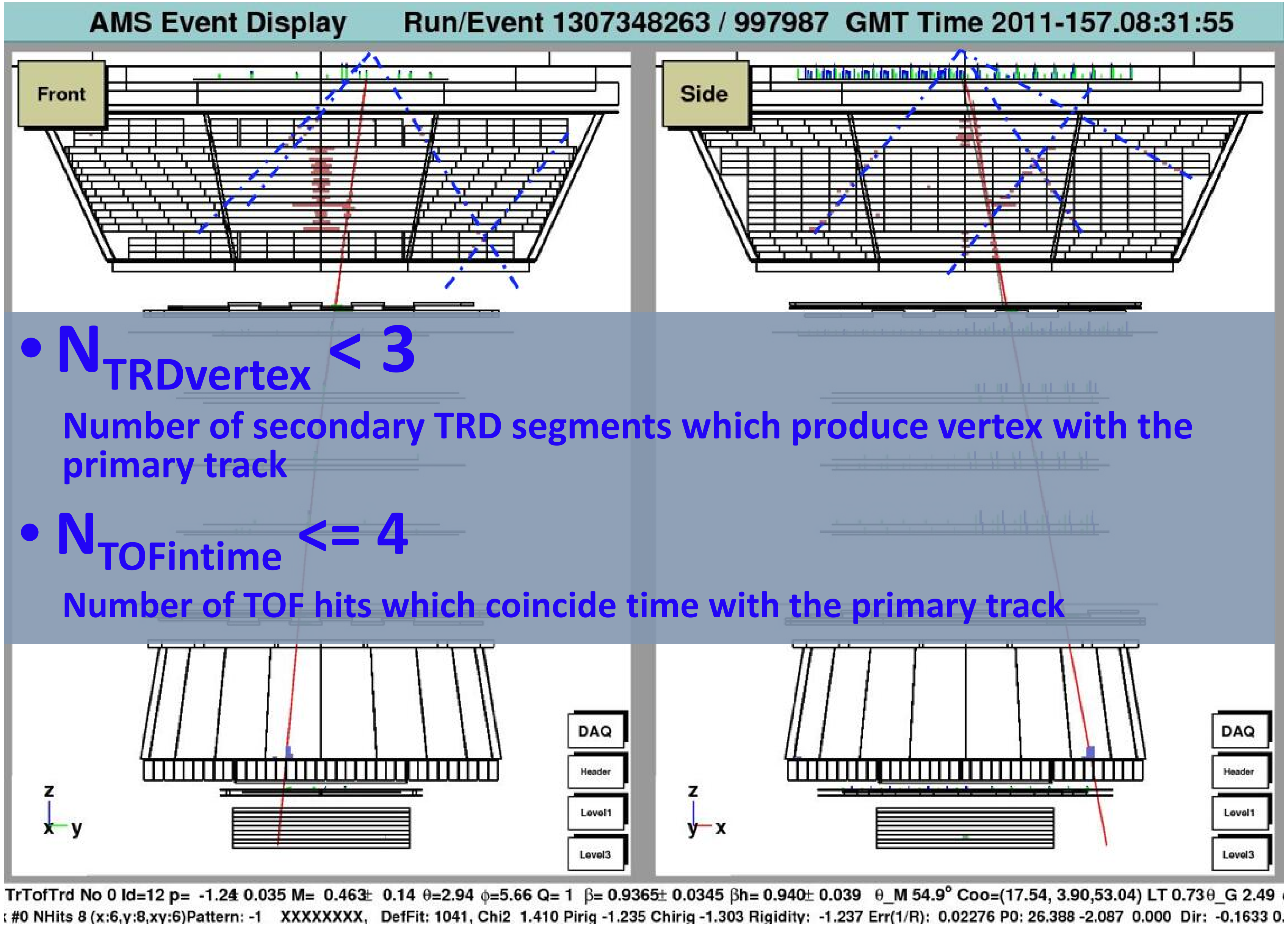

- $N_{TRDvertex} < 3$

  Number of secondary TRD segments which produce vertex with the primary track

- $N_{TOFintime} <= 4$

  Number of TOF hits which coincide time with the primary track

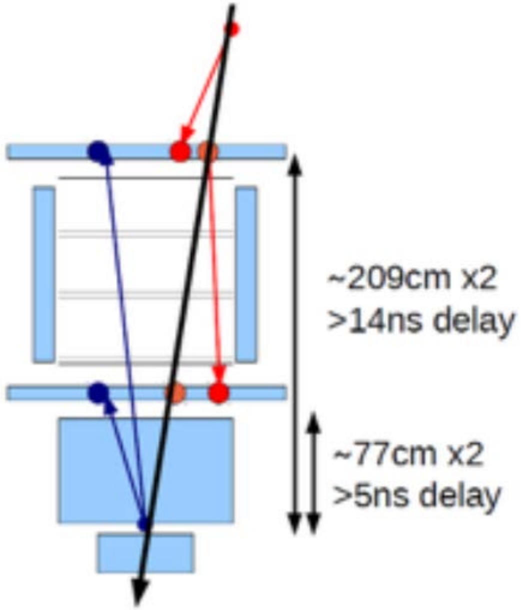

RICH Veto

Key parameters :

- **N_{pe} : Number of good reconstructed Photoelectrons corresponding to track (Remove noise p.e. produce by particle passing through PMT, remove noise p.e. produce by secondary particle)**

- **N_{exppe} : Expected number of Photoelectrons based on Electron assumption and Ray Tracing MC simulation**

RICH Veto : Idea

In Theory :

- $\beta_{threshold,AGL} = 0.95$
- The corresponding rigidity for $\bar{p}$ (p) with $\beta_{threshold,AGL}$ is 3 GV. Therefore below 3 GV, proton will not produce Cherenkov light when passing through AGL, while for electrons Cherenkov light emission is expected.

In Reality :

- Events with zero N_{pe} could be electrons where Cherenkov radiation was lost or absorbed due to one of possible effects like Rayleigh Scattering, total reflection in aerogel radiator, reflection or absorption on the mirror surface, falling into non-active area, light guide losses, etc.

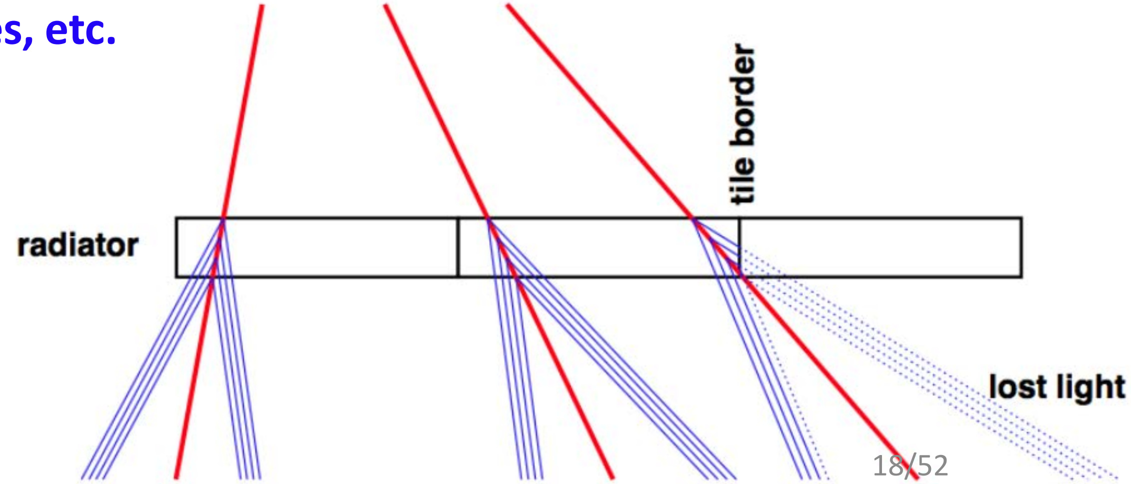

RICH Veto : N_{exppe}

Ray Tracing Integration Method:

- **Starting from the impact point of the particle on top of the radiator, a number of rays (NSTP) on a conical surface around the particle trajectory are propagated through the RICH to the detection plane. This procedure is repeated NSTL times along the particle path inside the radiator.**

$$N_{Exppe} = \int d\lambda d\phi dx \alpha \frac{q(\lambda)}{\lambda^2} \sin^2\theta_c(n,\beta) eff(\overrightarrow{r}, \overrightarrow{u}) f(l_r, l_f, l_g)$$

$$\sim \alpha \sum_{i=1}^{NL} \Delta\lambda_i \frac{q(\lambda_i)}{\lambda_i^2} \sin^2\theta_c(n,\beta) \Delta x$$

$$\sum_{i=1}^{NSTL} \Delta\phi \sum_{j=1}^{NSTP} eff(\overrightarrow{r_i}, \overrightarrow{u_j}) f(\overrightarrow{r_i}, \overrightarrow{u_j}).$$

RICH Veto : N_{exppe}

N_{exppe} distribution changes with rigidity for electron (left) and proton (right) in case N_{pe} = 0

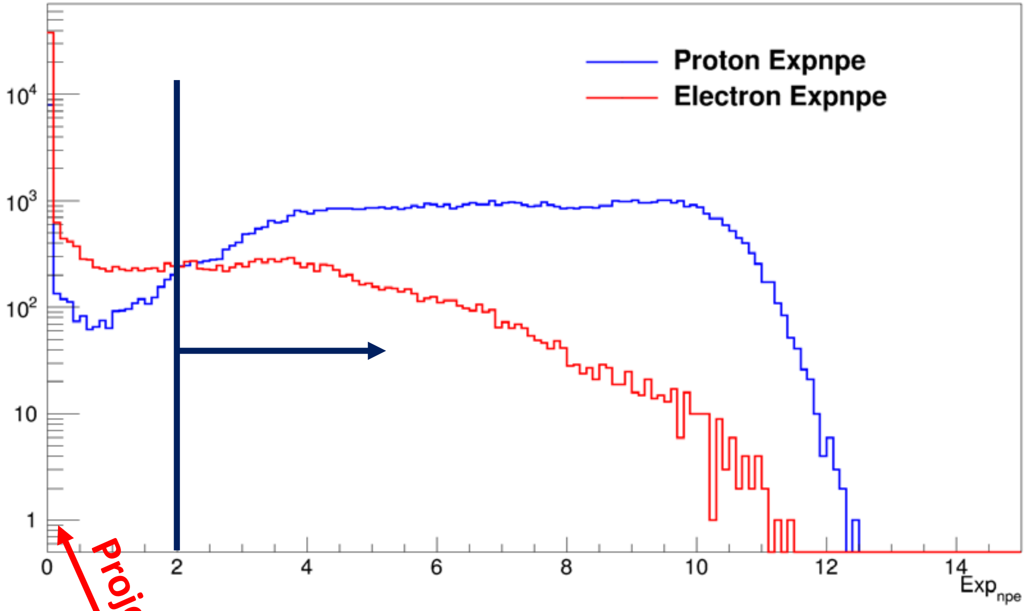

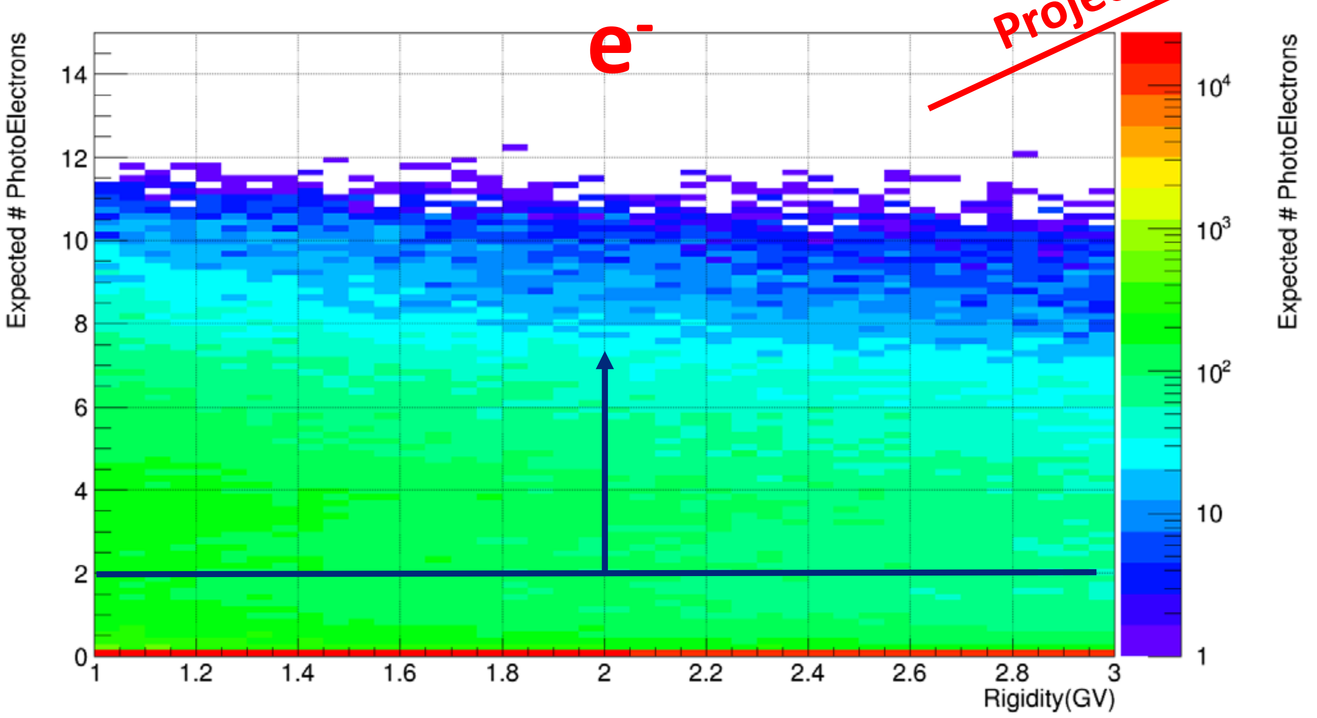

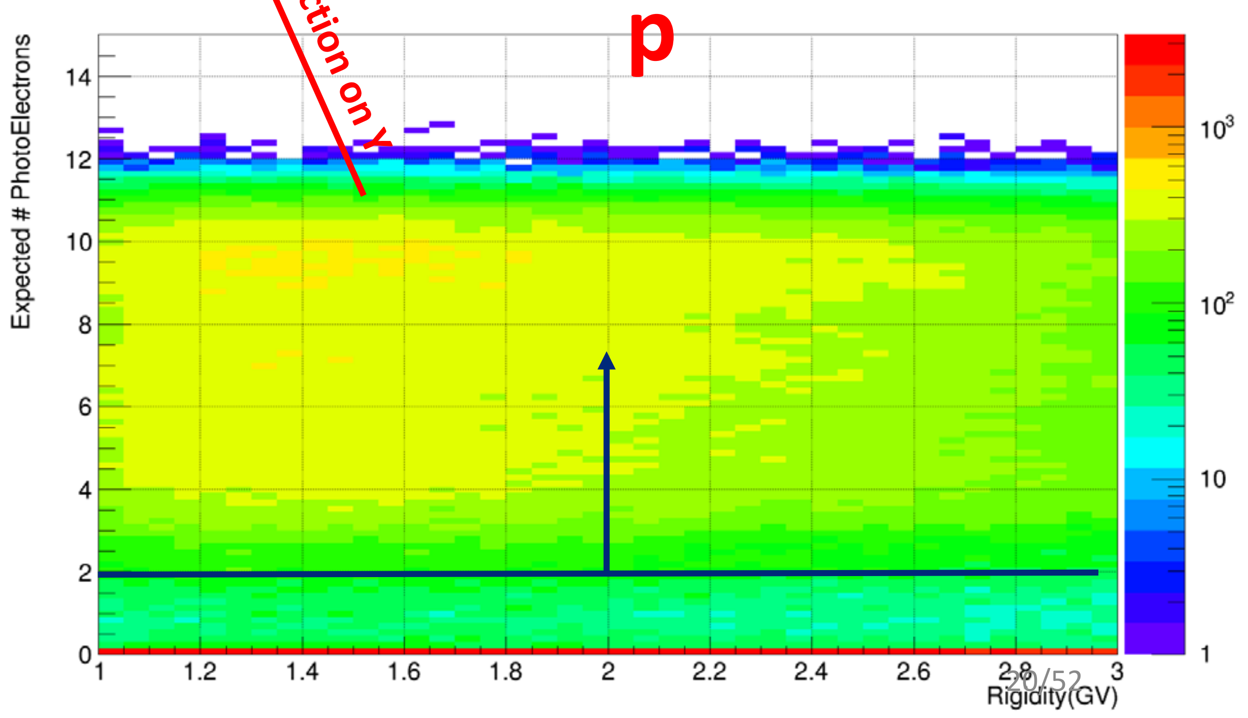

RICH Veto (R < 3 GV)

Efficiency : 20%

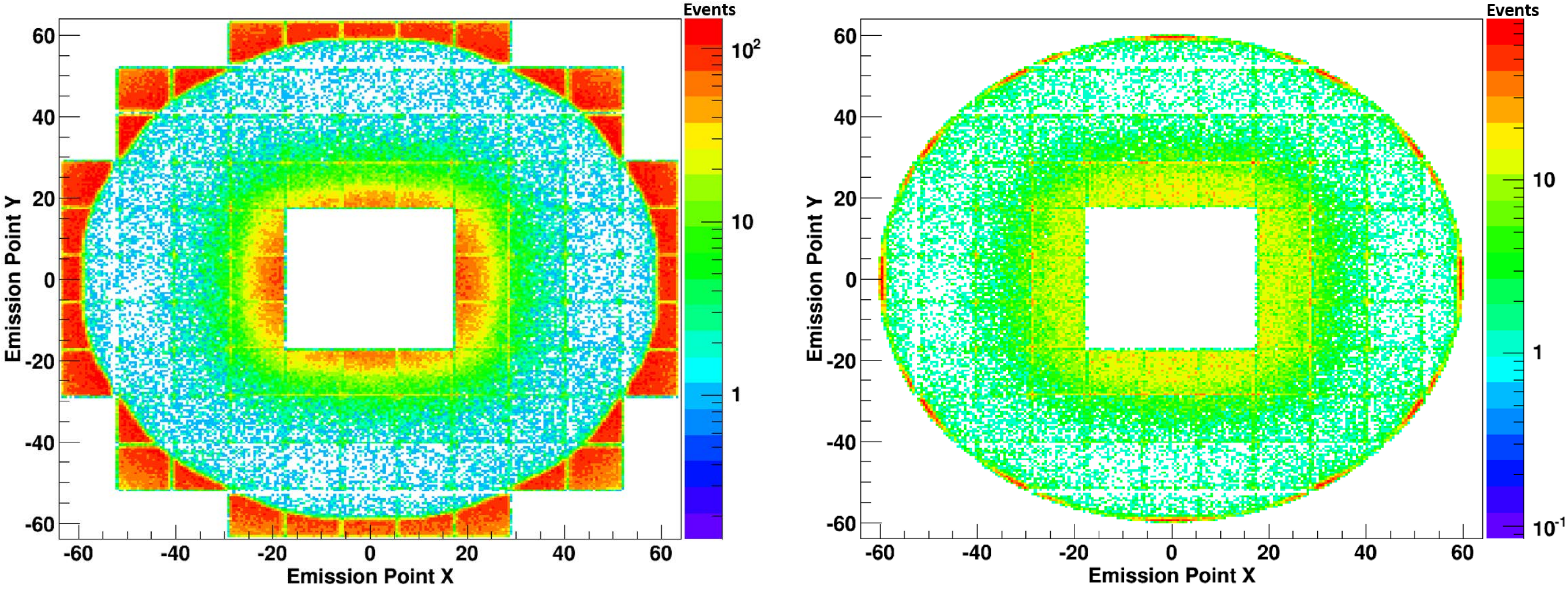

Simulated e^- : $N_{pe} = 0$

Simulated e^- : $N_{pe} = 0$ & $N_{exppe} > 2$

RICH Veto (R < 3 GV)

Efficiency : 88%

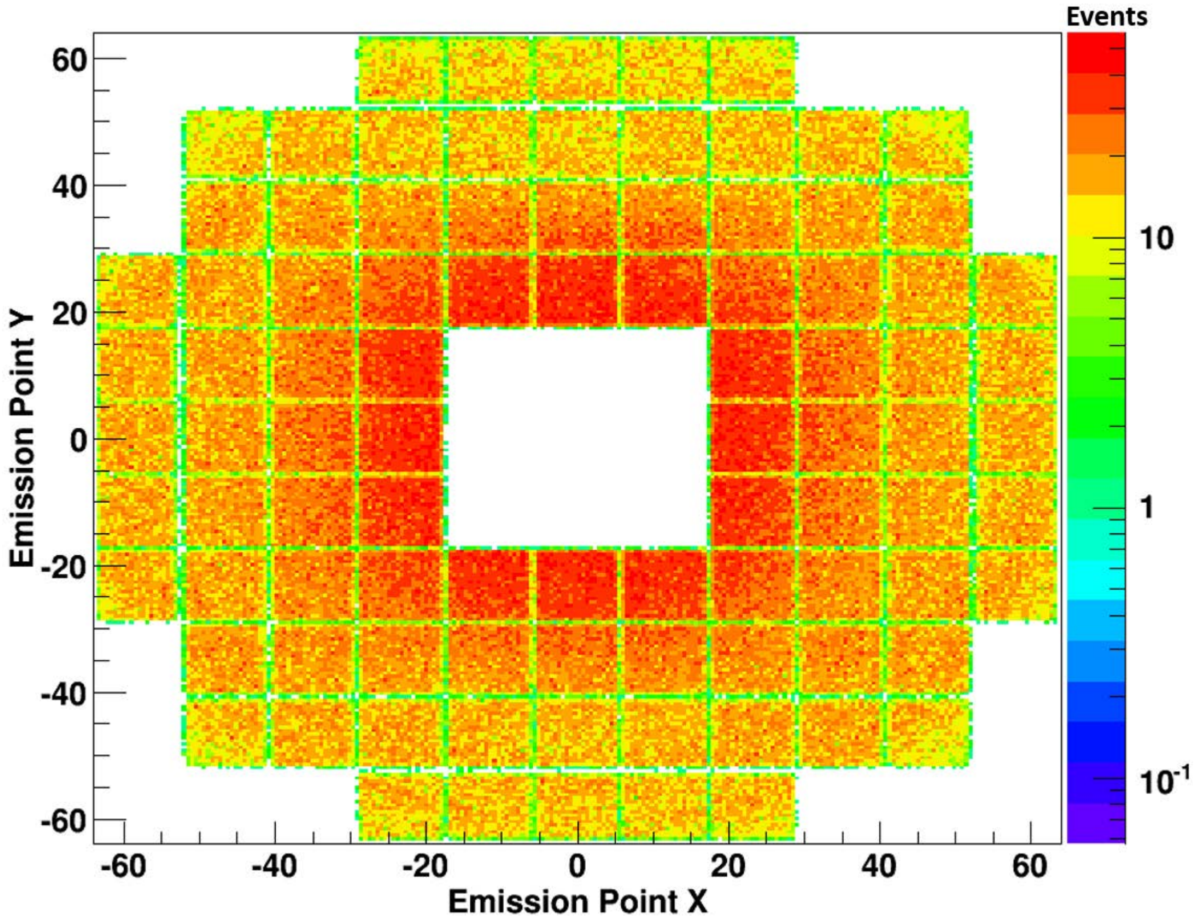

Simulated p : $N_{pe} = 0$

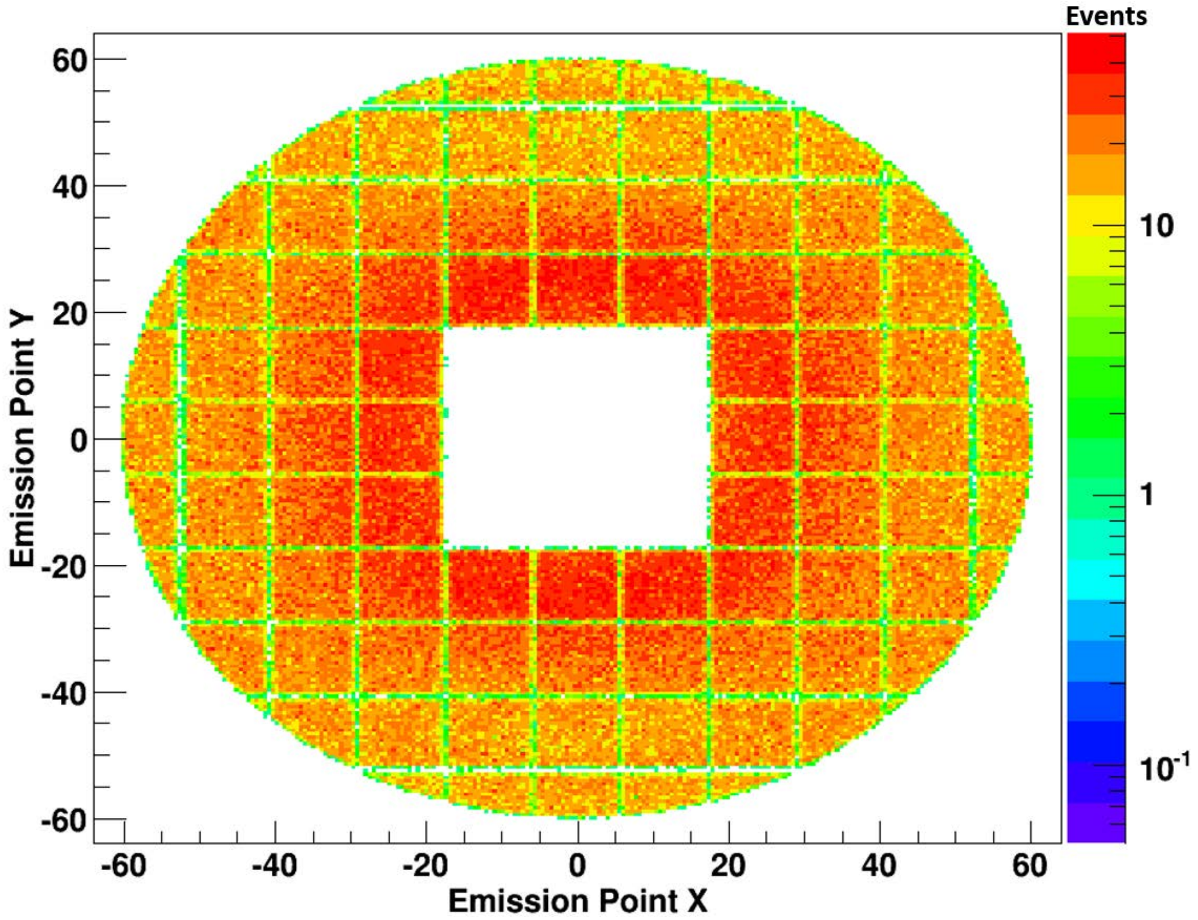

Simulated p : $N_{pe} = 0$ & $N_{exppe} > 2$

Mass ID by TOF

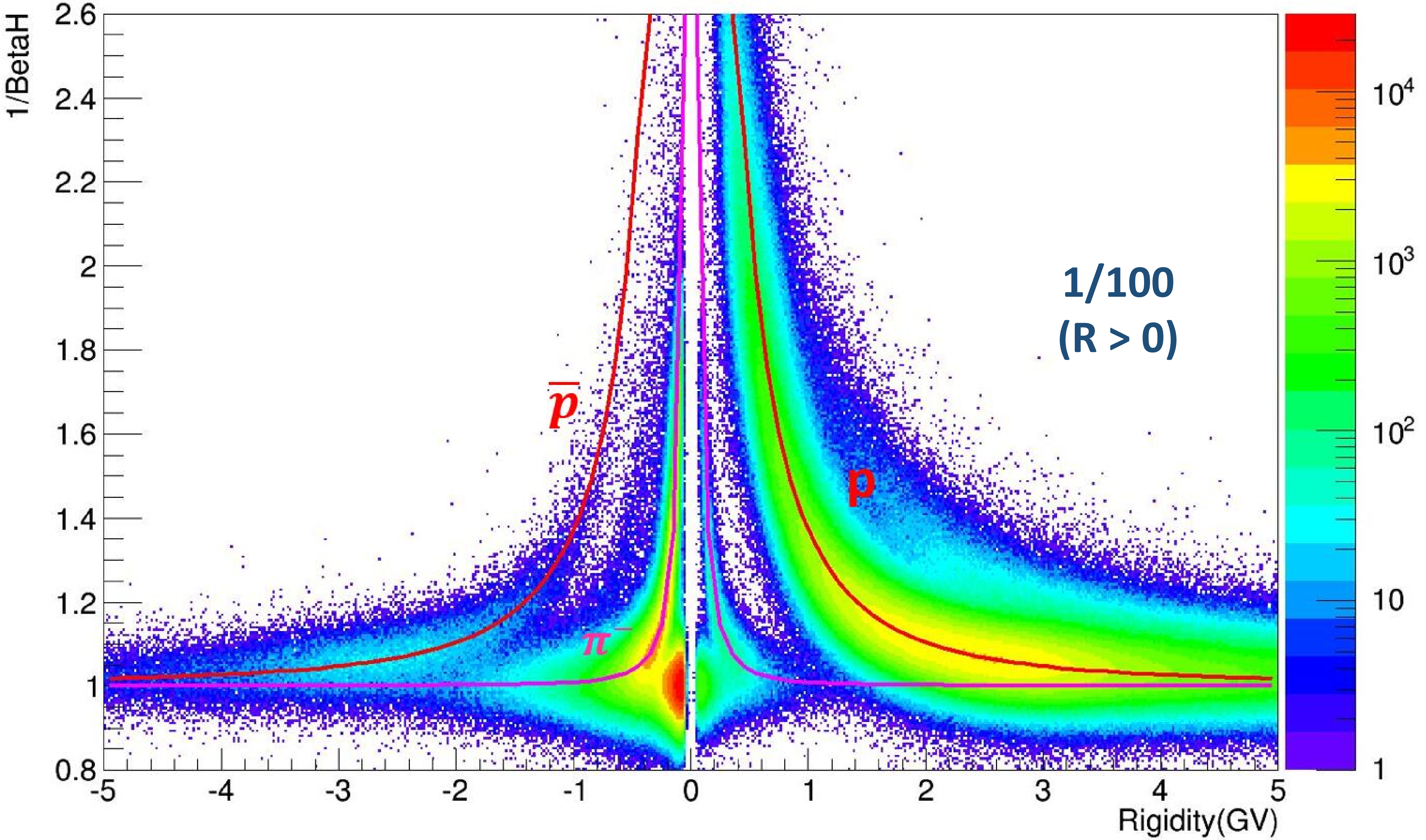

After RICH Veto : Cuts on N_{pe} == 0 and N_{exppe} > 2

Template Fit

- **Data sample to be fitted**
  - **negative events after rich veto selection**
- **Signal template**
  - **high statistic protons**
- **Background template**
  - **electrons and pions with RICH ring**

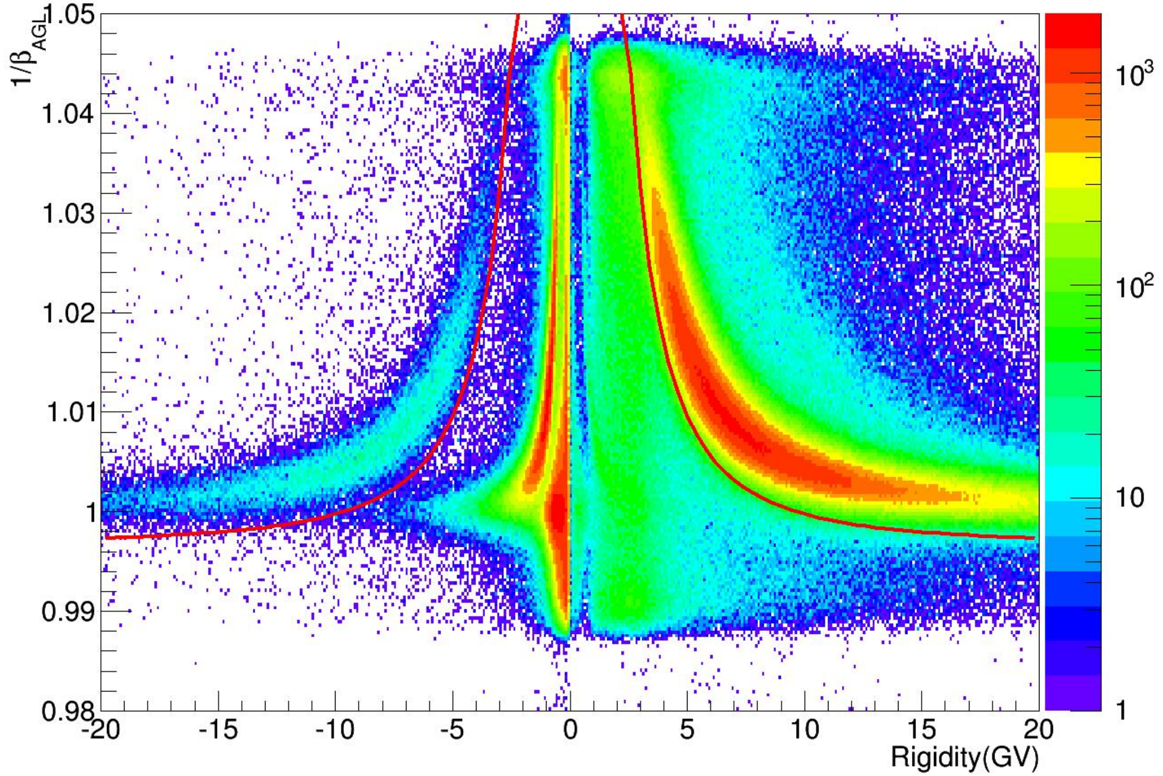

To make the fit rigidity independent, a normalization is done:

$$\Delta\beta_{ToF}/\sigma_{\beta^{-1}_{ToF}} = \left(\frac{1}{\beta_{ToF}} - \frac{1}{\beta_{rig,p}}\right)/\sigma_{\beta^{-1}_{ToF}}$$

$\beta_{rig,p}$ **is the theoretical value from rigidity measurement and assumption of proton mass.**

Template Fit example

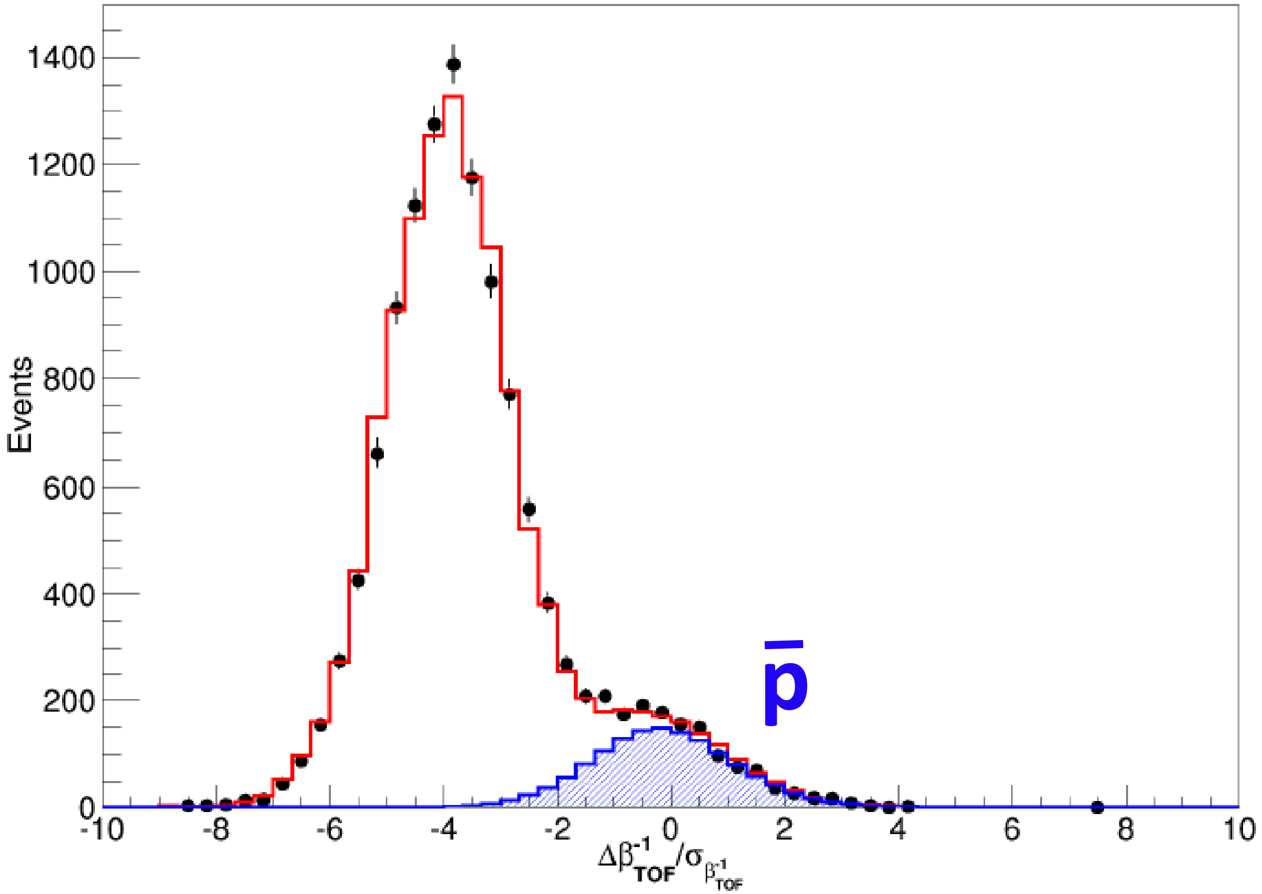

Before apply $N_{pe} = 0$ && $N_{Exppe} > 2$ cuts

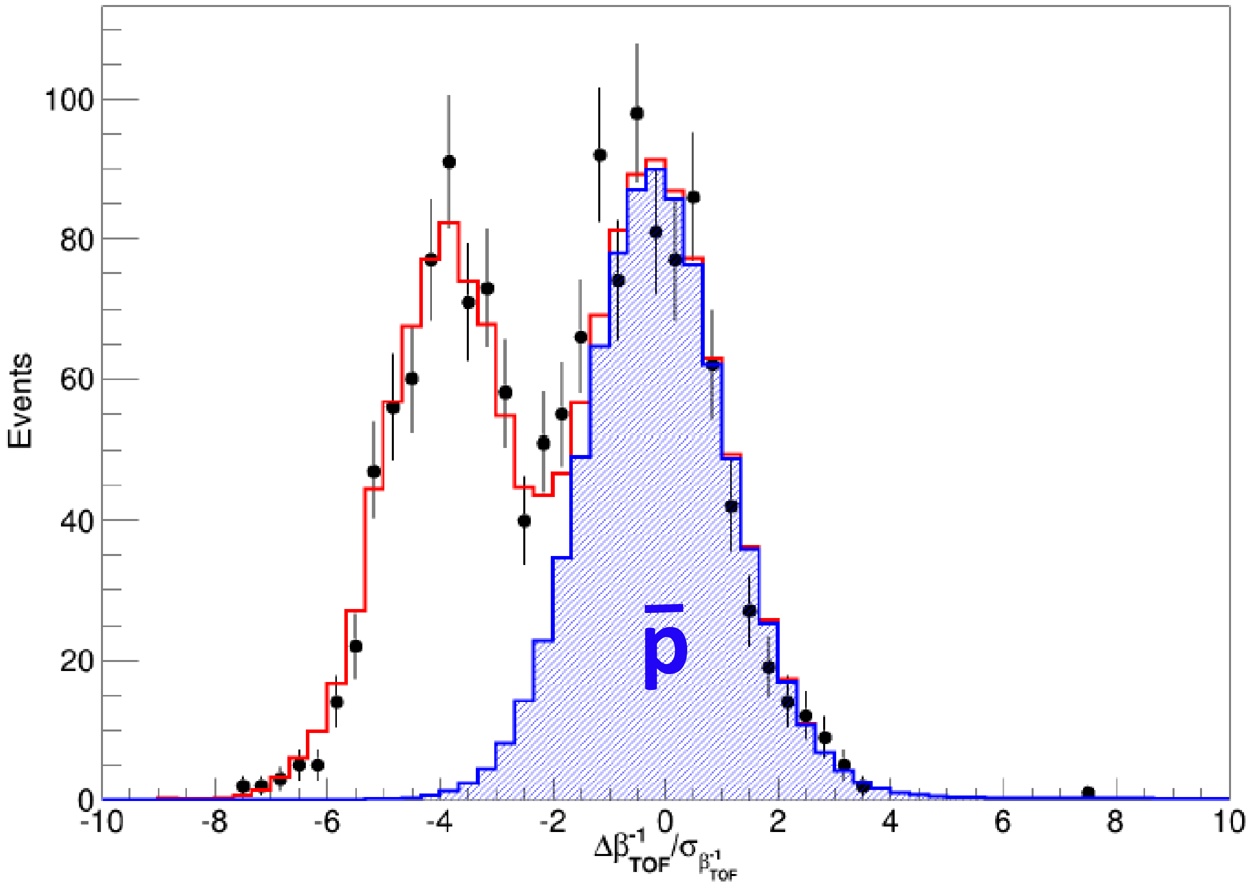

After apply $N_{pe} = 0$ && $N_{Exppe} > 2$ cuts

Middle rigidity region (3 - 50 GV)

Key analysis : TRD estimator

Goal : Maximize the statistics

- **Events within Ecal fiducial volume**

  Cut based analysis with TRD and Ecal BDT

- **Events outside Ecal fiducial volume**

  Template fit on TRD estimator

Particle ID in Middle rigidity region

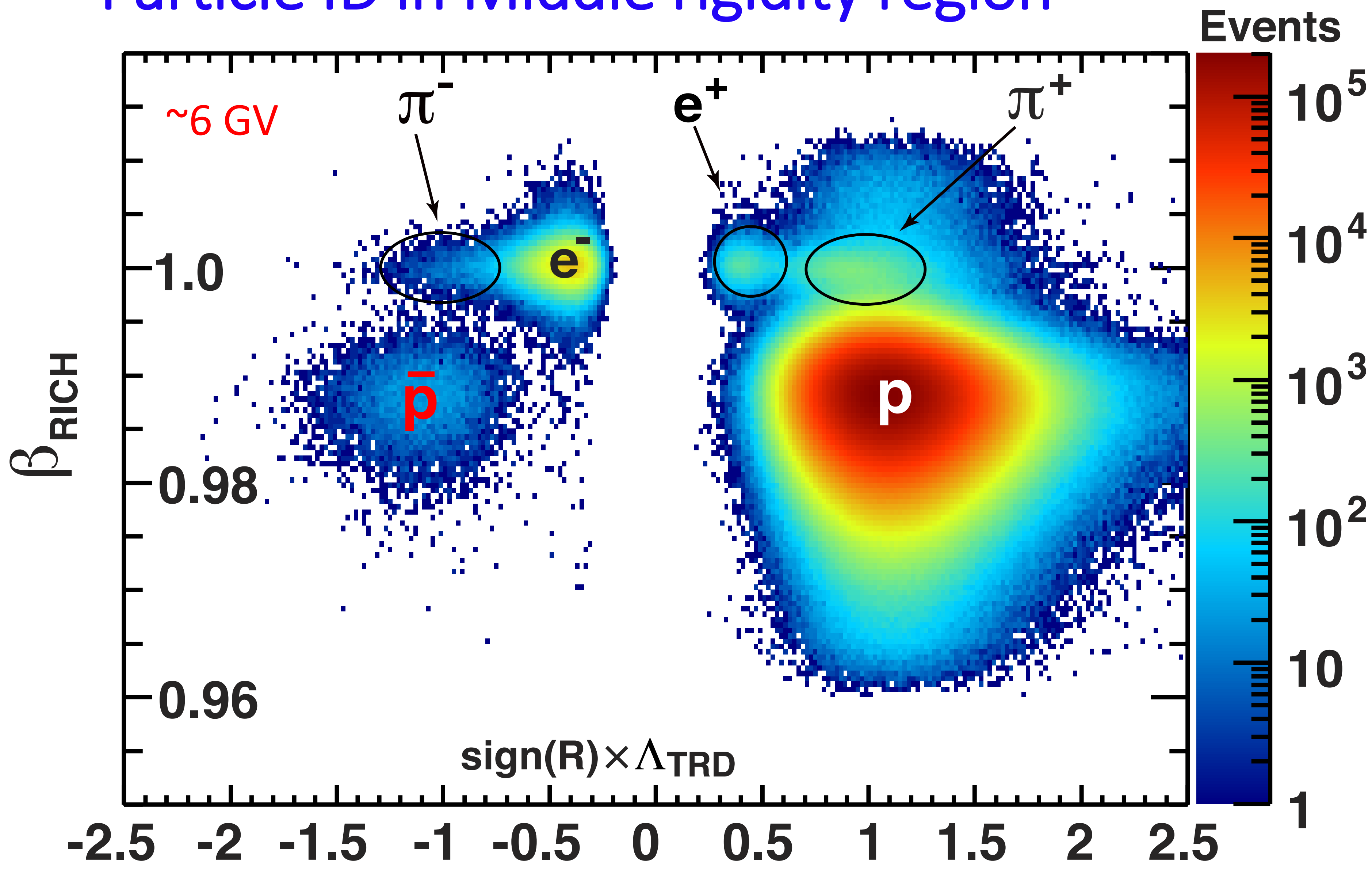

Antiproton signal is well separated from the backgrounds

RICH Beta Band

AGL

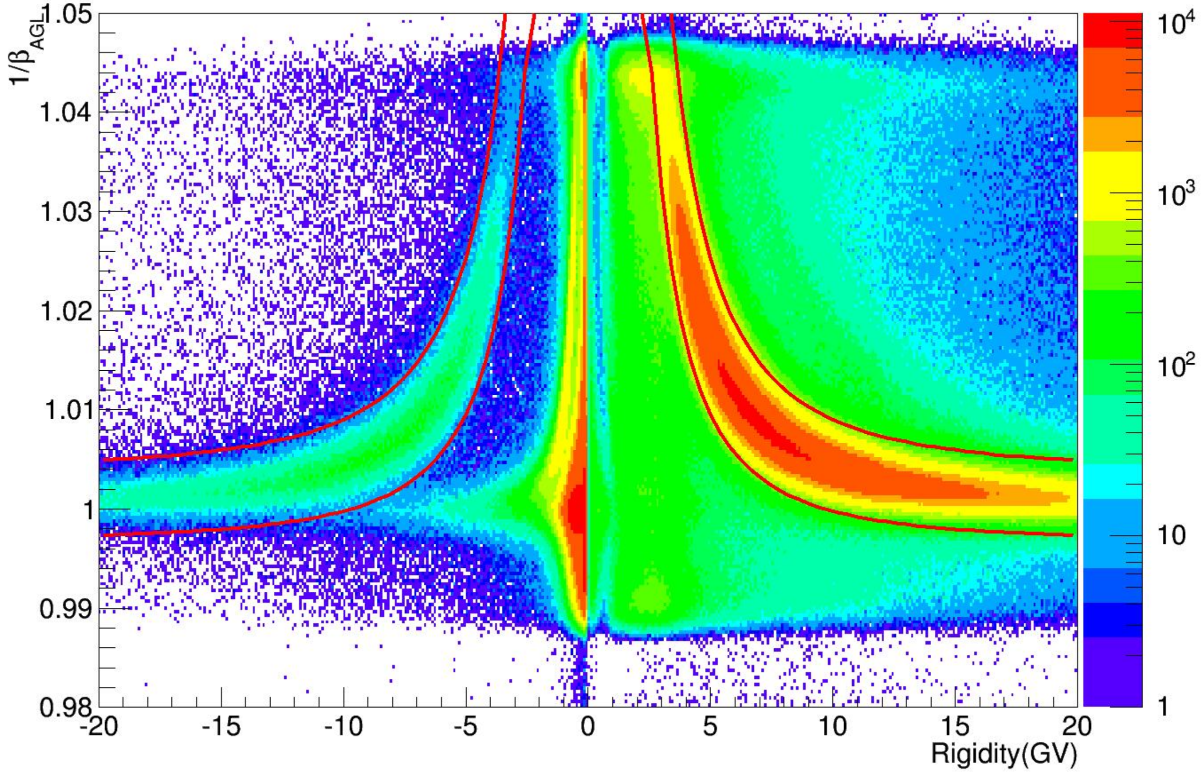

NaF

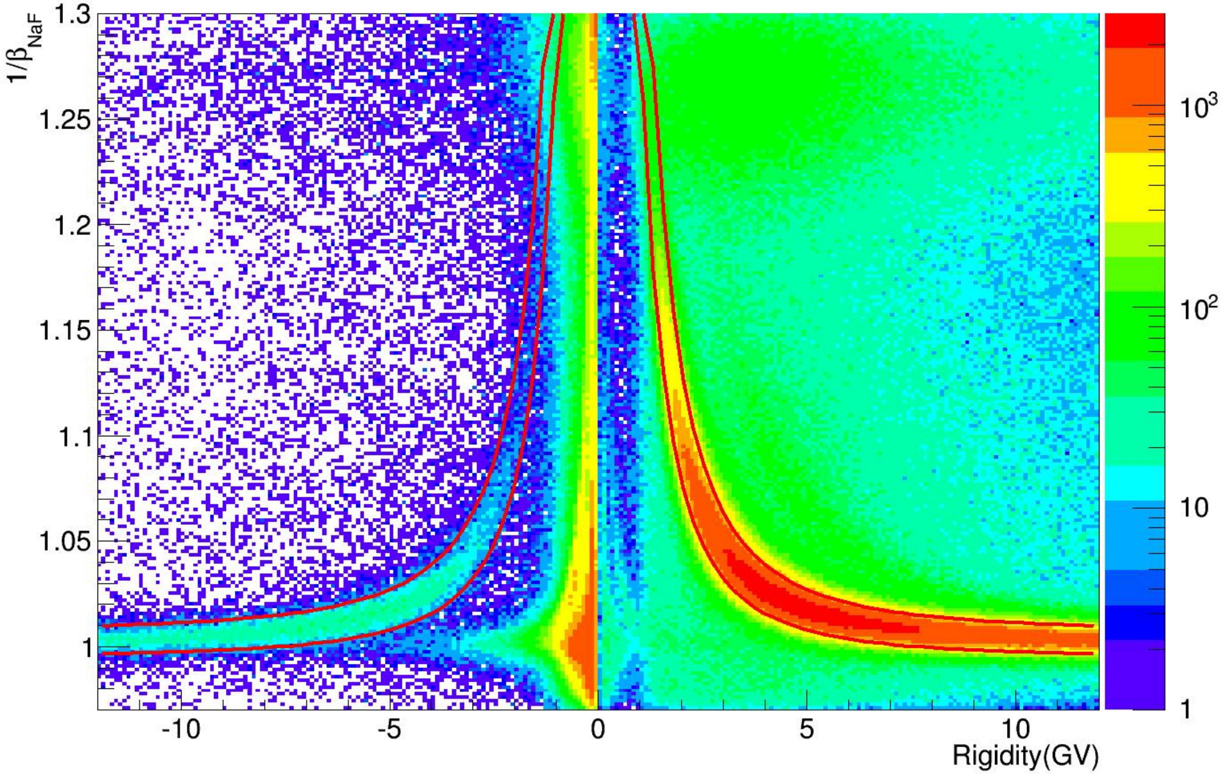

$$f(R) = (1 \pm \sigma_{beta}) \cdot \sqrt{(1 \pm \sigma_{rig}) \cdot (\frac{m_p}{R})^2 + 1}$$

Require events to locate within RICH beta band

Template fit on TRD estimator

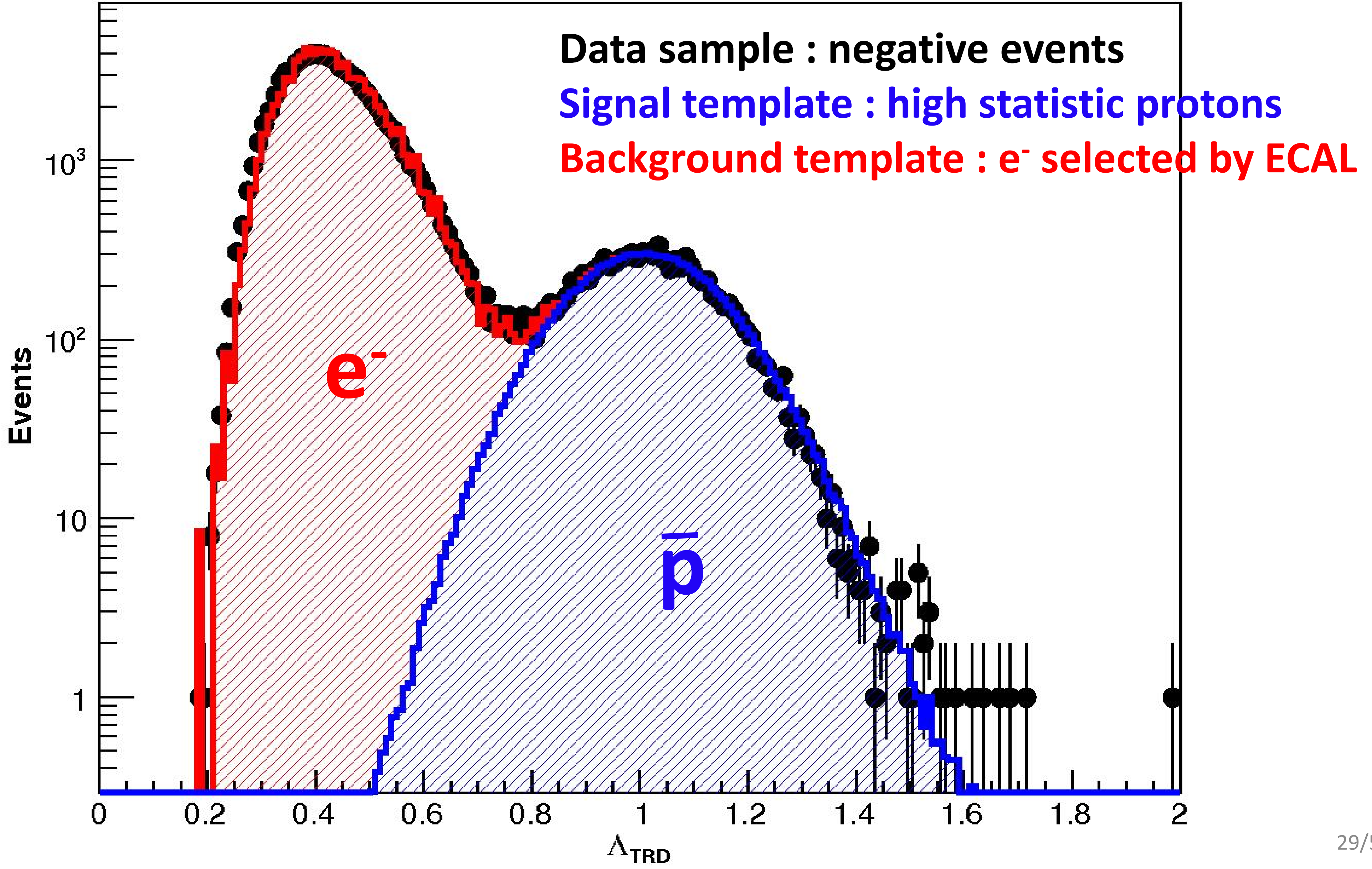

High rigidity region (> 50 GV)

Key analysis : Charge Confusion Estimator

Goal : Keep charge confusion (CC) under control

- **High energy antiprotons can only separate from protons with tracker, therefore tracker relative variables are used to construct Charge Confusion Estimator**

- **Template fit on Charge Confusion Estimator to get antiproton counting**

Tracker Relative Variables for Charge Confusion Estimator

Variables are basically rigidity independent after normalization

- **$R_{innL1}/R_{innL9} - 1$**
  - **Rigidity mismatch for InnL1 and InnL9 pattern**
- **$R_{FS}/R_{inn} - 1$**
  - **Rigidity mismatch for Full Span and Inner pattern**
- **$Log_{10}(Chi2Y)$**
  - **Tracker Fitting χ^2 on Y axis**
- **$Chi2Y_{FS} - Chi2Y_{inn}$**
  - **χ^2 mismatch for Full Span and Inner pattern**
- **$ResidualY_{L1}$**
  - **The residual for L1 hit position and Inner extrapolate L1 position**
- **$ResidualY_{L9}$**
  - **The residual for L9 hit position and Inner extrapolate L9 position**

Charge Confusion Estimator

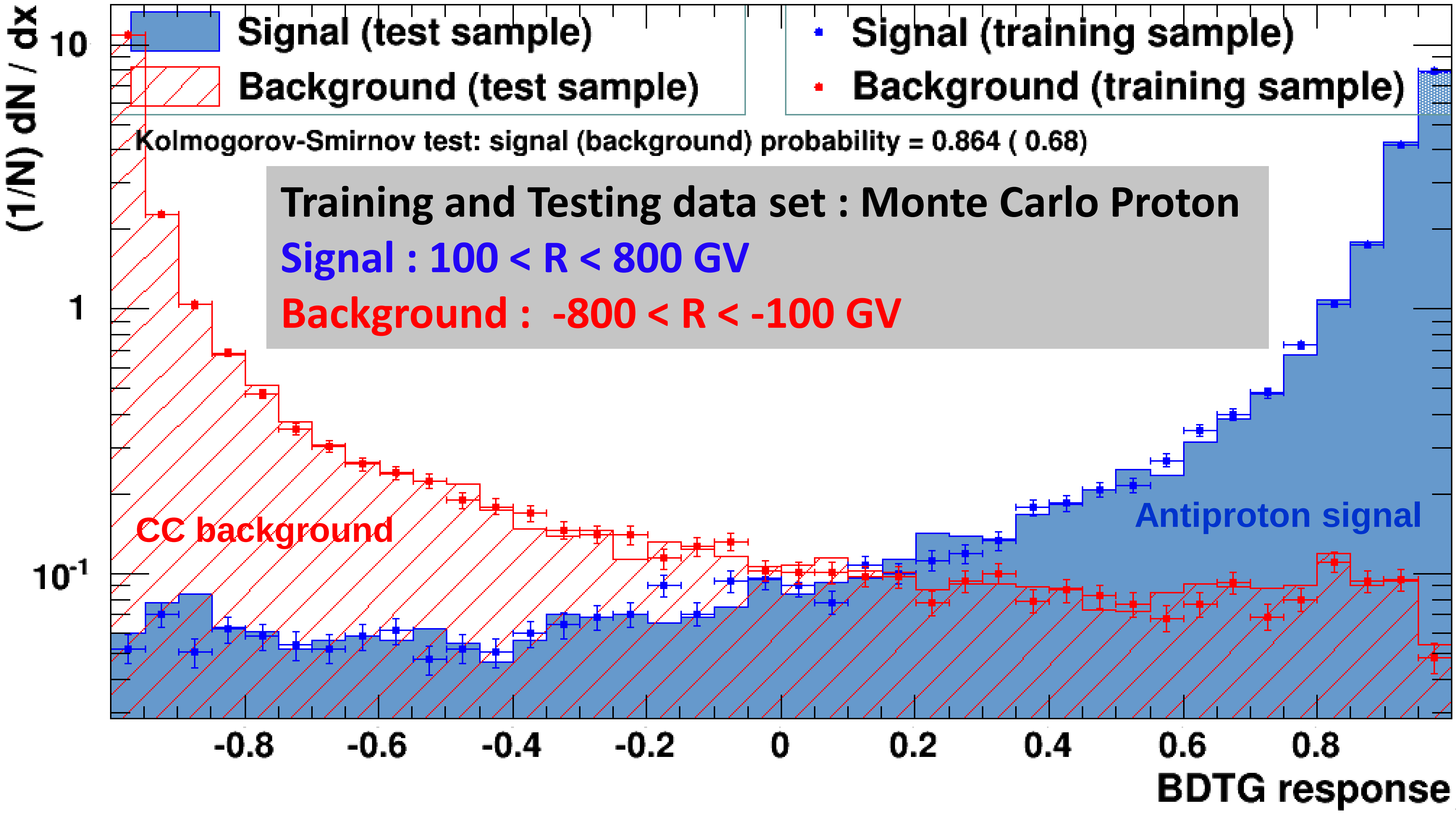

Template fit on Charge Confusion Estimator

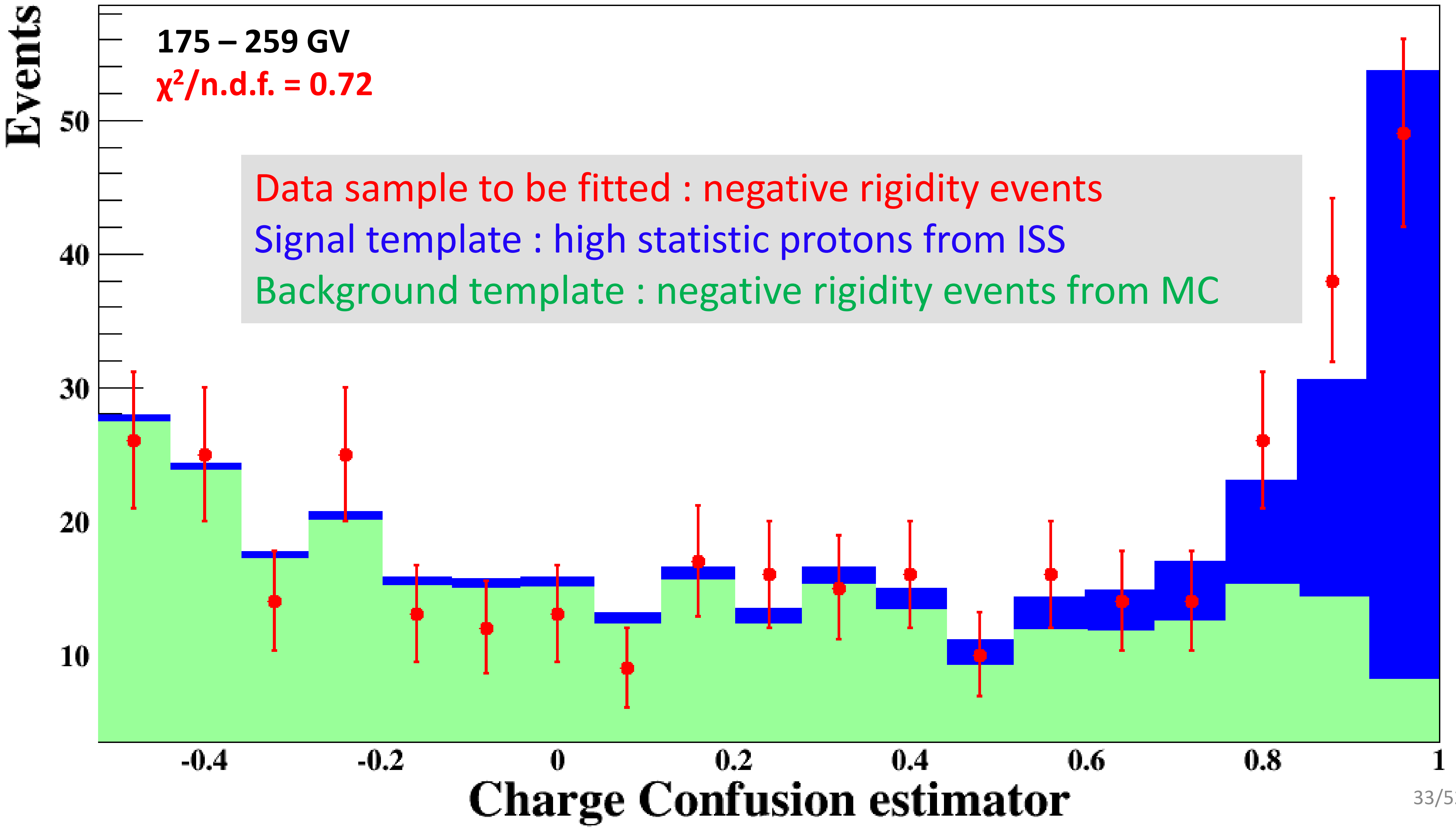

Acceptance Correction

Flux

$$\Phi_i^{\bar{p}} = \frac{N_i^{\bar{p}}}{A_i^{\bar{p}} T_i \Delta R_i}$$

Ratio

$$\left(\frac{\bar{p}}{p}\right)_i = \frac{\Phi_i^{\bar{p}}}{\Phi_i^{p}} = \frac{N_i^{\bar{p}}}{N_i^{p}} \cdot \frac{A_i^{p}}{A_i^{\bar{p}}}$$

$$\frac{A_i^{p}}{A_i^{\bar{p}}} = \left(\frac{N_{sel}^{p}}{N_{gen}^{p}}\right)_i \cdot \left(\frac{N_{gen}^{\bar{p}}}{N_{sel}^{\bar{p}}}\right)_i$$

The acceptance for p and $\bar{p}$ is not the same, mainly due to the different cross section of p+C and $\bar{p}$+C

- **Monte Carlo simulation approach to calculate acceptance.**
- **N_{gen} events generated, N_{sel} events pass the same selection as ISS data.**

Unfolding : Folded Acceptance

$$(\frac{\bar{p}}{p})_i = \frac{\Phi_i^{\bar{p}}}{\Phi_i^{p}} = \frac{N_i^{\bar{p}}}{N_i^{p}} \cdot \frac{A_i^{p}}{A_i^{\bar{p}}} = \frac{\widetilde{N}_i^{\bar{p}}}{\widetilde{N}_i^{p}} \cdot \frac{\widetilde{A}_i^{p}}{\widetilde{A}_i^{\bar{p}}}$$

- **Iteration method (Step i):**
  - **Reweight MC proton by proton flux : ϕ^p**
  - **Reweight MC antiproton by $\phi^p \times (\bar{p}/p)_{i-1}$**
  - **Calculate the acceptance correction factor $(A_p/A_{\bar{p}})_i$**
  - **Apply the correction and update the antiproton ratio $(\bar{p}/p)_i$**

i→i+1

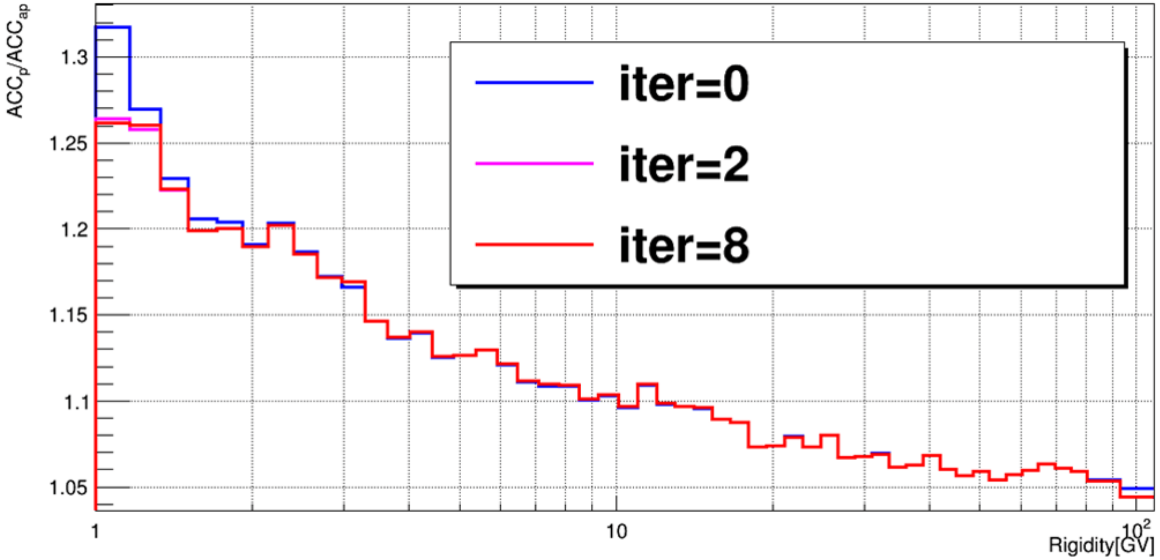

Systematic Error

- **Charge Confusion**
  - **Scan fit range to change template shape**
- **Template Fluctuation**
  - **At high energy, fluctuate charge confusion template**
  - **At Middle and low energy, fluctuate background template**
- **Acceptance**
  - **Cross section ratio uncertainty**
- **Selection**
  - **Vary cut values of variables**
- **Rigidity Scale**
  - **Tracker misalignment**

Systematic Error : Charge Confusion

- **Scan fit range to change template shape**
- **Fit the result by Gaussian function and assign the sigma as systematic error cause by Charge Confusion.**

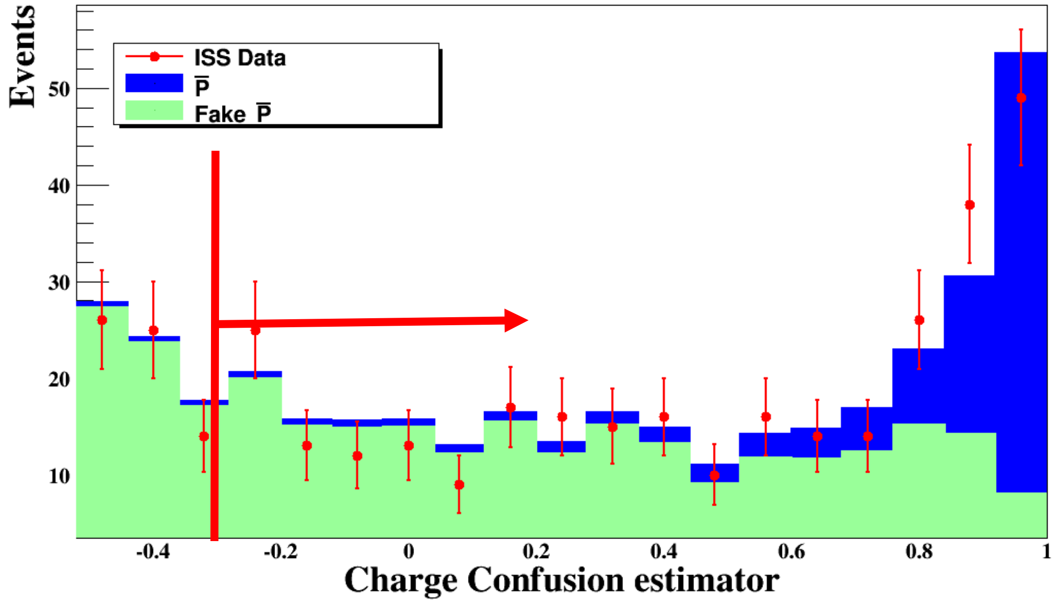

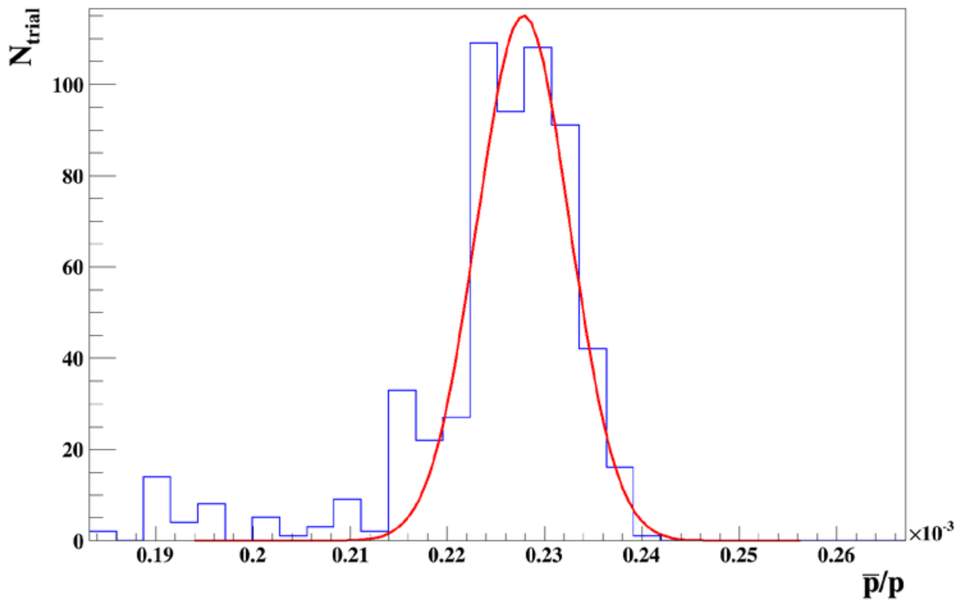

Systematic Error : Template Fluctuation

- **Fluctuate background template within statistical error**

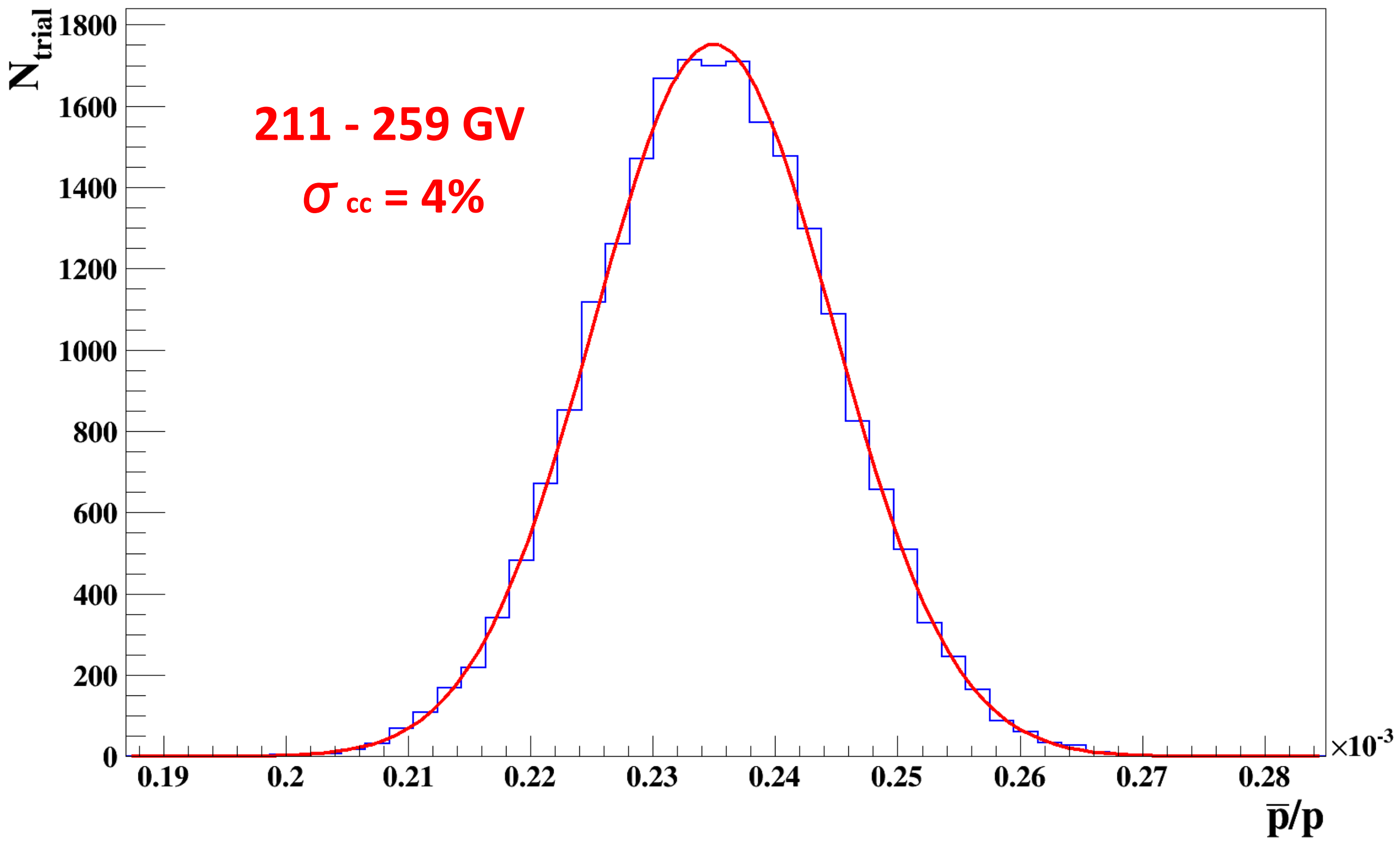

Systematic Error : Acceptance

- **By changing proton MC inelastic cross section ± 10% we can know how much influence on acceptance correction ratio.**

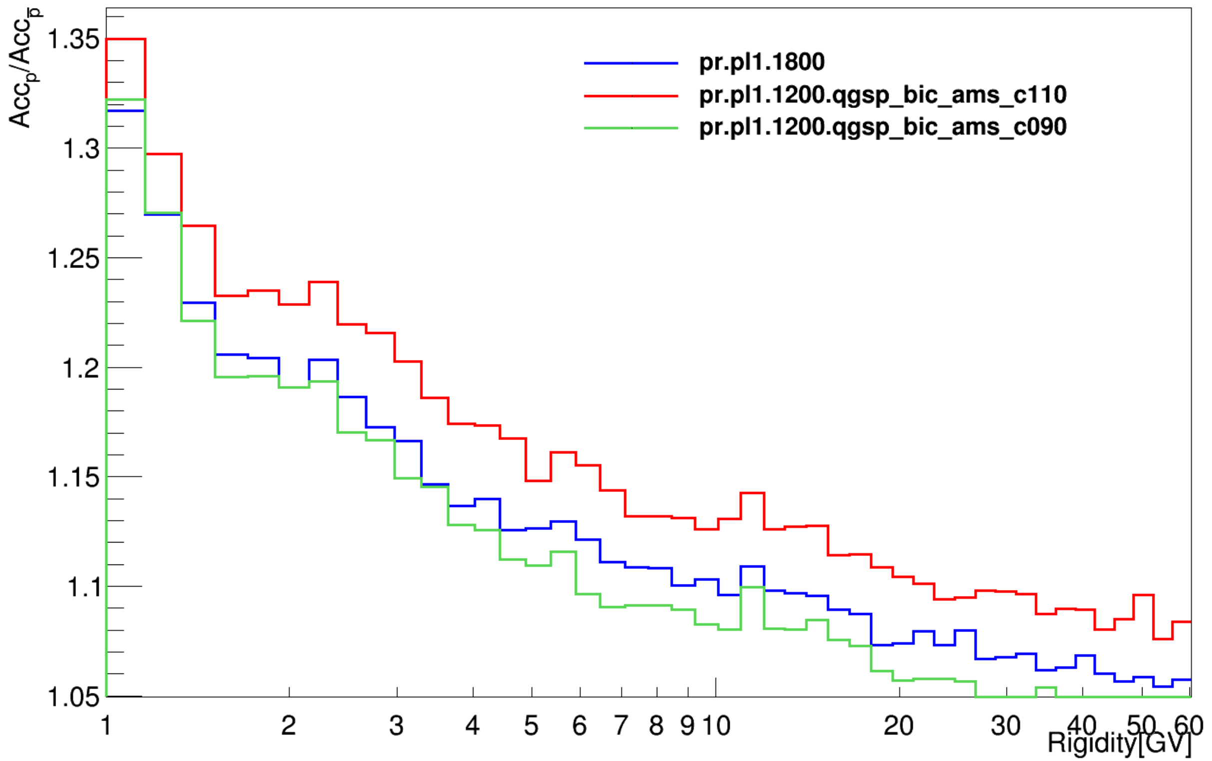

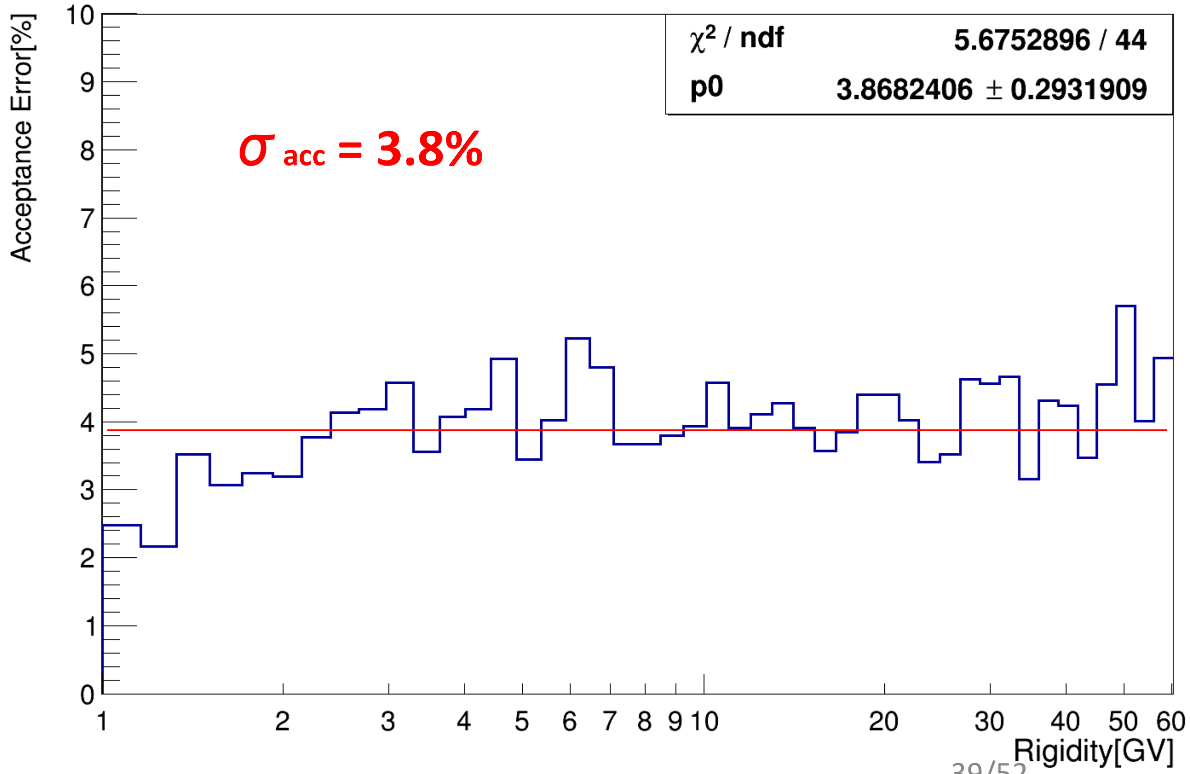

Systematic Error : Selection

- **Vary cut values of the variables that are not sensitive to charge confusion.**
- **The width subtracted by pure fluctuation gives the systematic error of selection dependence.**

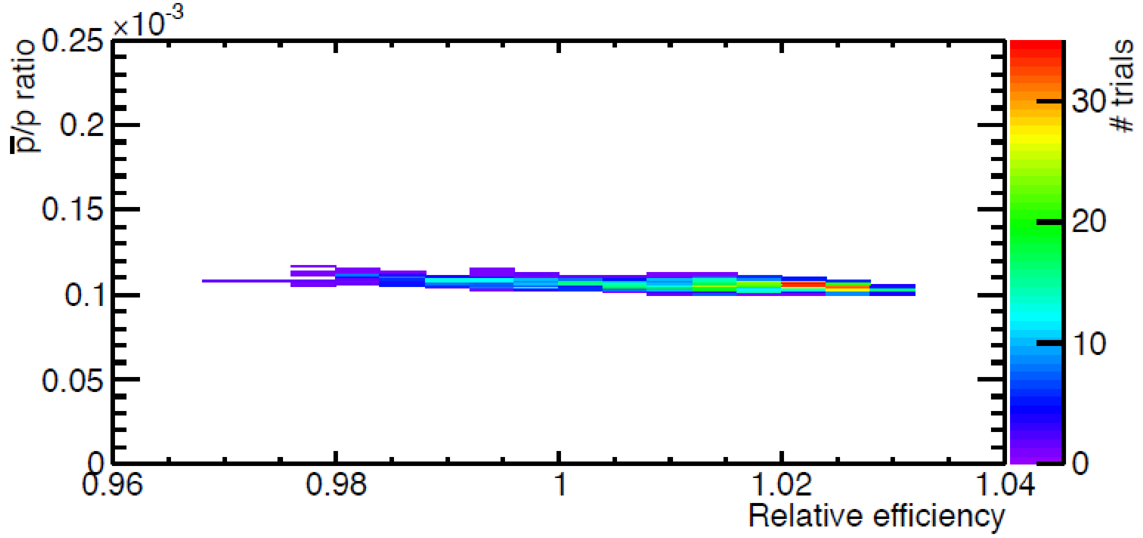

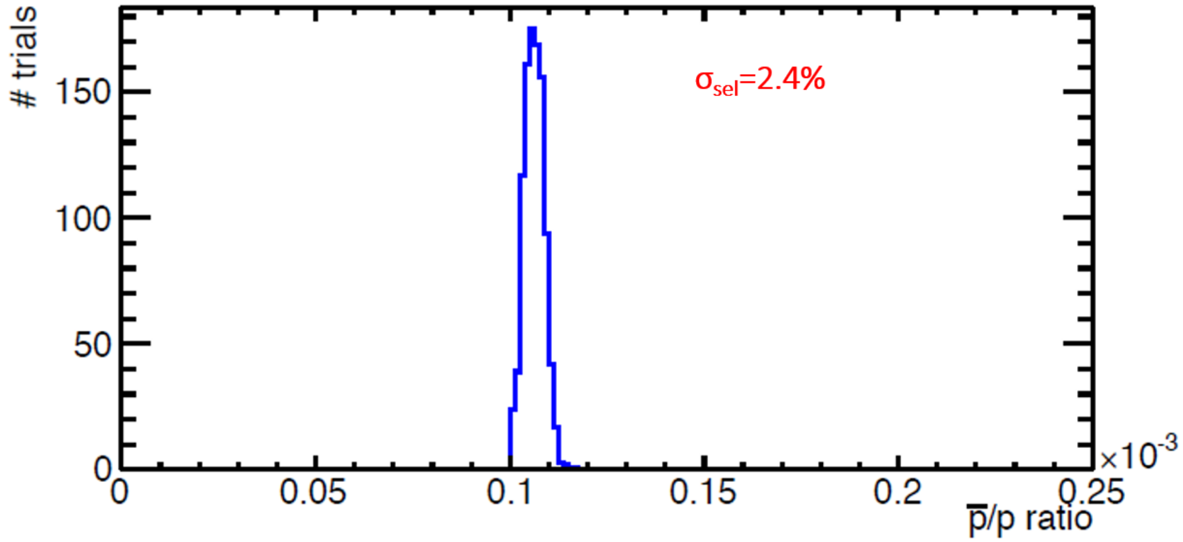

Systematic Error : Rigidity Scale

- **The error on the absolute rigidity scale due to the residual misalignment of the tracker planes was estimated by comparing the electron/positron energy measured in the ECAL with the momentum in the tracker. It was estimated to be 1/26 TV^{-1}.**

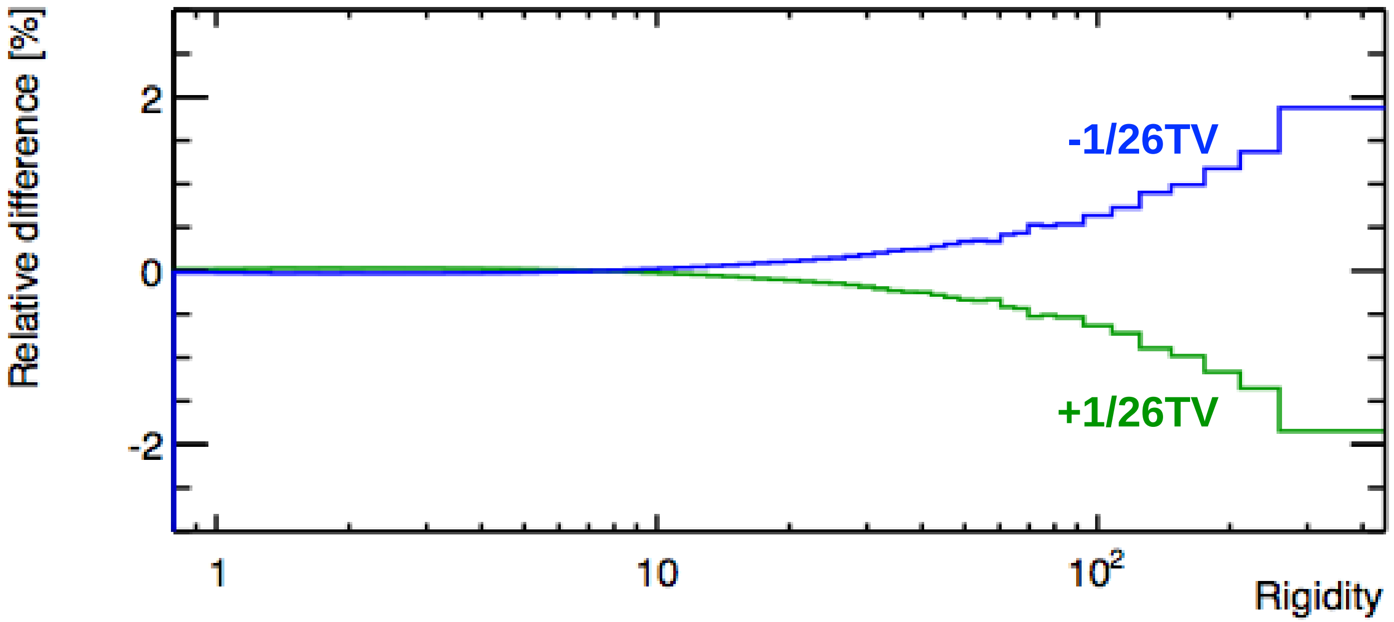

Error Breakdown : Systematic Error

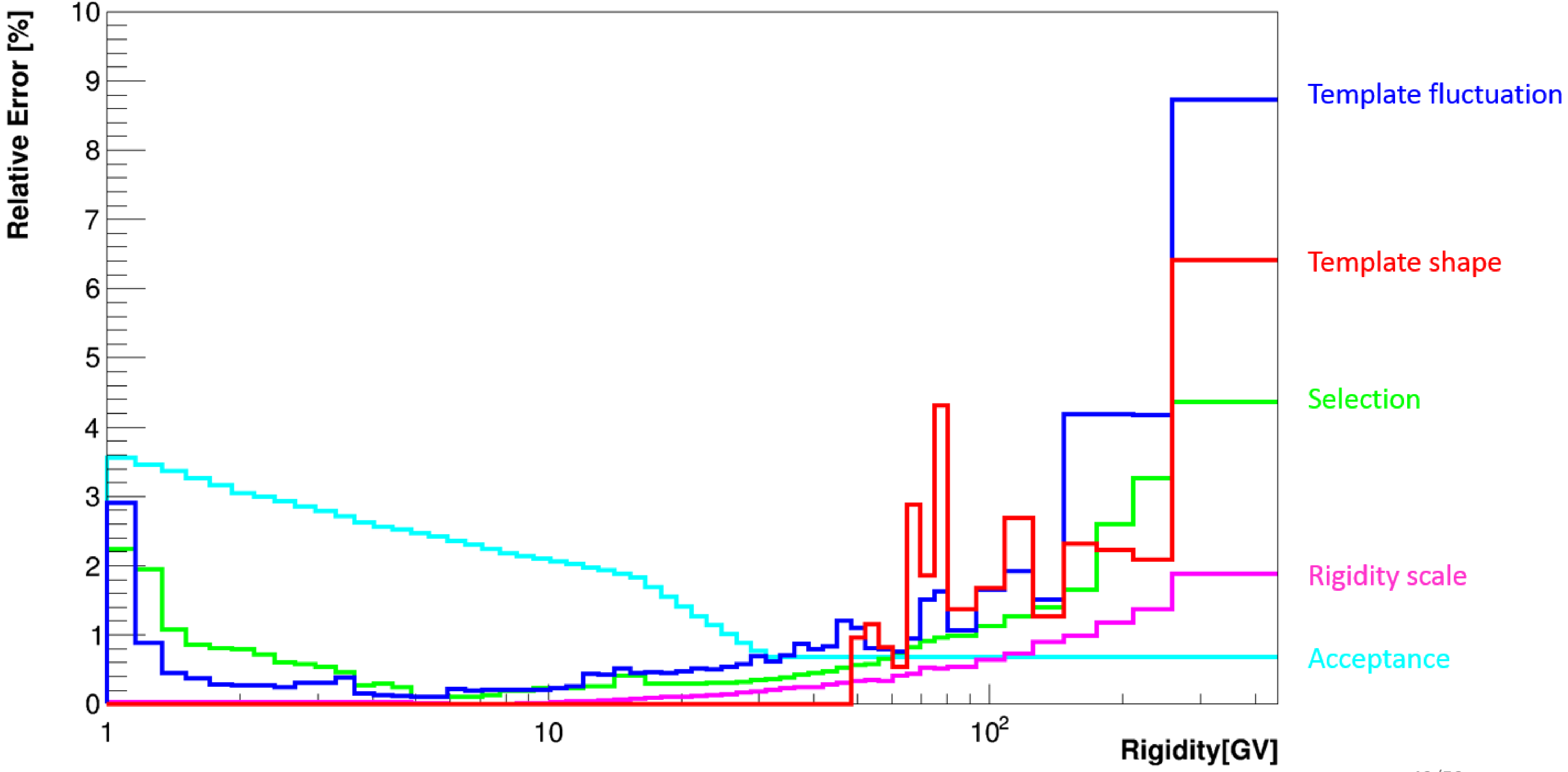

Error Breakdown : Total Error

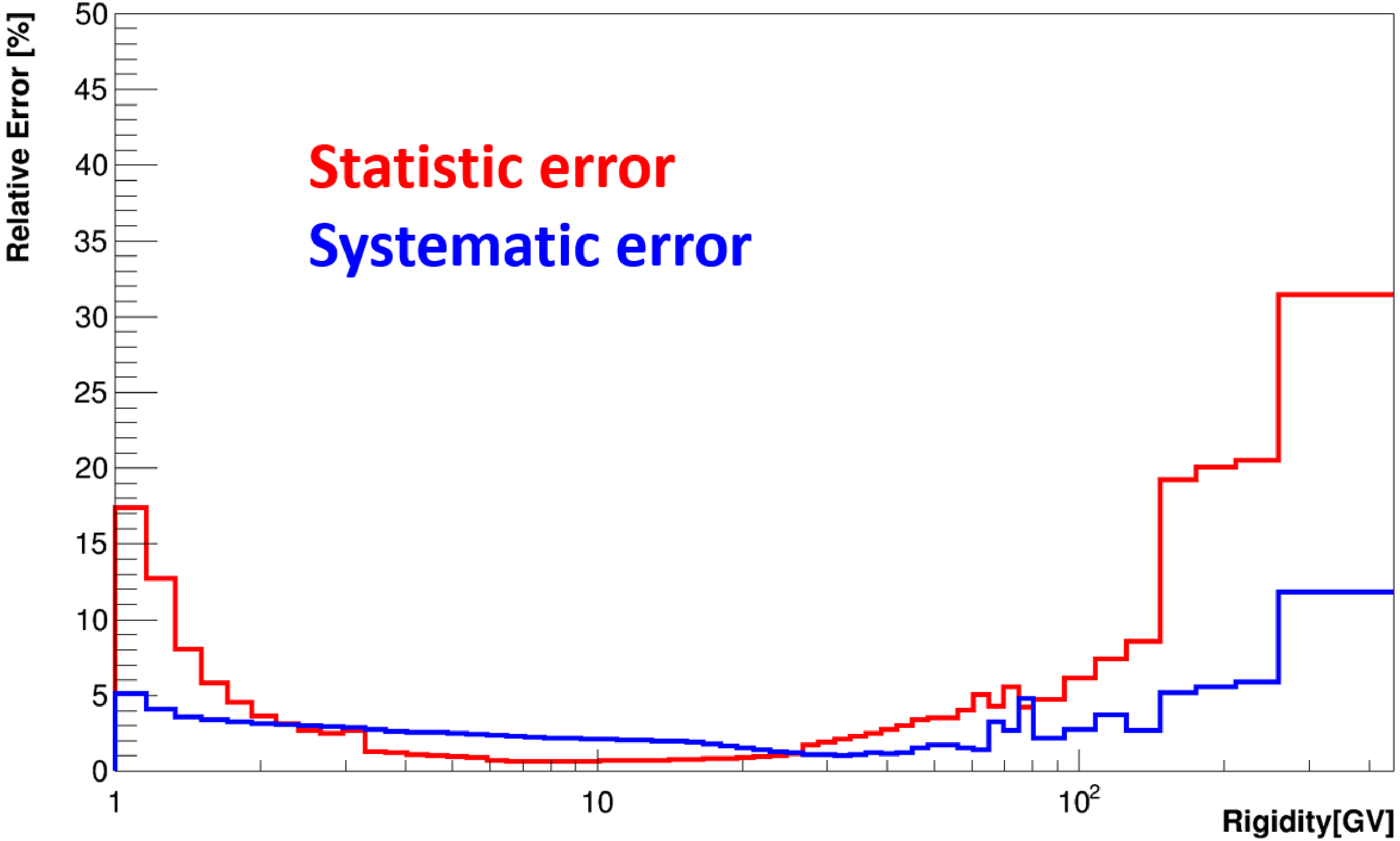

Antiproton/proton flux ratio

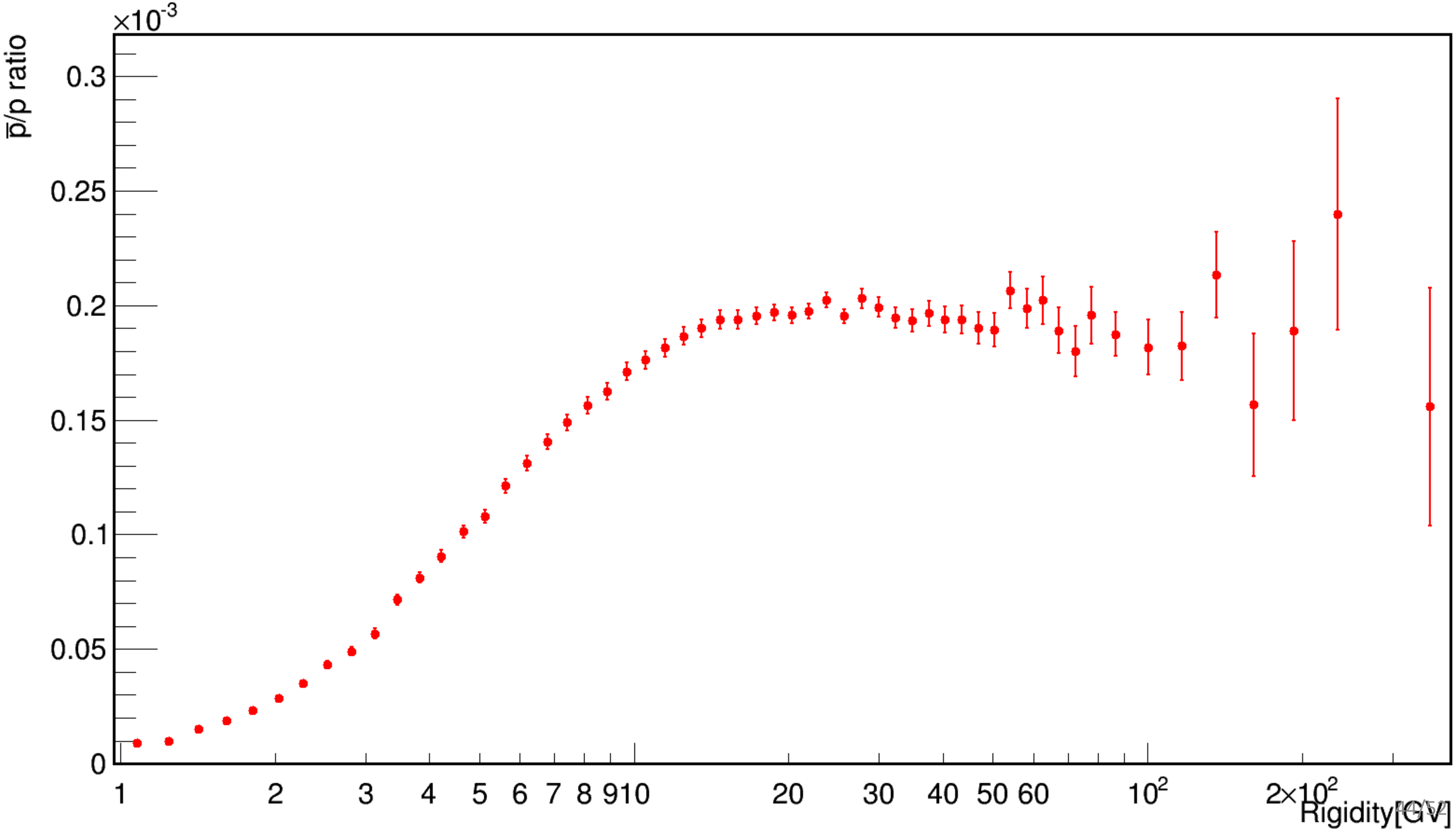

Result Comparison

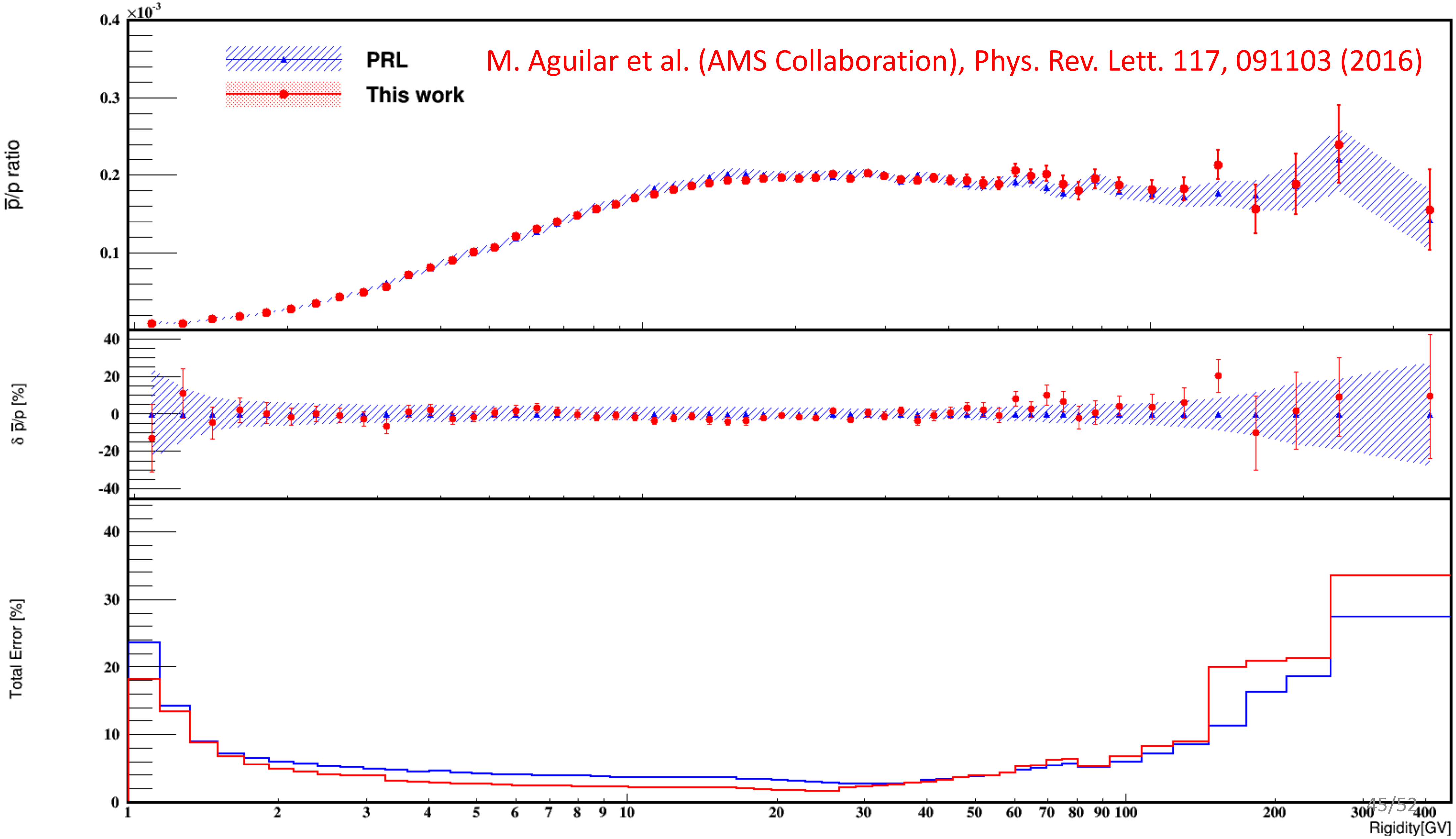

Unexpected: The Spectra of Protons and Antiprotons:

If $\bar{p}$ are secondaries, their rigidity dependence should be different than p:

$p + ISM \rightarrow \bar{p} + \ldots$

Unexpectedly $\bar{p}$ and p have the same rigidity dependence.

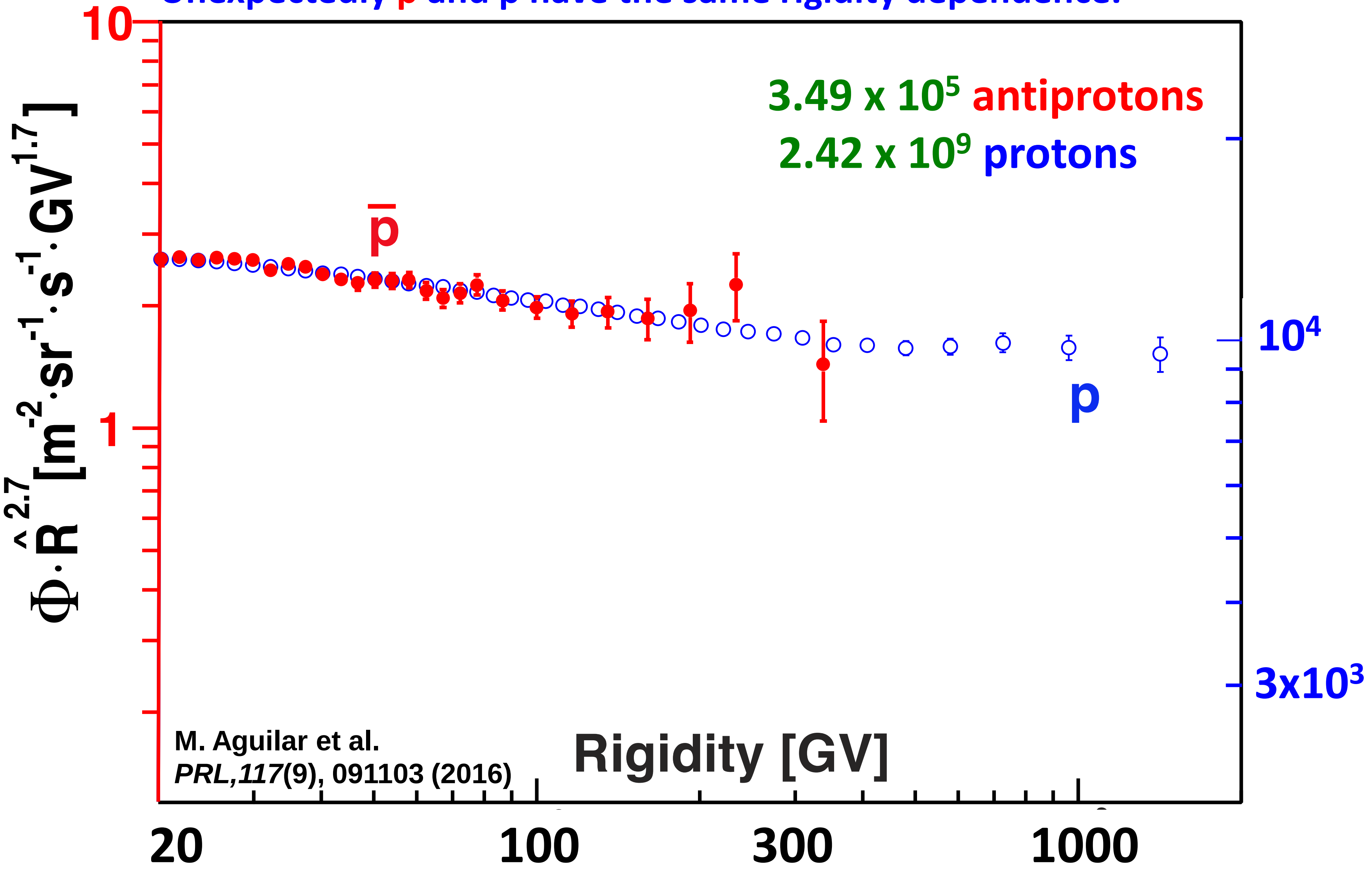

Unexpected results: the rigidity dependence of e^+, $\bar{p}$, p are identical from ~60 to ~500 GV

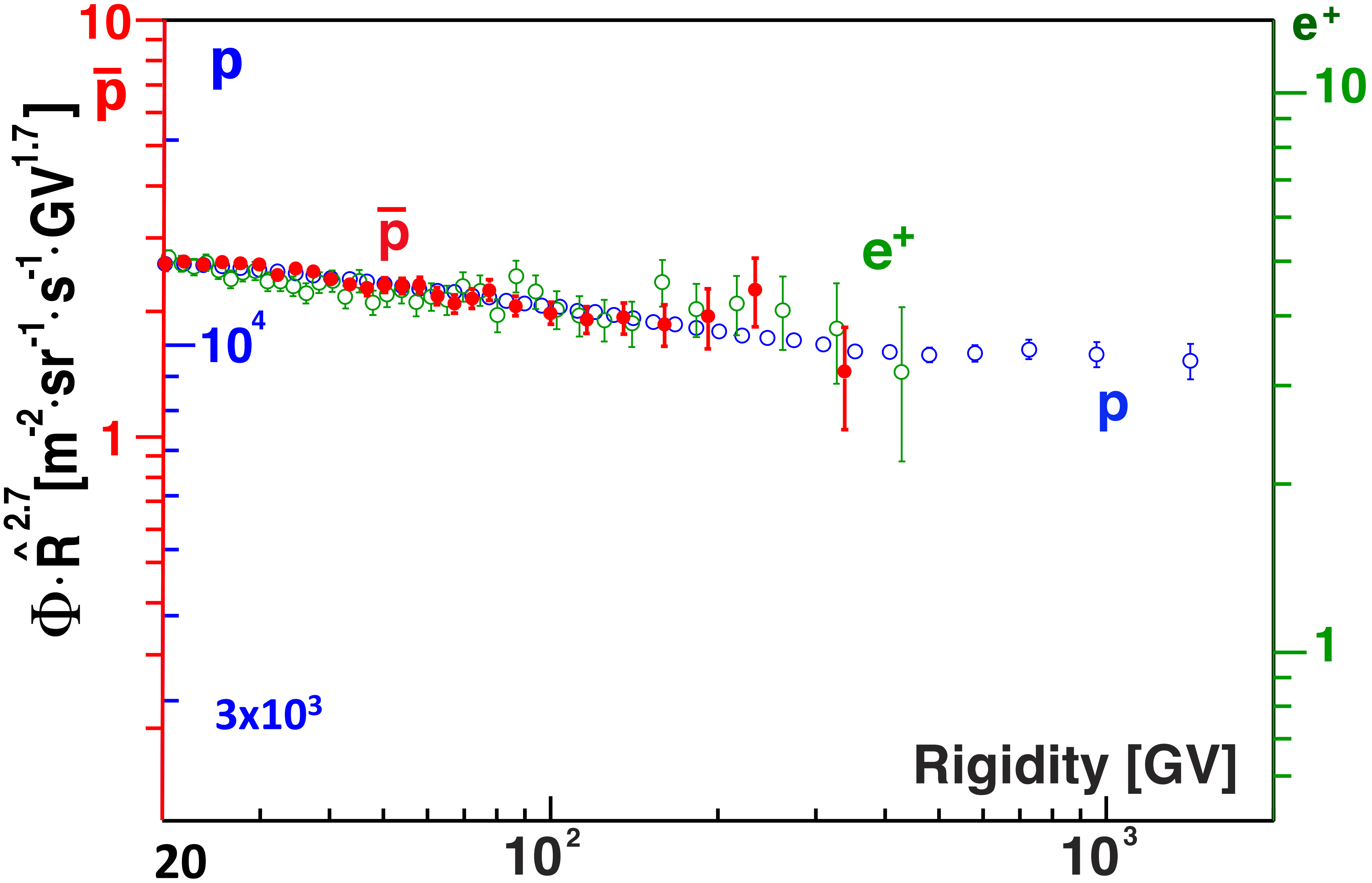

Unexpected results: the rigidity dependence of e^+, $\bar{p}$, p are identical from ~60 to ~500 GV

e^- has a different rigidity dependence.

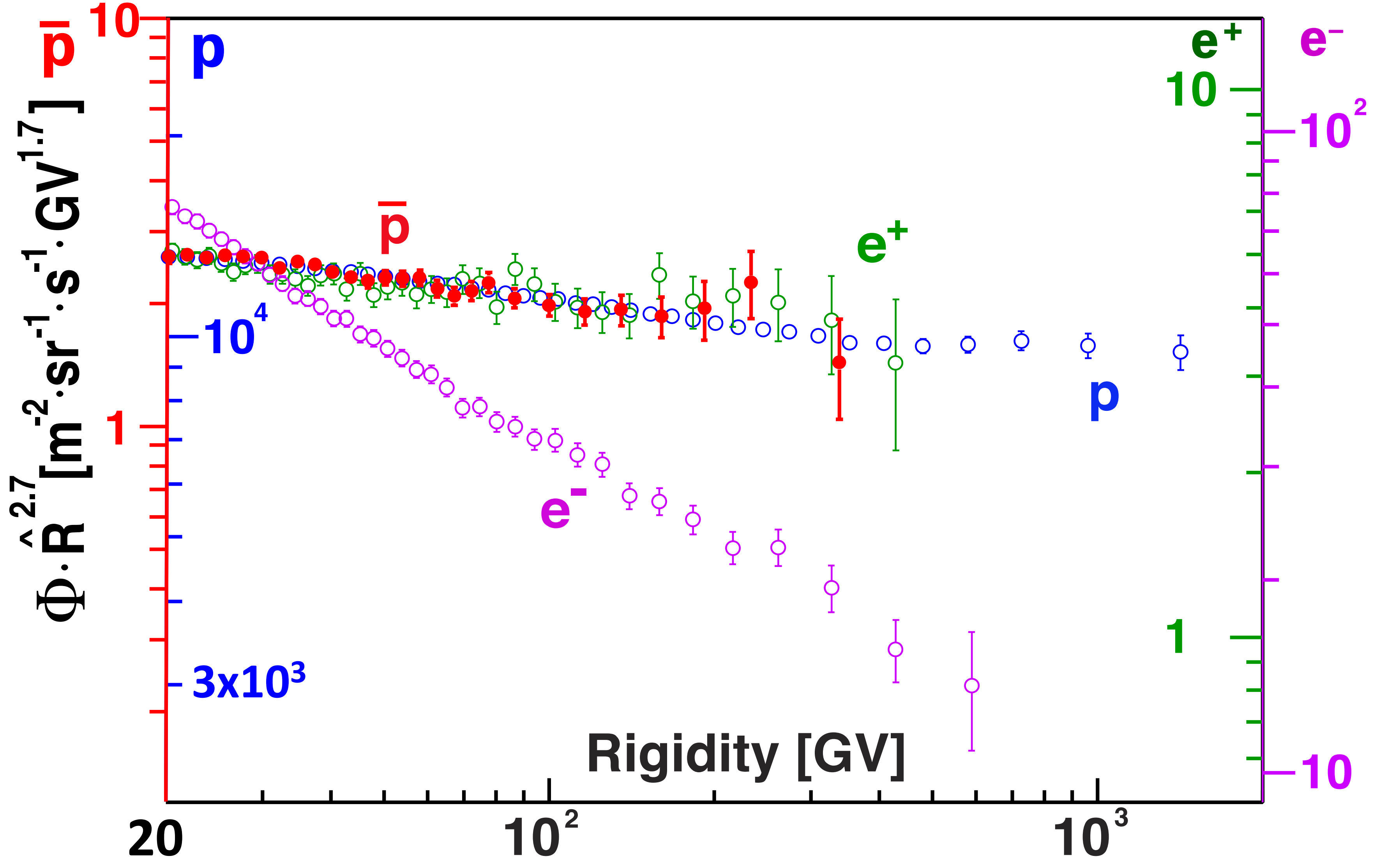

AMS $\bar{p}/p$ results and modeling

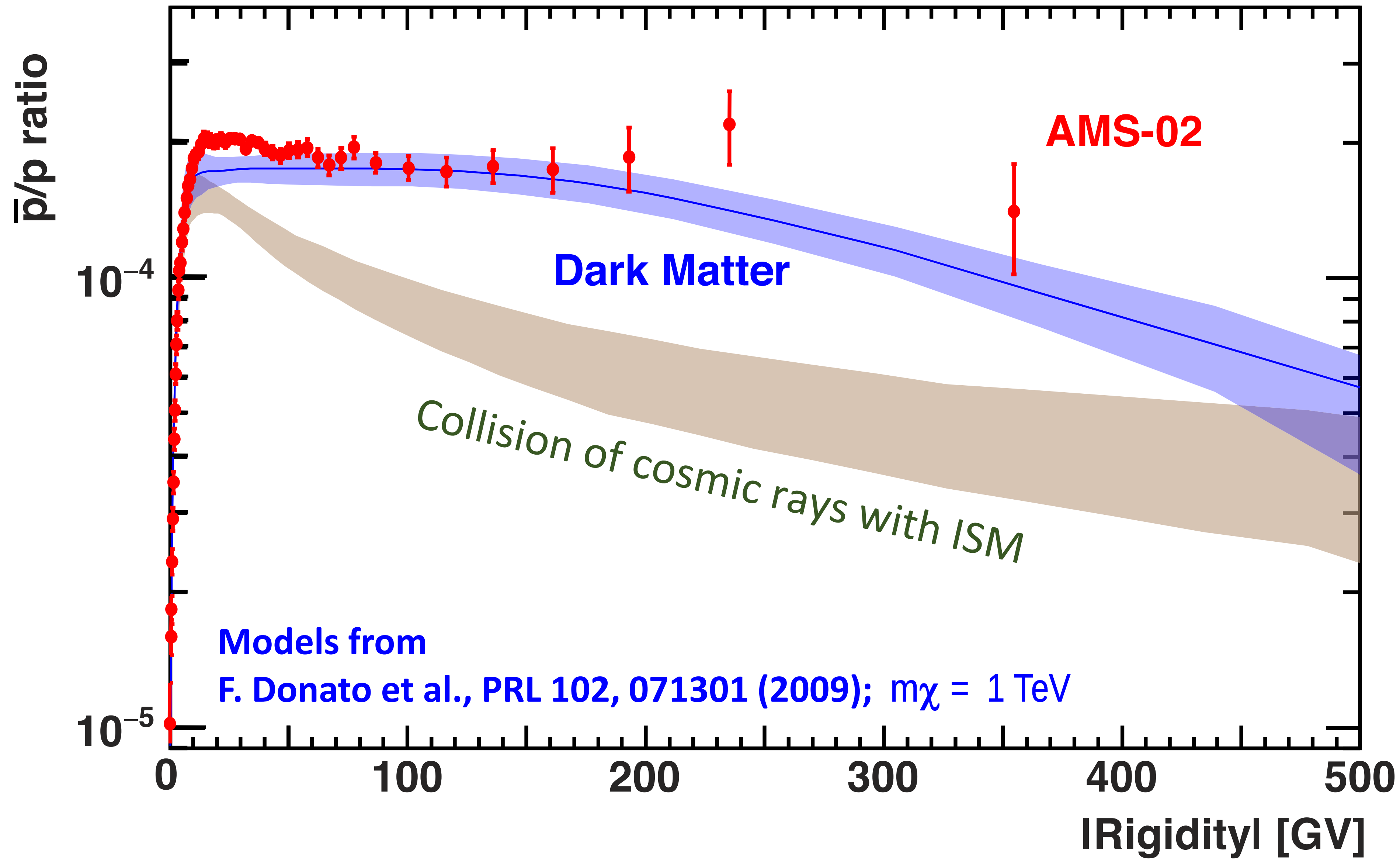

Recent models of antiproton production

From collision of cosmic rays with interstellar medium:

J. Feng, et.al., Phys. Rev. D. 94, 123007 (2016)
G.Giesen, et. al., JCAP 09 (2015) 023
C.Evoli et. al., JCAP 12 (2015) 039
R.Kappl, et. al., JACP 10(2015) 034
...

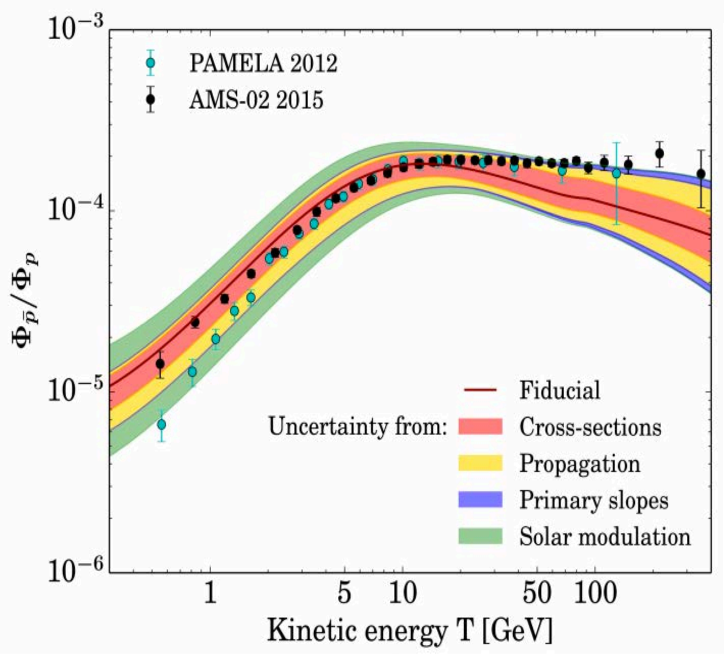

G.Giesen, et. al., JCAP 09 (2015) 023

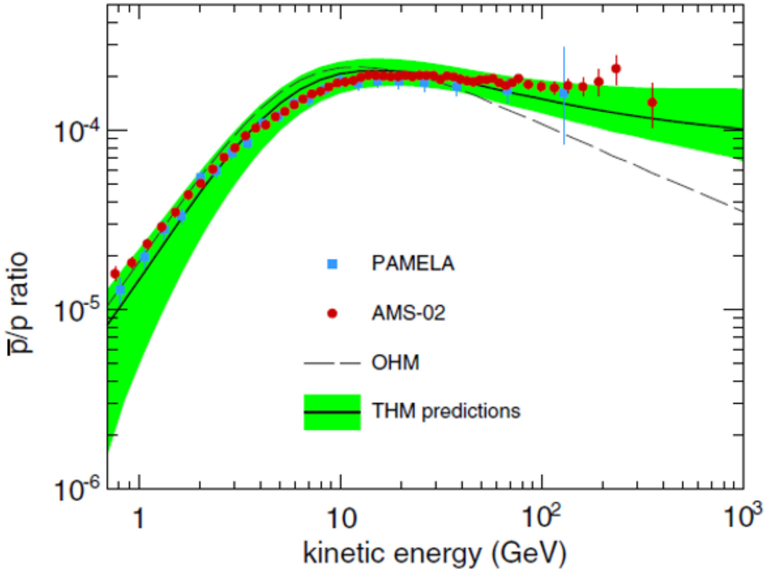

J. Feng, et.al., Phys. Rev. D. 94, 123007 (2016)

Dark matter contribution to explain the antiproton excess around 10 GV:

A. Cuoco, et. Al.*Phys. Rev. Lett.* 118, 191102
M.Y. Cui, et. al. *Phys. Rev. Lett.* 118, 191101 (2017)

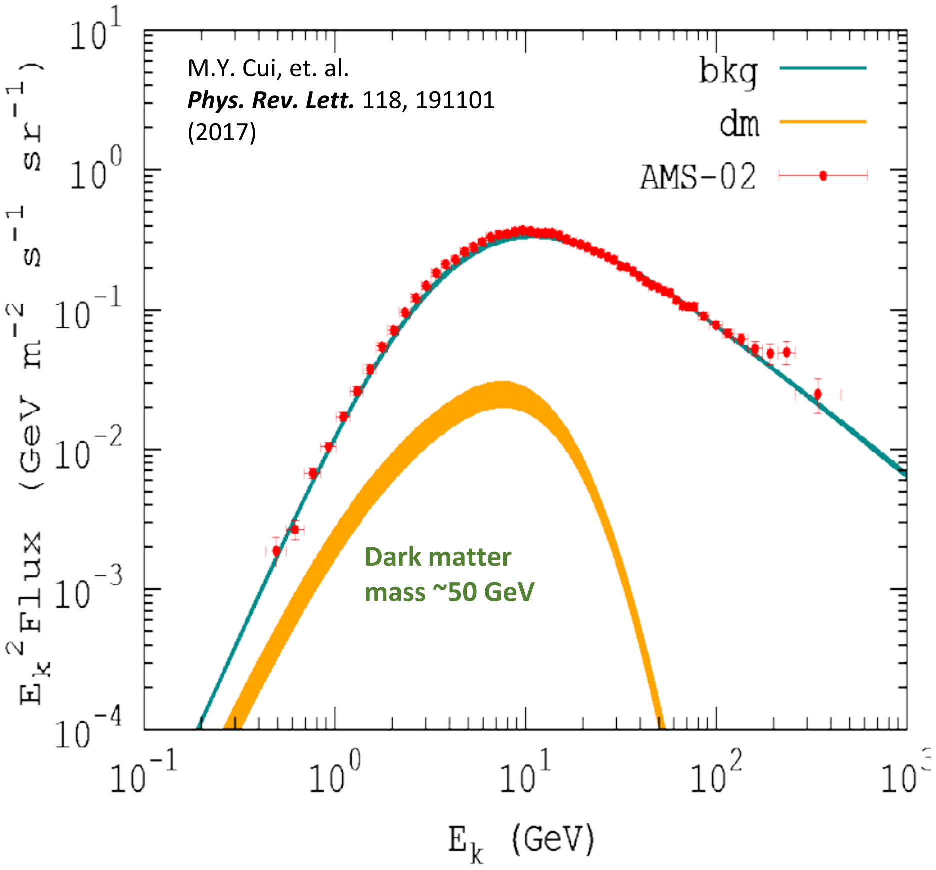

The precision and comprehensive data from AMS allows for the exploration of new phenomena

Measuring antiproton through the life time of Space Station

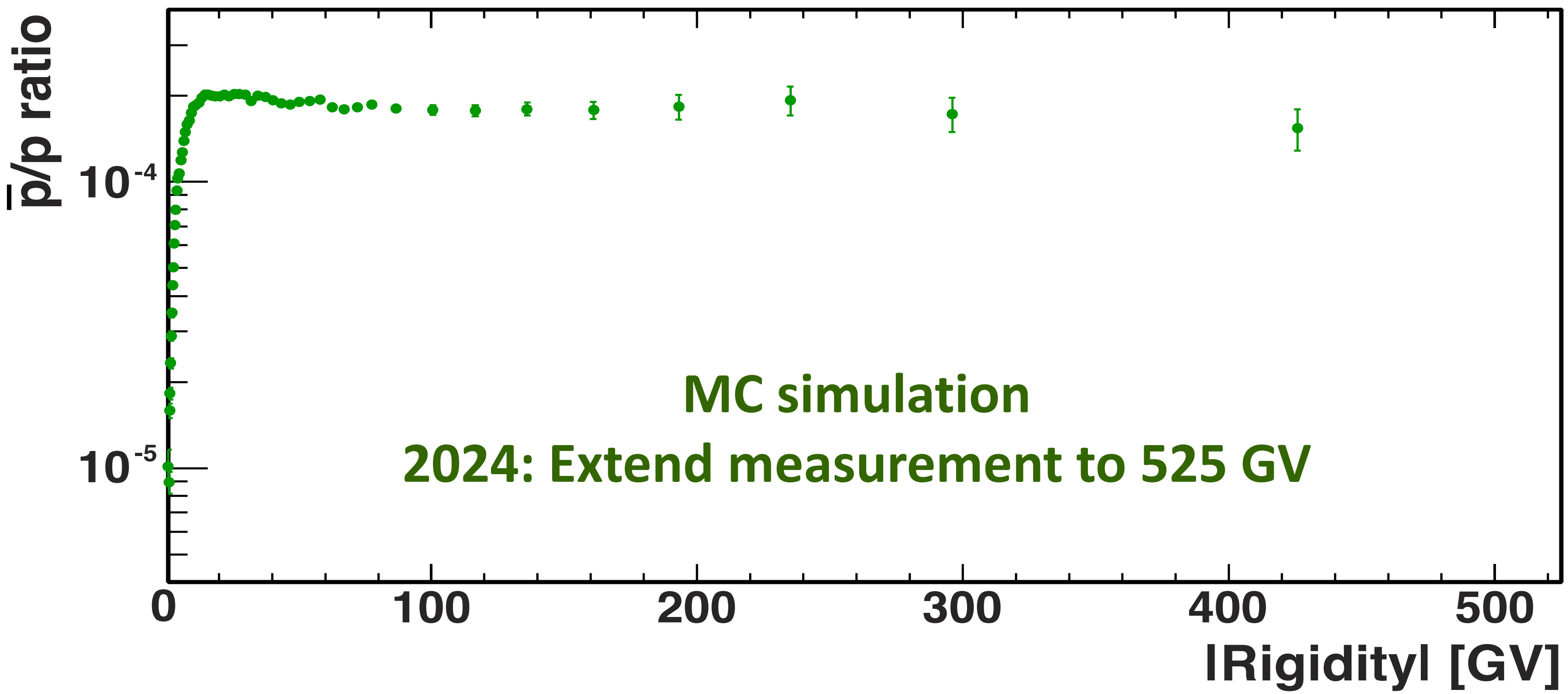

By collecting more data,
AMS will explore to higher rigidity with better accuracy

Thanks for your attention !

Ziyuan.Li / Sun-Yet-Sen University

IHEP, Beijing, Aug.22,2017

Back Up

In 6 years AMS has collected over 100 billion events.

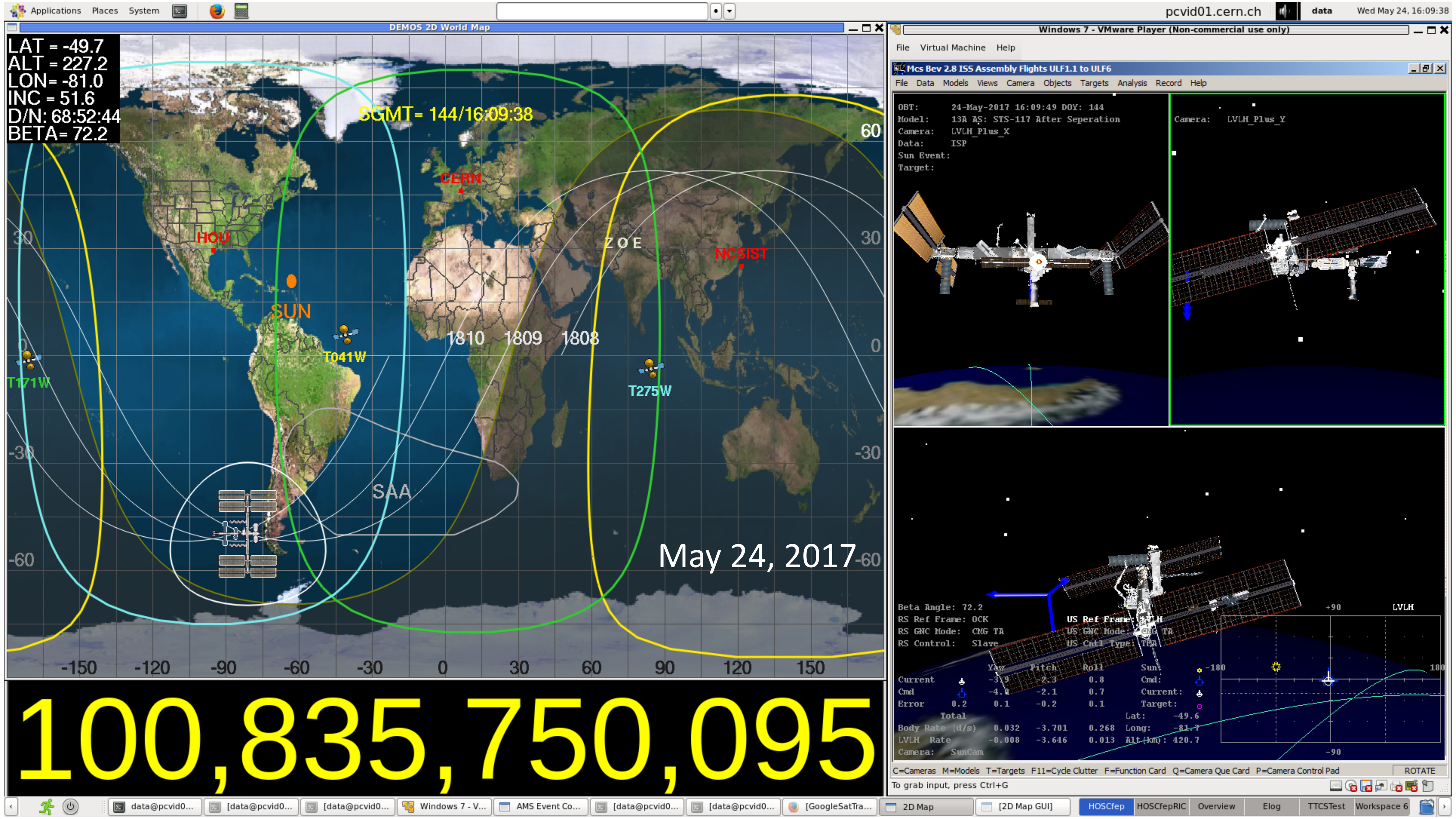

AMS will continue to collect data in the life time of ISS (2024)

TRD performance on the ISS

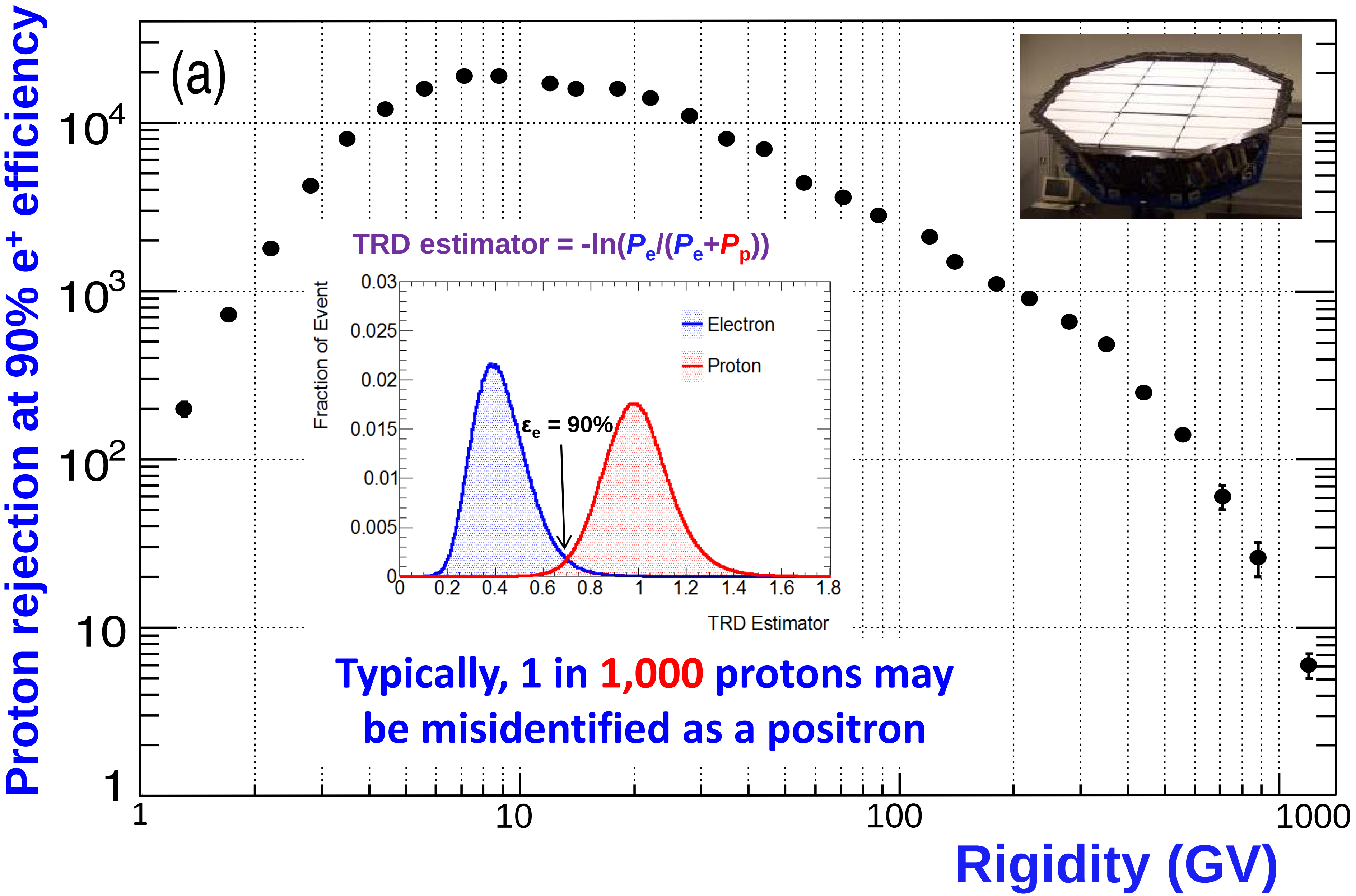

ECAL Performance on the ISS

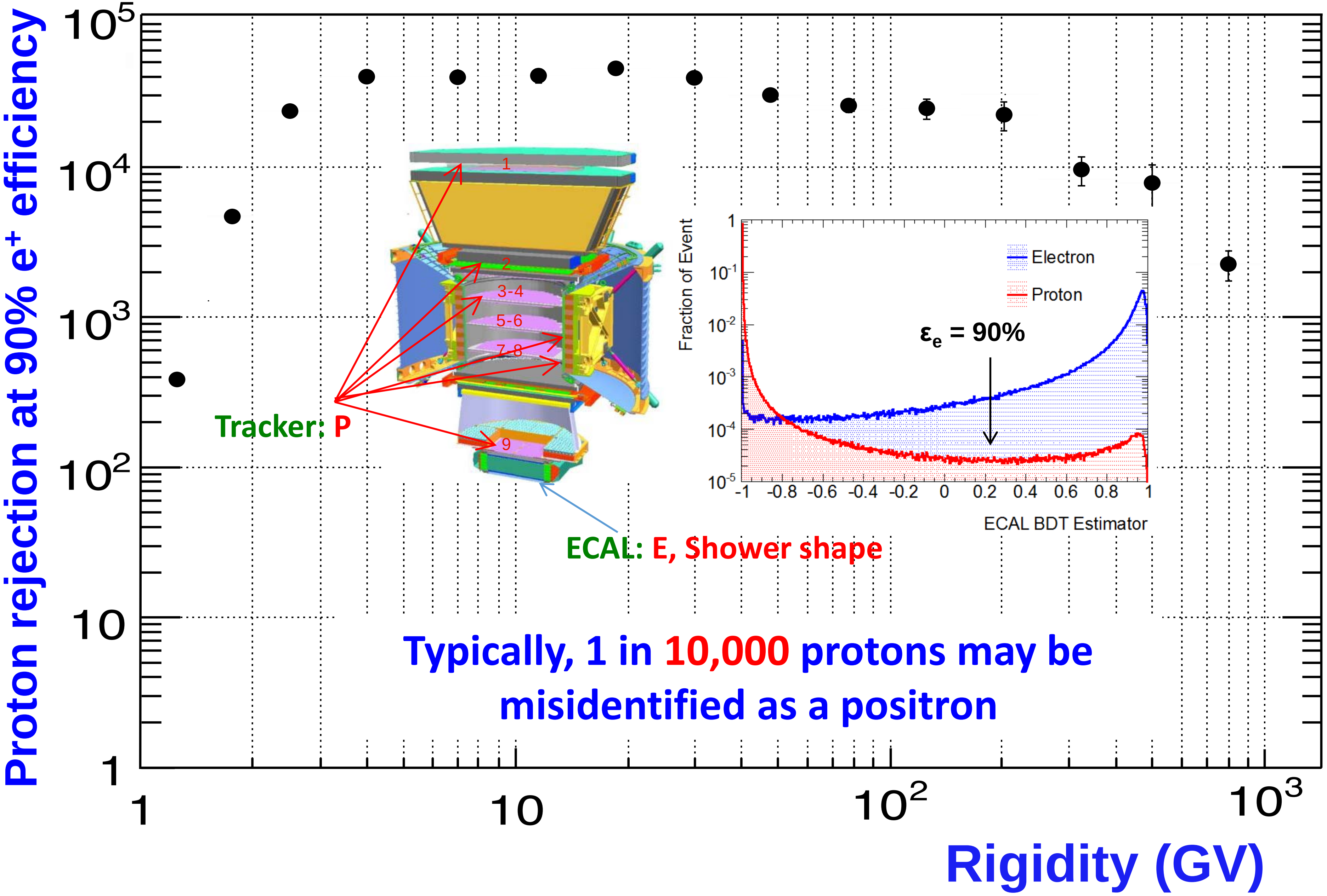

Detector Calibration and Monte Carlo simulation

Detector calibration

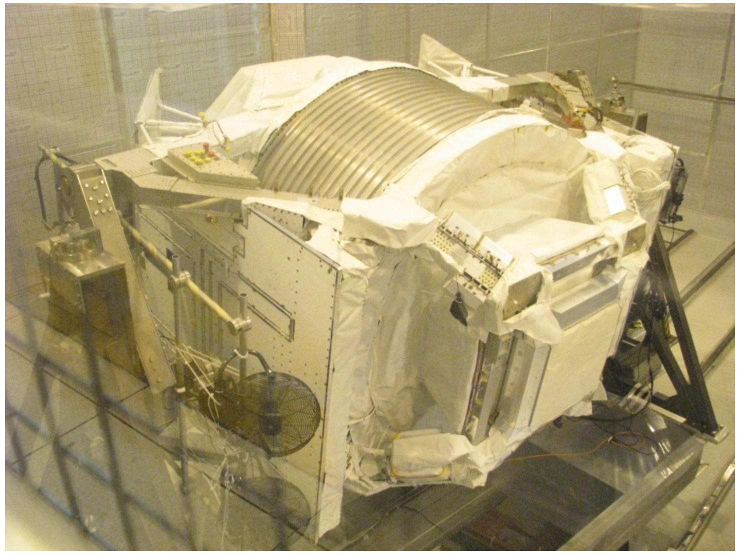

Monte Carlo simulation

10,000 CPU cores at CERN
+ regional centers

Intensive Test Beam @ CERN:

Particle type: p, $e^{\pm}$, $\pi^{\pm}$
Energy (10–400 GeV)
Position (2000)

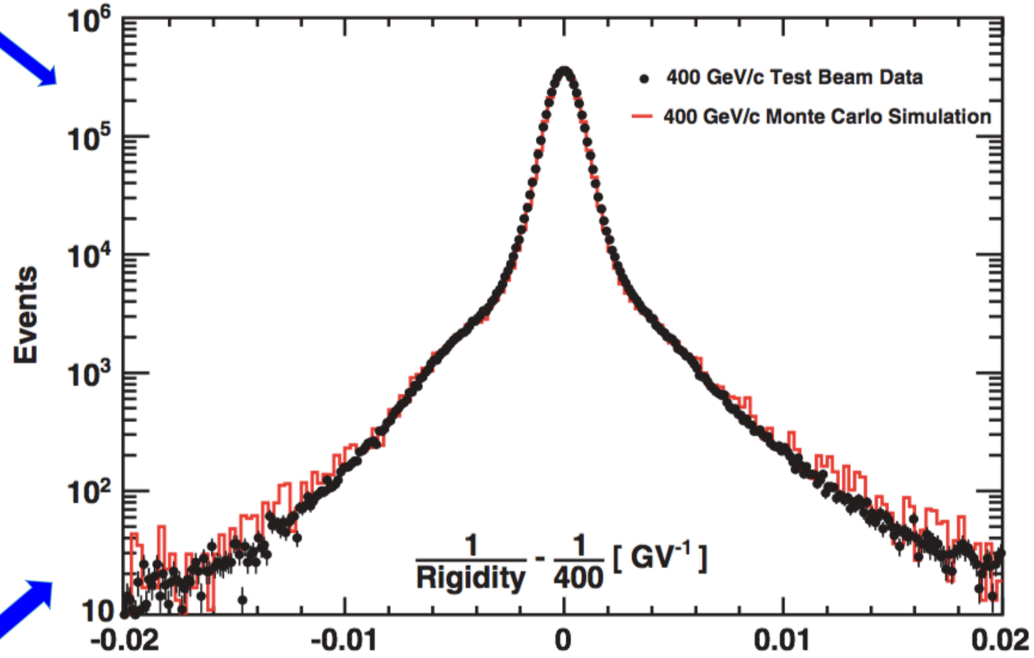

Monte Carlo simulation:

1. Interactions (physics and materials)
2. Digitization (electronics)

Results in data-like events

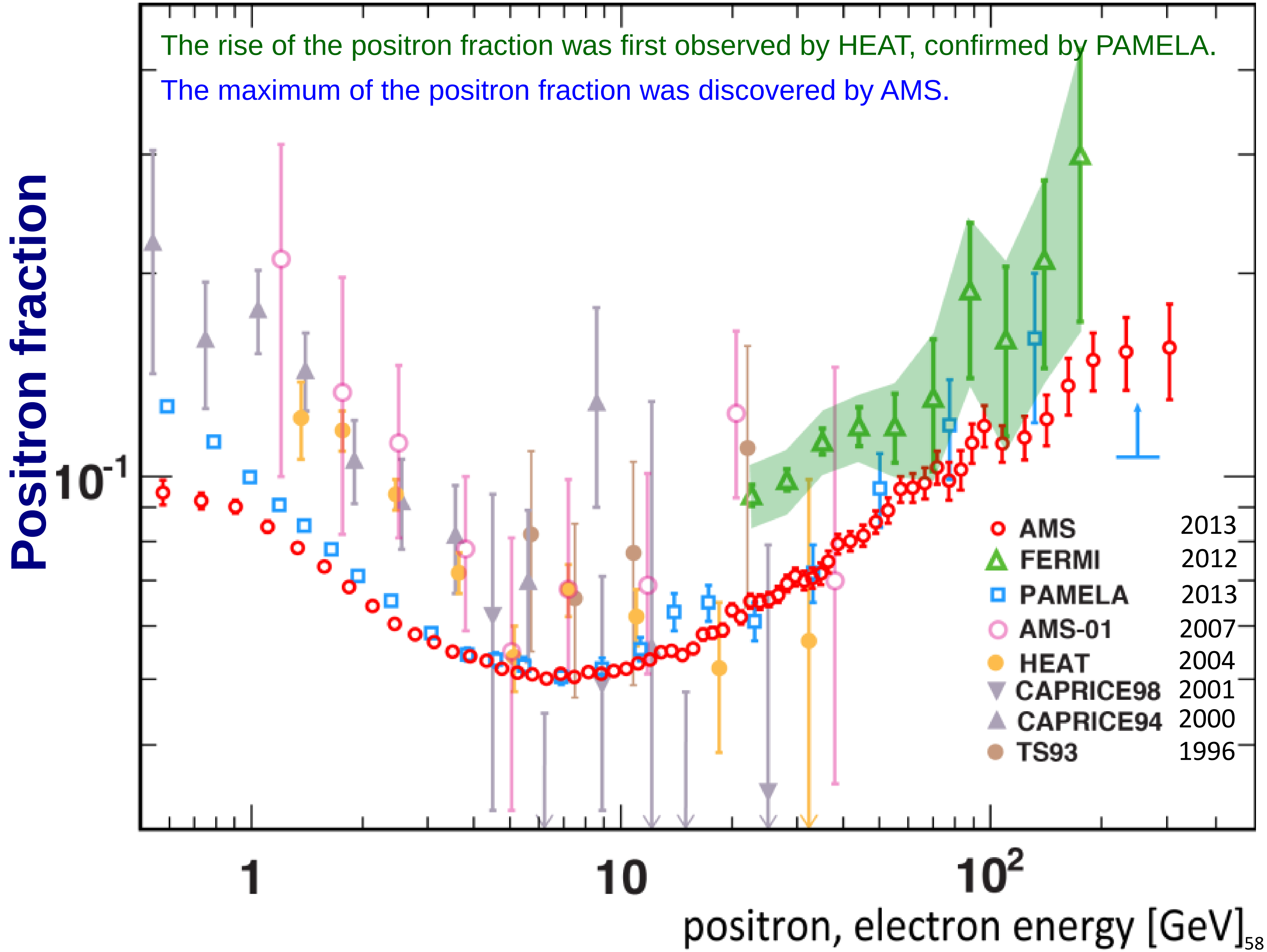
The rise of the positron fraction was first observed by HEAT, confirmed by PAMELA.
The maximum of the positron fraction was discovered by AMS.
Positron fraction
10^{-1}
1
10
10^2
positron, electron energy [GeV]
AMS 2013
FERMI 2012
PAMELA 2013
AMS-01 2007
HEAT 2004
CAPRICE98 2001
CAPRICE94 2000
TS93 1996

Positron Fraction: 5 years data

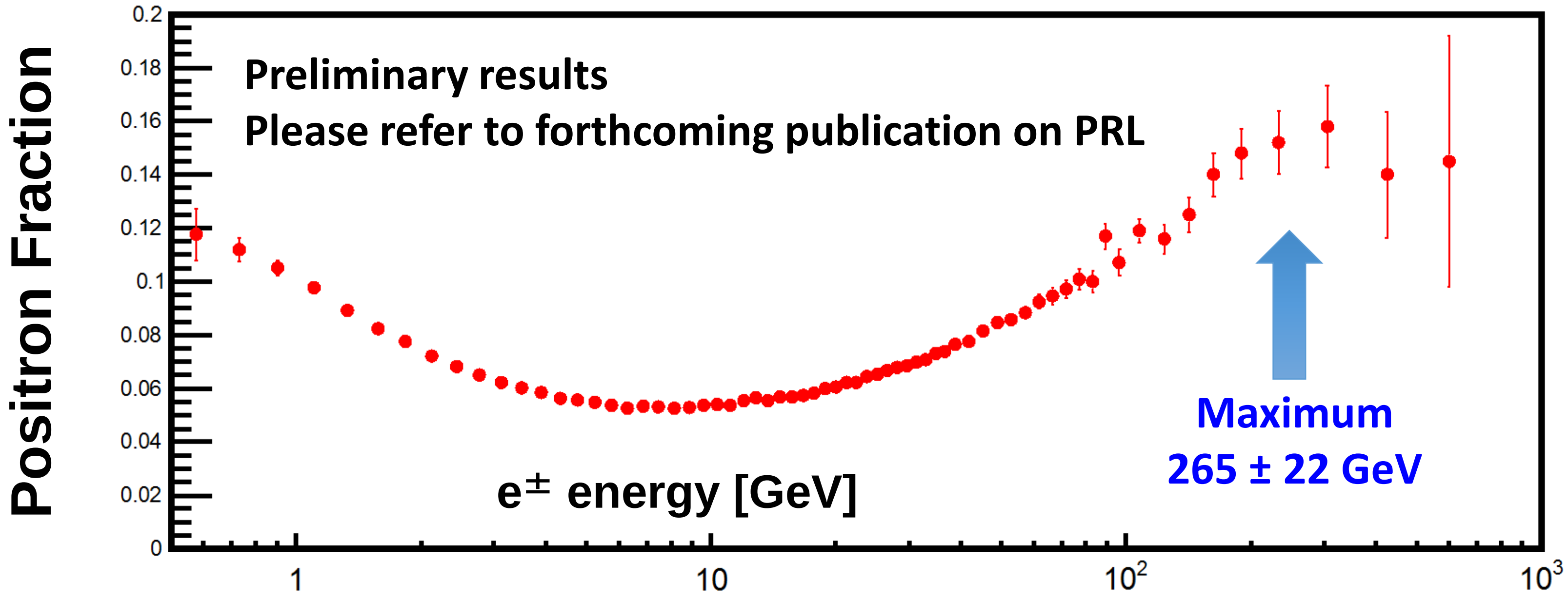

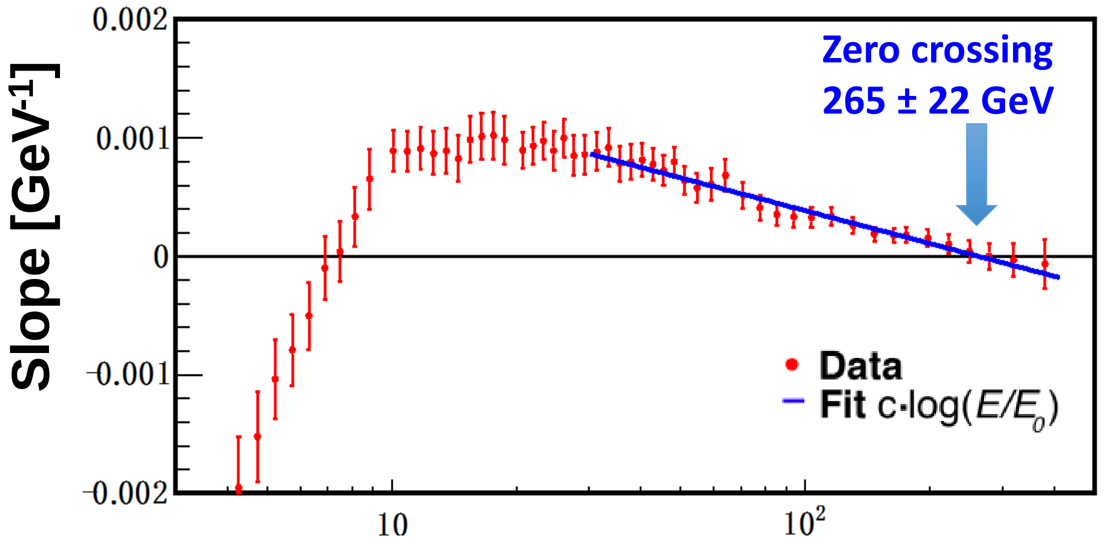

Additional source of high energy electrons and positrons

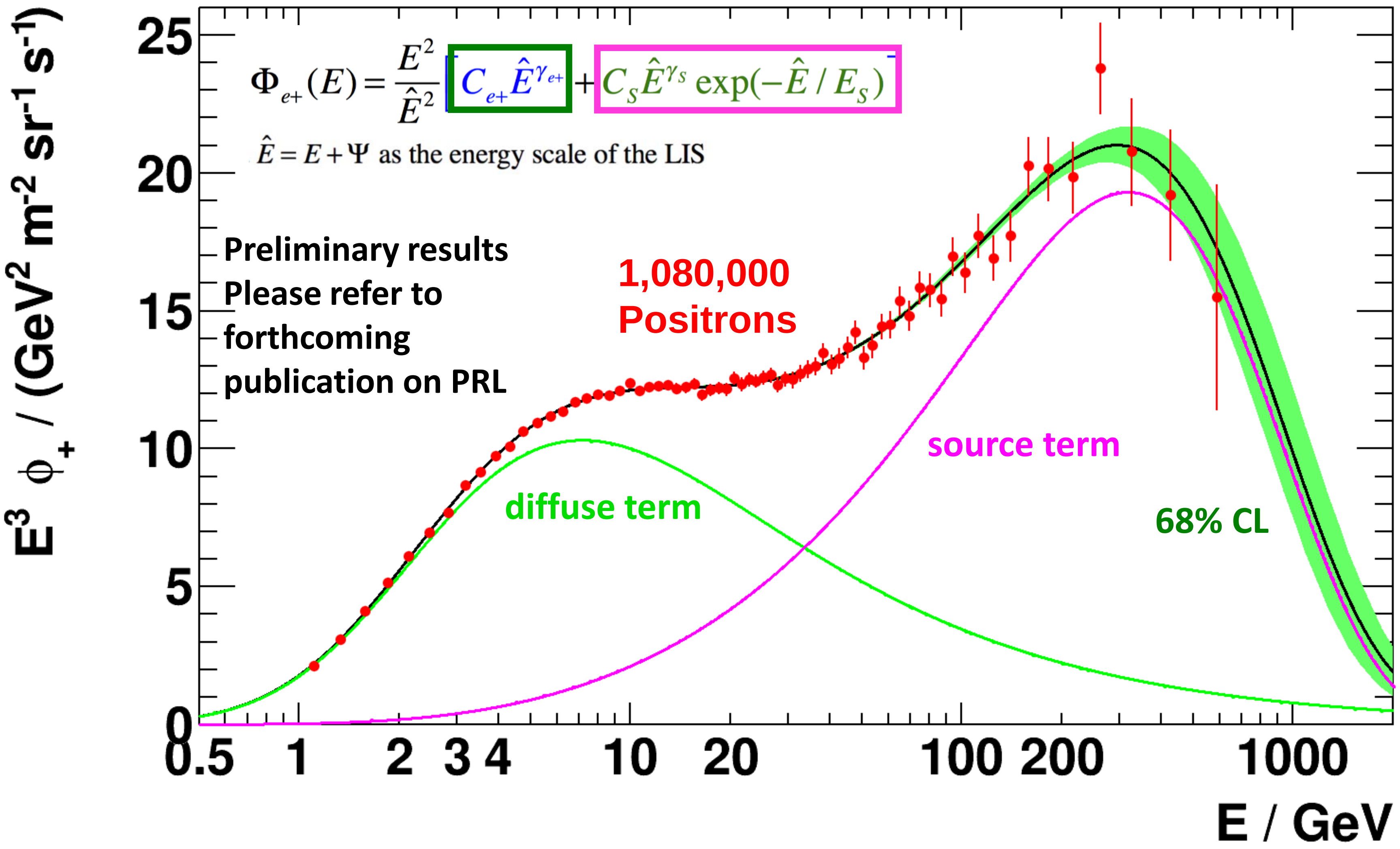

Primary source of cosmic ray positron

Additional source of high energy electrons and positrons

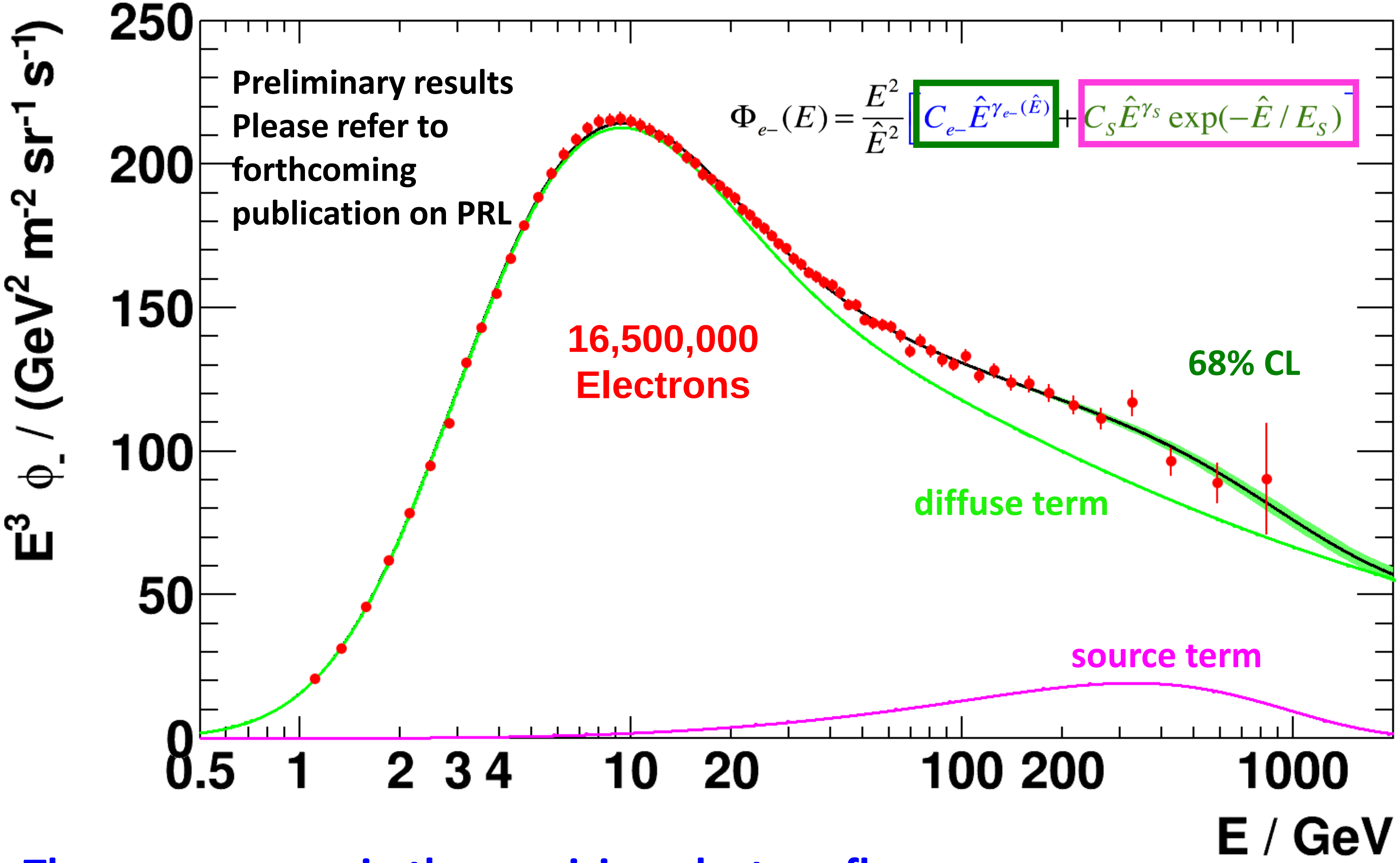

- The **same source** in the precision electron flux
- Common source of electrons and positrons by **Charge Symmetry Process**
- Require comprehensive modelling of cosmic rays to understand its origin

Alternative Models to explain the AMS Positron Flux and Positron Fraction Measurements

- **Modified Propagation of Cosmic Rays**
- **Supernova Remnants**
- **Pulsars**

Examples:

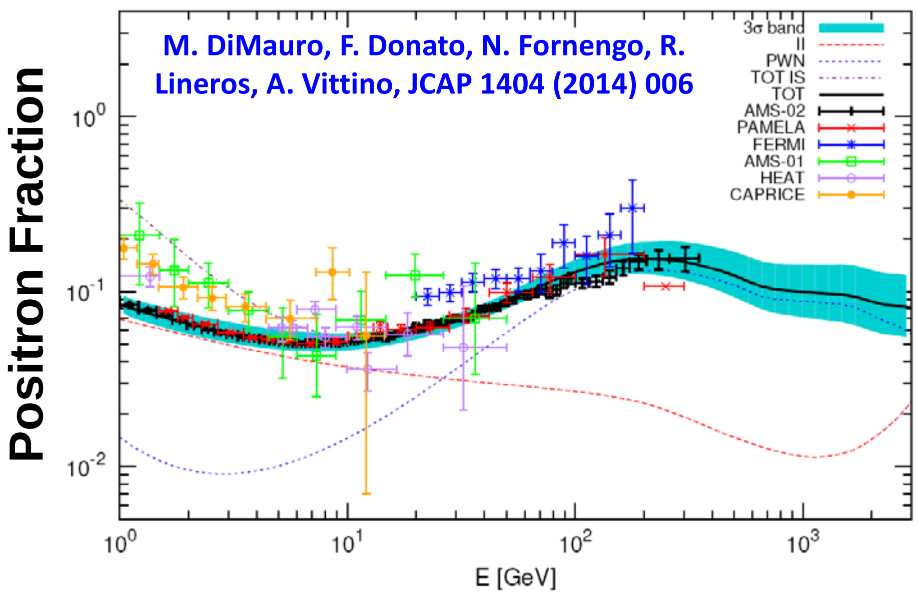

By 2024, AMS will distinguish Dark Matter from Pulsars

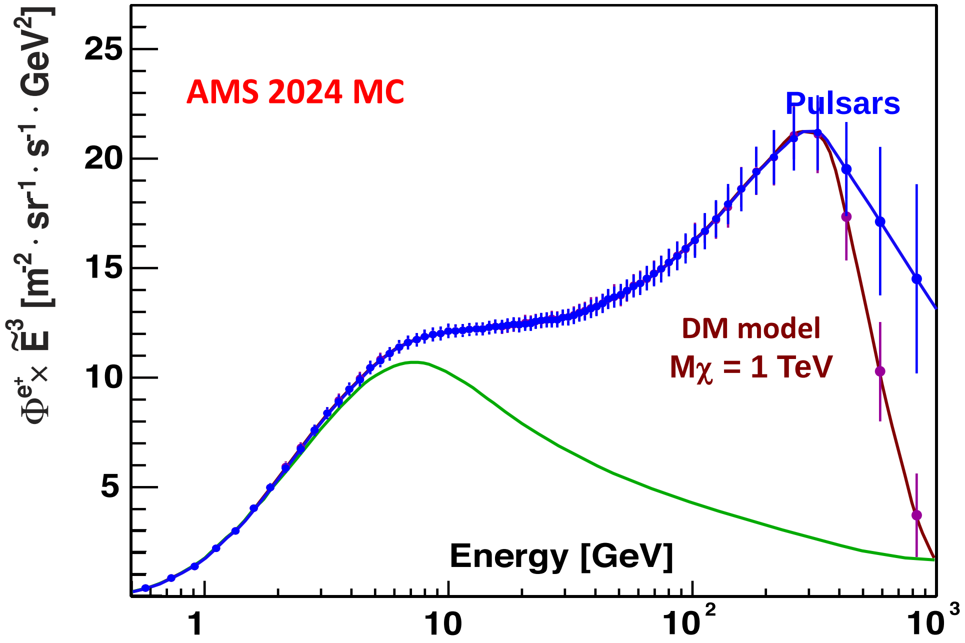

AMS Measurements on Positron, Electron anisotropy and on antiprotons will also help distinguish different models

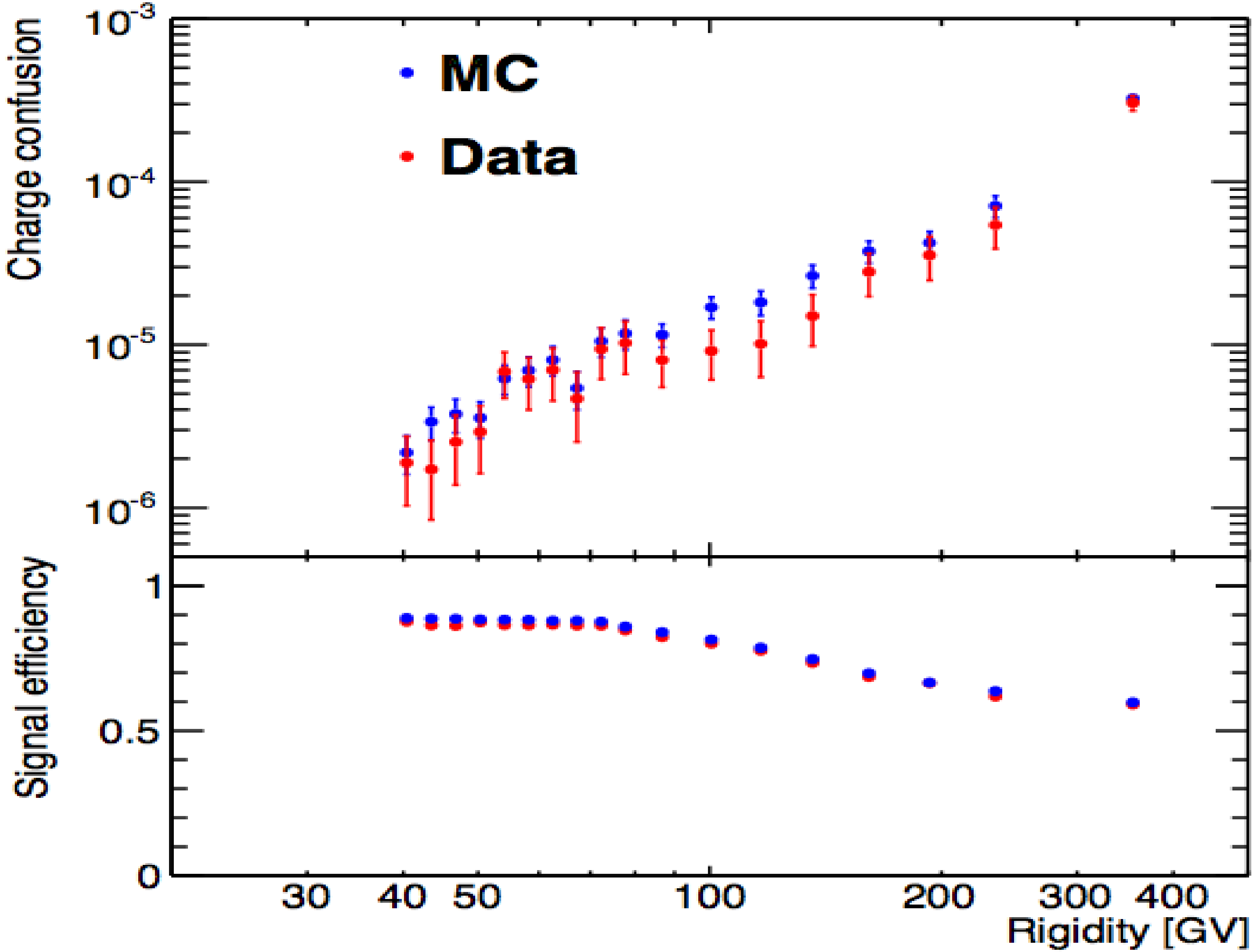
Charge confusion
MC
Data
10^{-3}
10^{-4}
10^{-5}
10^{-6}
Signal efficiency
1
0.5
0
30
40
50
100
200
300
400
Rigidity [GV]

Cross section difference

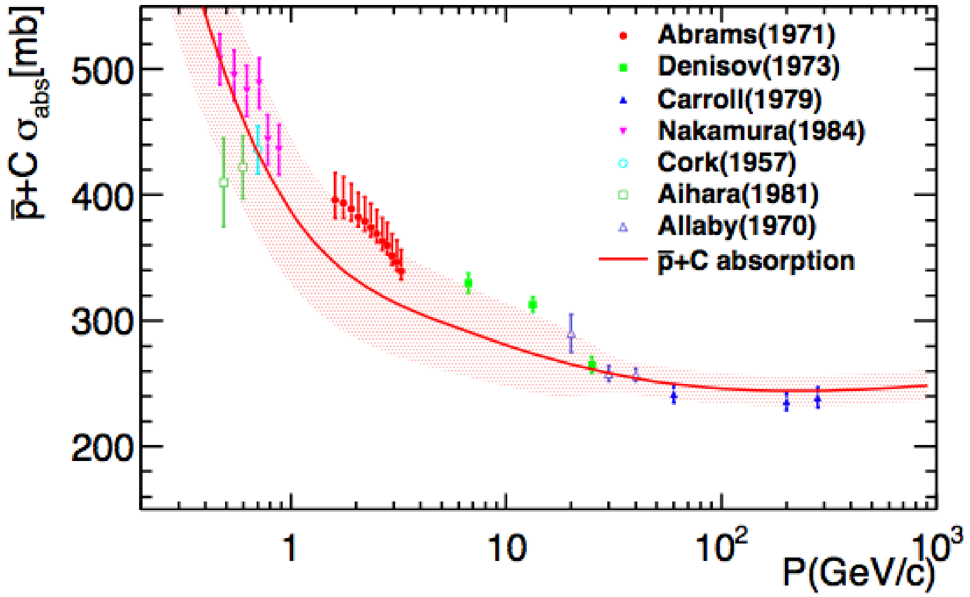

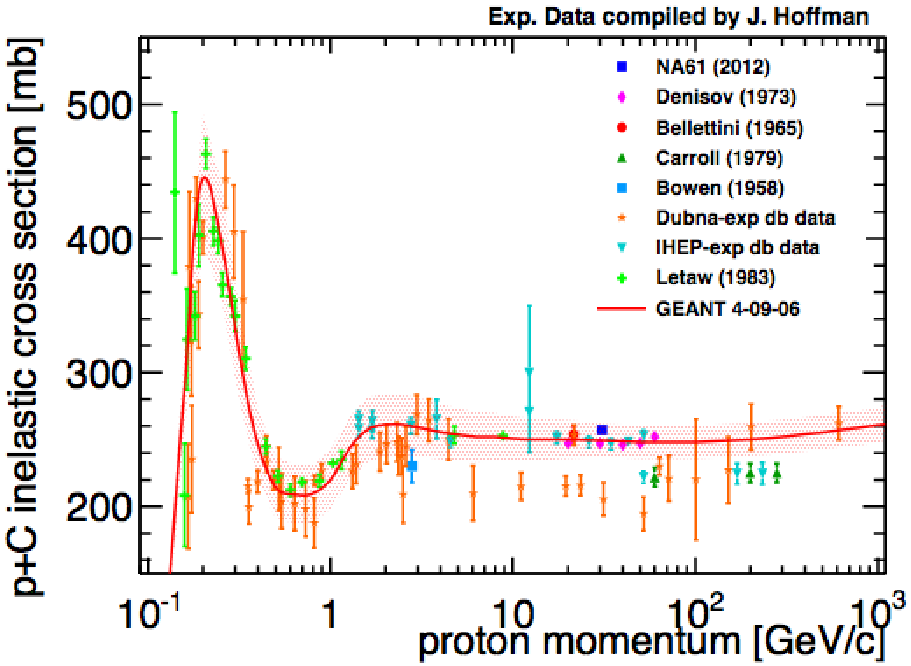

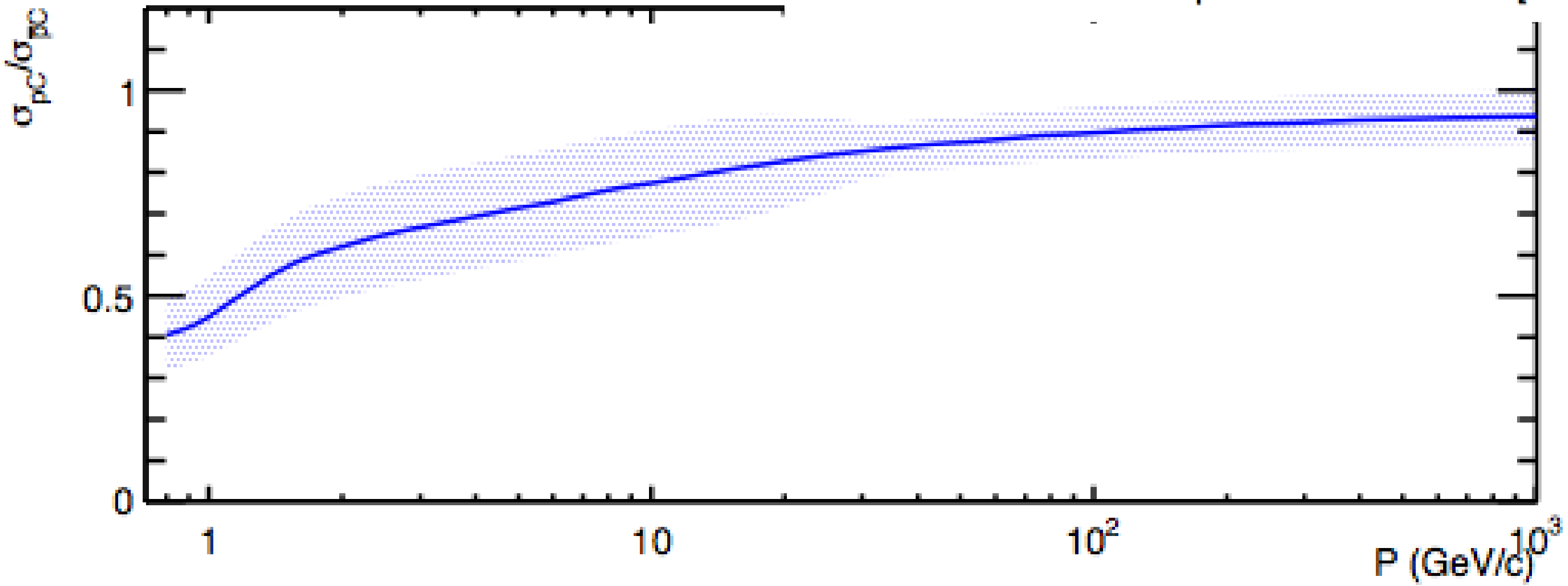

AMS proton flux

New information: The proton flux cannot be described by a single power law = CR^{γ}

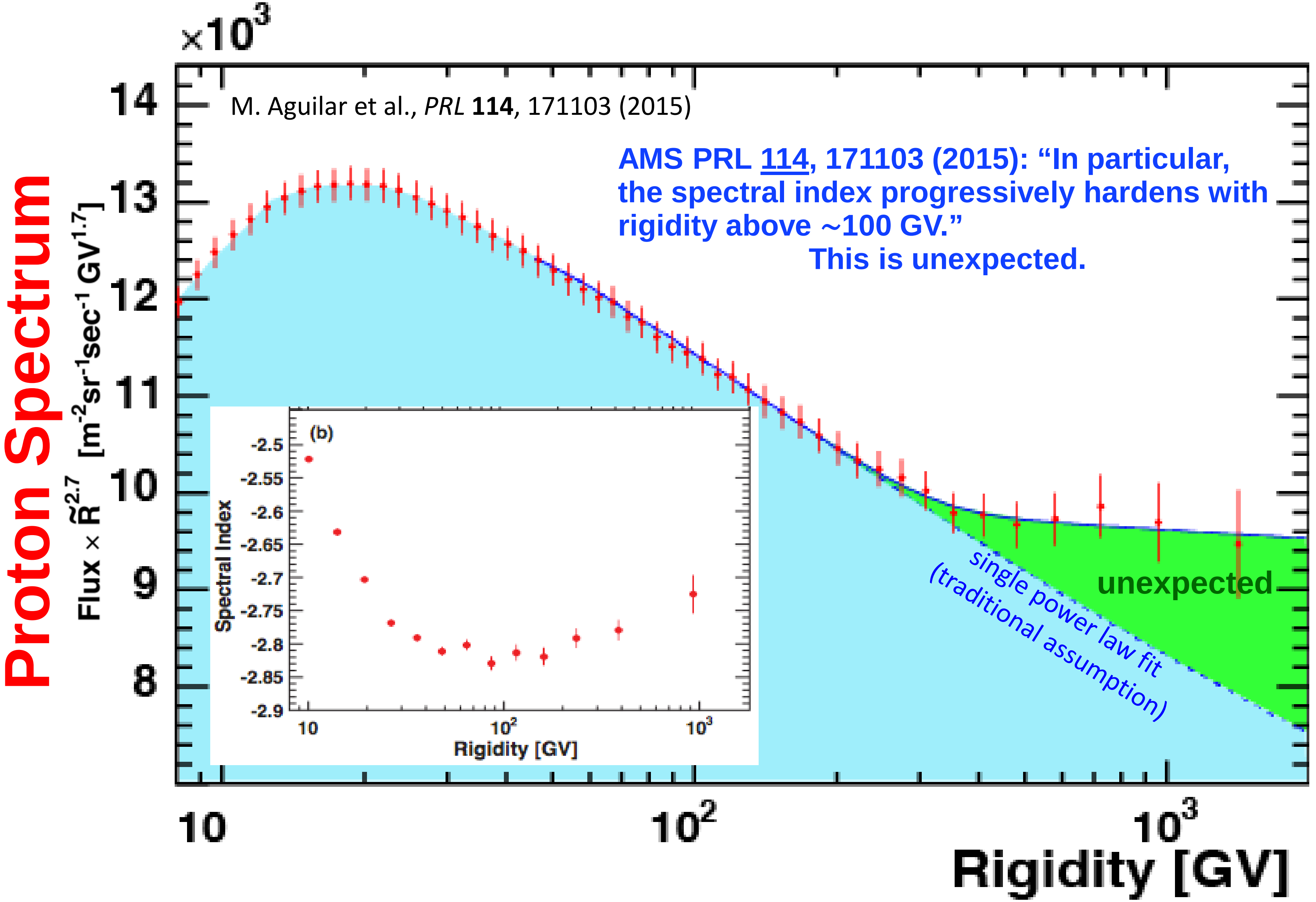

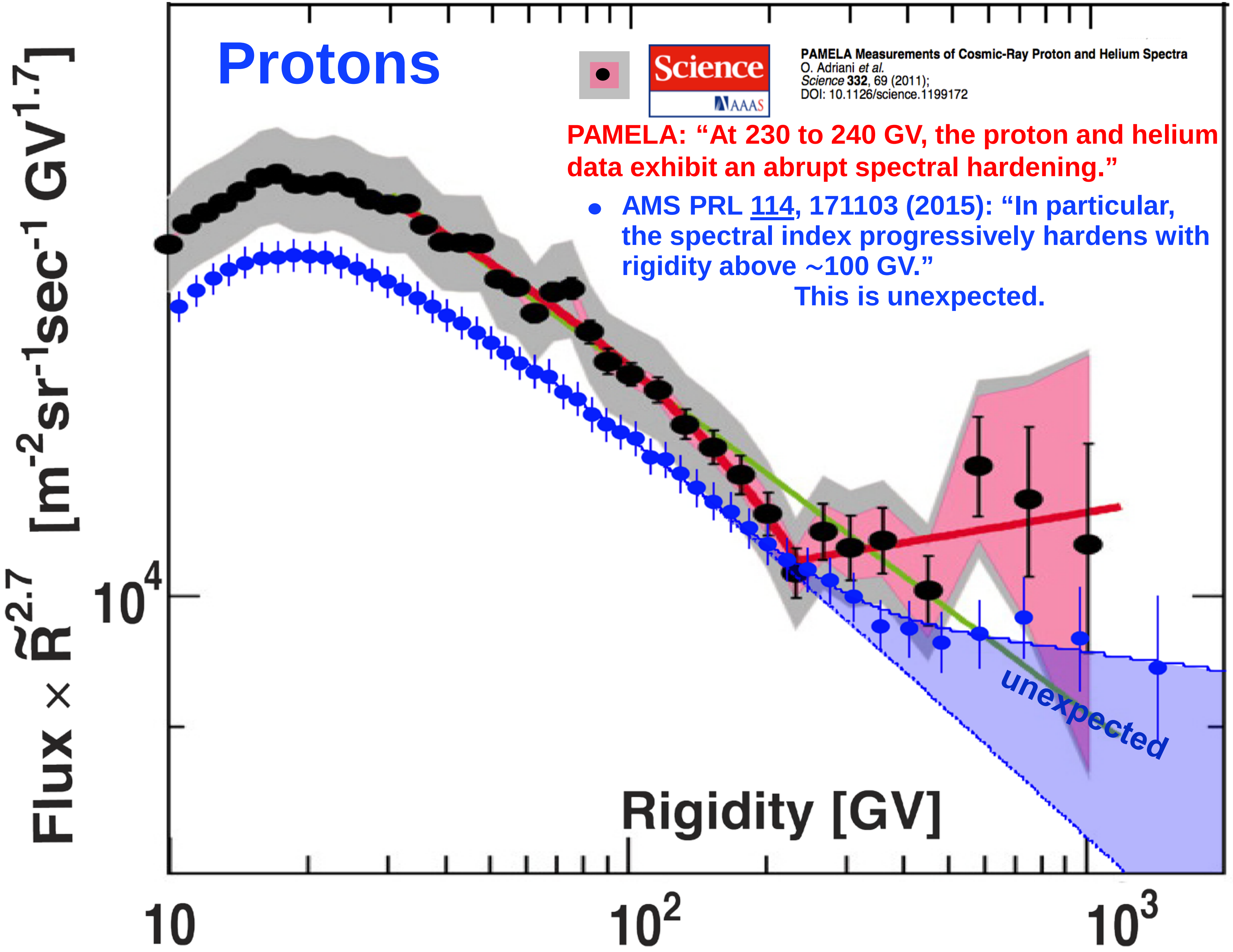
Protons
Science
AAAS
PAMELA Measurements of Cosmic-Ray Proton and Helium Spectra
O. Adriani et al.
Science 332, 69 (2011);
DOI: 10.1126/science.1199172
PAMELA: "At 230 to 240 GV, the proton and helium data exhibit an abrupt spectral hardening."
AMS PRL 114, 171103 (2015): "In particular, the spectral index progressively hardens with rigidity above ~100 GV."
This is unexpected.
unexpected
Flux × R̃^2.7 [m^-2sr^-1sec^-1 GV^1.7]
10^4
Rigidity [GV]
10
10^2
10^3

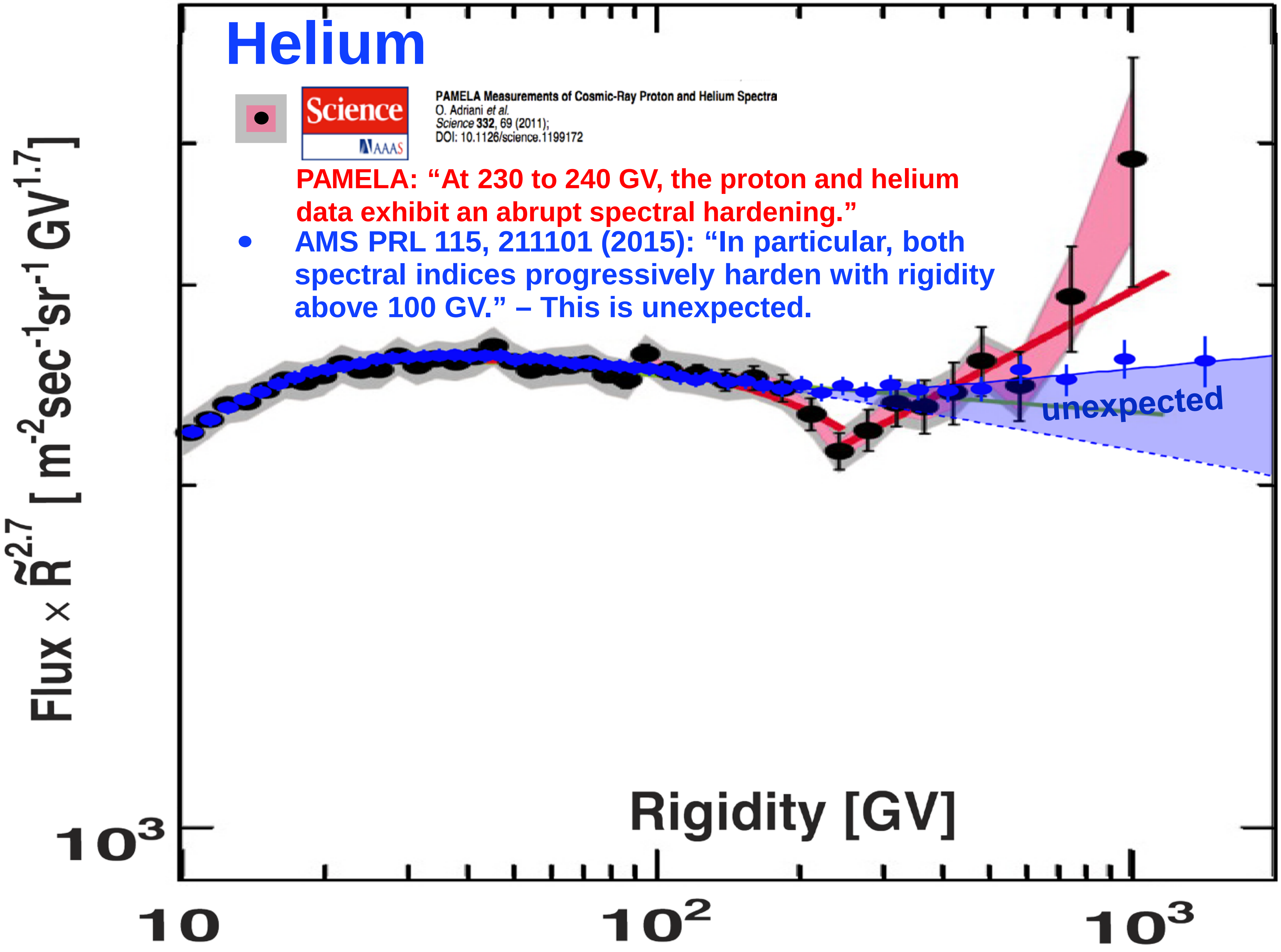
Helium
Science
AAAS
PAMELA Measurements of Cosmic-Ray Proton and Helium Spectra
O. Adriani et al.
Science 332, 69 (2011);
DOI: 10.1126/science.1199172
PAMELA: "At 230 to 240 GV, the proton and helium data exhibit an abrupt spectral hardening."
AMS PRL 115, 211101 (2015): "In particular, both spectral indices progressively harden with rigidity above 100 GV." – This is unexpected.
unexpected
Flux × R̃$^{2.7}$ [m^{-2}sec^{-1}sr^{-1} GV$^{1.7}$]
10^3
Rigidity [GV]
10
10^2
10^3